

# ECMWF Newsletter

Number 138 – Winter 2013/14

European Centre for Medium-Range Weather Forecasts

Europäisches Zentrum für mittelfristige Wettervorhersage

Centre européen pour les prévisions météorologiques à moyen terme

Ten years of ENVISAT  
data at ECMWF

---

Skill of ECMWF's  
monthly forecasts

---

Representation of stable  
boundary layers

---

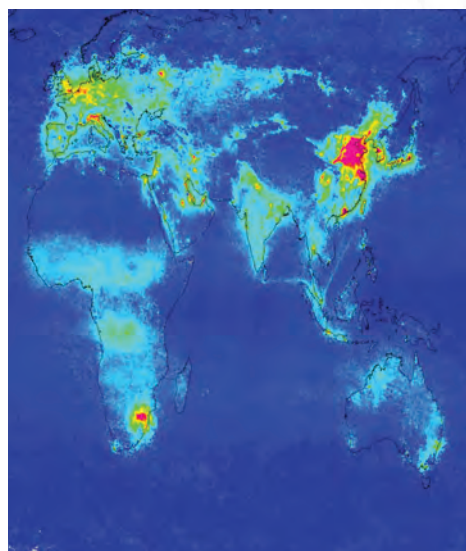
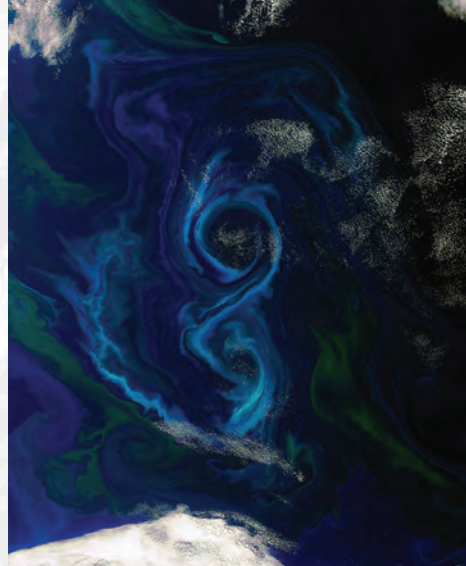
Seasonal forecasts of  
crop irrigation needs

---

3D visualization of  
ensemble forecasts

---

[www.ecmwf.int/publications/newsletter](http://www.ecmwf.int/publications/newsletter)



## **PUBLICATION POLICY**

The *ECMWF Newsletter* is published quarterly. Its purpose is to make users of ECMWF products, collaborators with ECMWF and the wider meteorological community aware of new developments at ECMWF and the use that can be made of ECMWF products. Most articles are prepared by staff at ECMWF, but articles are also welcome from people working elsewhere, especially those from Member States and Co-operating States. The *ECMWF Newsletter* is not peer-reviewed.

Editor: Bob Riddaway

Typesetting and Graphics: Anabel Bowen with the assistance of Corinne O'Sullivan.

Any queries about the content or distribution of the *ECMWF Newsletter* should be sent to [Bob.Riddaway@ecmwf.int](mailto:Bob.Riddaway@ecmwf.int)

Guidance about submitting an article is available at [www.ecmwf.int/publications/newsletter/guidance.pdf](http://www.ecmwf.int/publications/newsletter/guidance.pdf)

---

## **CONTACTING ECMWF**

Shinfield Park, Reading, Berkshire RG2 9AX, UK

Fax: +44 118 986 9450

Telephone: National 0118 949 9000

International +44 118 949 9000

ECMWF website [www.ecmwf.int](http://www.ecmwf.int)

---

Front cover: four images illustrating various aspects of ENVISAT. See page 44 for information about the images and associated credits.

© Copyright 2014

European Centre for Medium-Range Weather Forecasts, Shinfield Park, Reading, RG2 9AX, England

Literary and scientific copyright belong to ECMWF and are reserved in all countries. This publication is not to be reprinted or translated in whole or in part without the written permission of the Director-General. Appropriate non-commercial use will normally be granted under condition that reference is made to ECMWF.

The information within this publication is given in good faith and considered to be true, but ECMWF accepts no liability for error, omission and for loss or damage arising from its use.

## 2014 and beyond

Looking forward, 2014 is already promising to be a year that will see the Centre exploit a number of important new opportunities to continue to advance the science and practice of global numerical weather prediction (NWP).

One of the major contributing factors to seizing these opportunities is the installation of our new Cray XC30 supercomputer. Providing around three times our current computing capability by utilising over 150,000 processor cores, it will be giving us the power to carry out the research we need to be able to introduce improvements to our predictions. Also in 2014 we are starting our Scalability initiative. Scalability is key to addressing a challenge ECMWF and other modelling centres have to enable their codes to operate effectively and efficiently on the increasingly large number of processors and on new emerging supercomputer architecture. This initiative will be collaborative and will involve academia, NWP experts and computer vendors from the international community and is focussed on being ready for the next generation of supercomputers. One of the very exciting aspects of this project is that it is key in enabling us to continue our quest to reduce initial condition error, model uncertainties and forecast errors. A fundamental way to do that is by increasing the resolution (detail) that our forecasts contain as well as improving our utilisation of observations to determine more accurate initial conditions.

Other areas that have already produced great scientific benefits for weather prediction – reanalysis and atmospheric composition – are also poised to take significant strides forward this year. The importance of being able to use today's science and models to calculate a reliable, consistent and credible record of the global climate of the twentieth century has been recognised by the European Commission (EC) in funding a new collaborative ERA-CLIM2 project led by ECMWF to start in 2014. Such reanalyses are likely to form an important part of the new Copernicus climate change service under development by the EC. The progress being made regarding the integration of atmospheric composition into global analysis and forecast models, for example

pioneered by the MACC programme led by ECMWF, will continue and hopefully transition into an operational phase in the Copernicus atmosphere service.

Weather and climate continue to be critical areas of focus for society and as a publicly-funded organisation we will play our part in communicating the science that underpins them. Recent extreme weather leading, for example, to flooding events in Europe and cold outbreaks in North America have created a huge appetite not only for accurate forecasts but also for explanations about why this is happening. As a research institute, as well as an operational centre, we intend to use our new website, to be launched in 2014, to present the research and explain, as far as possible, the science.

The Centre is of course also pursuing its global cooperation including with the US National Weather Service and the China Meteorological Administration amongst others. Also on the international stage, the Centre will be hosting major workshops in 2014 including ones on climate services, global flooding and high-performance computing.

These and other opportunities sit alongside the vital on-going work by ECMWF to develop and produce its numerical weather predictions. We expect to introduce a new model cycle in 2014 that will address, for example, long standing model biases in the upper troposphere–lower stratosphere and the tendency for forecasts to predict too many occurrences of light rain. It will also include improvements in data assimilation and a better calibration of the ensemble information in the medium and extended range.

These developments rely on talented people collaborating worldwide and having state-of-the-art computing facilities at their disposal as well as access to the global observations that are so critical to initialise and evaluate global forecasts.

I invite you to read more about our activities in this edition of our newsletter, and across the various areas of our new website as it develops.

**Alan Thorpe**

### CONTENTS

#### EDITORIAL

2014 and beyond ..... 1

#### NEWS

Metview's 20<sup>th</sup> anniversary ..... 2

New model cycle 40r1 ..... 3

Retirement of Jean-Jacques Morcrette ..... 4

Handling hyperspectral infrared satellite observations ..... 5

MACC-II General Assembly ..... 5

Use and development of Meteorological Operational Systems ..... 6

ERA-Interim monitors the global warmth of 2013 ..... 8

Parameter estimation and inverse modelling for atmospheric composition ..... 10

Update on the new website ..... 10

ECMWF's contribution to GEO ..... 11

New items on the ECMWF website ..... 12

Applying for Special Projects ..... 12

#### METEOROLOGY

Ten years of ENVISAT data at ECMWF ..... 13

Have ECMWF monthly forecasts been improving? ..... 18

Improving the representation of stable boundary layers ..... 24

iCOLT – Seasonal forecasts of crop irrigation needs at ARPA-SIMC ..... 30

#### COMPUTING

GPU based interactive 3D visualization of ECMWF ensemble forecasts ..... 34

#### GENERAL

ECMWF calendar 2014 ..... 38

ECMWF Council and its committees ..... 39

TAC Representatives, Computing Representatives and Meteorological Contact Points ..... 40

ECMWF publications ..... 41

Contact information ..... 41

## Metview's 20<sup>th</sup> anniversary

**IAIN RUSSELL, FERNANDO II, SÁNDOR KERTÉSZ, JUAN-JOSÉ DOMÍNGUEZ**

The 20<sup>th</sup> anniversary of the first internal release of Metview was celebrated at ECMWF in December 2013. Metview is ECMWF's meteorological workstation software for accessing, manipulating and visualising meteorological data, incorporating both an interactive and a batch mode. It is used by analysts and researchers, inside and outside ECMWF, to analyse observation, analysis and model data.

Work on Metview was started in 1991 as a co-operative project between ECMWF and INPE/CPTEC (Brazil) with assistance from Météo-France. After two years of initial development, the first release of Metview was ready in December 1993. Its cutting-edge graphical user interface and powerful Macro language made it the easiest way to handle ECMWF's data, and Metview was released to Member States in October 1995.

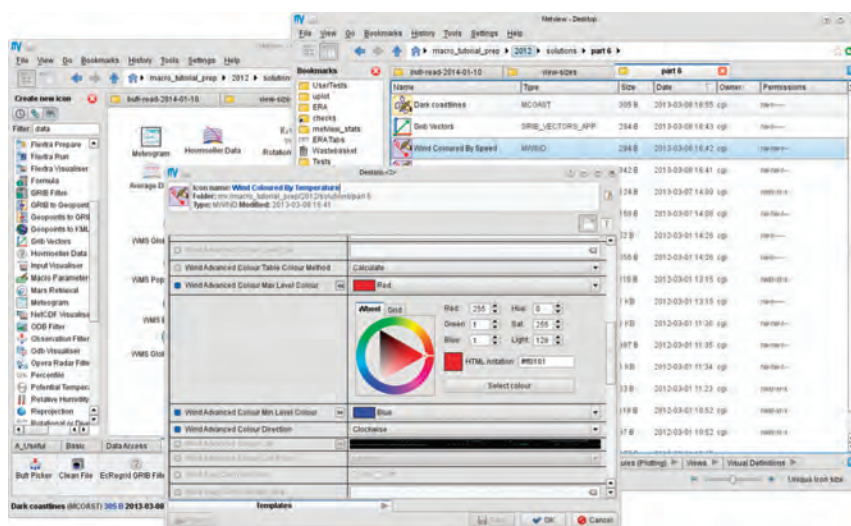
Metview's success and power are the result of offering a single unified interface which brings together many technologies developed at ECMWF for handling and visualising meteorological data. These include access to the MARS data archive, handling of GRIB, BUFR and ODB data, grid-point interpolation, and a high-quality meteorological plotting engine. Feedback and contributions from both inside and outside ECMWF have ensured that it continues to meet the needs of its users.

December also saw the default version of Metview used at ECMWF upgraded from 3 to 4. Version 4 retains much backwards compatibility with version 3, and the Metview developers are assisting users to migrate where needed.

The future of Metview sees some exciting developments. A new user interface will enable new users to learn Metview more easily and give experienced users quicker access to its functionality. Work has also been done to interface Metview's powerful data manipulation capabilities with



**The Metview 20<sup>th</sup> anniversary celebration.** The celebration held on 6 December 2013 was well attended by developers, both past and present, and users from ECMWF.



**The new user interface for Metview.** This will help unlock the power of Metview for both new and experienced users.

the 3D visualisation provided by software from VAPOR (Visualization and Analysis Platform for Ocean, Atmosphere and Solar Researchers). And of course Metview will continue to support research, monitoring and training at ECMWF while tackling

the challenges of increased model resolution and data volumes. More information about Metview and VAPOR is available at:

<http://software.ecmwf.int/metview>  
<https://www.vapor.ucar.edu/>

# New model cycle 40r1

**PETER BAUER,  
DAVID RICHARDSON**

On 19 November 2014, a new model cycle of the Integrated Forecasting System (IFS) was implemented. This affected the high-resolution forecast (HRES) and ensemble forecast (ENS).

This cycle includes several significant model changes, such as a revised convection scheme that addresses the long-standing issue of convection over land producing rainfall too early during the day. Updates of vertical diffusion and orographic drag alleviate systematic wind shear and wind-turning errors in the boundary layer. Surface-atmosphere coupling for forested areas has been increased and inconsistencies of the treatment of snow albedo between surface and radiation scheme have been removed, both addressing the 2-metre temperature model error.

Following the vertical resolution increase of HRES and the associated data assimilation in the previous cycle (Cy38r2), Cy40r1 introduces a corresponding upgrade for the ENS to 91 levels with the model top being raised to 0.01 hPa. This enhances the representation of clouds, boundary layers and the interaction between troposphere and stratosphere. The interaction of the atmosphere with the dynamical ocean model has been improved through a tendency coupling starting at initial time. Land surface parameters are perturbed in the ENS initial conditions and produce more realistic ENS spread for 2-metre temperature and moisture. Wave effects on ocean circulation have been added. The EDA (Ensemble of Data Assimilations) has been enhanced by increasing the ensemble size from 10 to 25 and it now provides a flow-dependent estimation of background error co-variances for the 4DVAR assimilation. Perturbations are also included for soil moisture observations with this cycle.

Cycle 40r1 also includes a number of changes to satellite data usage. More temperature and humidity observations

Domain	Parameter	Level	Anomaly correlation										RMS error									
			Forecast day										Forecast day									
			1	2	3	4	5	6	7	8	9	10	1	2	3	4	5	6	7	8	9	10
Europe	Relative humidity	300 hPa	▲	▲	▲	▲	▲	▲	▲	▲	▲	▲	▲	▲	▲	▲	▲	▲	▲	▲	▲	
		700 hPa	▲	▲	▲	▲	▲	▲	▲	▲	▲	▲	▲	▲	▲	▲	▲	▲	▲	▲	▲	▲
	Temperature	100 hPa	▼	▼	▼	▼	▼	▼	▼	▼	▼	▼	▼	▼	▼	▼	▼	▼	▼	▼	▼	▼
		500 hPa	▲	▲	▲	▲	▲	▲	▲	▲	▲	▲	▲	▲	▲	▲	▲	▲	▲	▲	▲	▲
		850 hPa	▲	▲	▲	▲	▲	▲	▲	▲	▲	▲	▲	▲	▲	▲	▲	▲	▲	▲	▲	▲
		1000 hPa	▲	▲	▲	▲	▲	▲	▲	▲	▲	▲	▲	▲	▲	▲	▲	▲	▲	▲	▲	▲
	Wind	200 hPa	▲	▲	▲	▲	▲	▲	▲	▲	▲	▲	▲	▲	▲	▲	▲	▲	▲	▲	▲	▲
		850 hPa	▲	▲	▲	▲	▲	▲	▲	▲	▲	▲	▲	▲	▲	▲	▲	▲	▲	▲	▲	▲
	Geopotential	100 hPa	▼	▼	▼	▼	▼	▼	▼	▼	▼	▼	▼	▼	▼	▼	▼	▼	▼	▼	▼	▼
		500 hPa	▲	▲	▲	▲	▲	▲	▲	▲	▲	▲	▲	▲	▲	▲	▲	▲	▲	▲	▲	▲
850 hPa		▲	▲	▲	▲	▲	▲	▲	▲	▲	▲	▲	▲	▲	▲	▲	▲	▲	▲	▲	▲	
Extratropical Northern Hemisphere	10 m wind over ocean	▲	▲	▲	▲	▲	▲	▲	▲	▲	▲	▲	▲	▲	▲	▲	▲	▲	▲	▲	▲	
		▲	▲	▲	▲	▲	▲	▲	▲	▲	▲	▲	▲	▲	▲	▲	▲	▲	▲	▲	▲	
		▲	▲	▲	▲	▲	▲	▲	▲	▲	▲	▲	▲	▲	▲	▲	▲	▲	▲	▲	▲	
	Relative humidity	300 hPa	▲	▲	▲	▲	▲	▲	▲	▲	▲	▲	▲	▲	▲	▲	▲	▲	▲	▲	▲	▲
		700 hPa	▲	▲	▲	▲	▲	▲	▲	▲	▲	▲	▲	▲	▲	▲	▲	▲	▲	▲	▲	▲
	Temperature	100 hPa	▲	▲	▲	▲	▲	▲	▲	▲	▲	▲	▲	▲	▲	▲	▲	▲	▲	▲	▲	▲
		500 hPa	▲	▲	▲	▲	▲	▲	▲	▲	▲	▲	▲	▲	▲	▲	▲	▲	▲	▲	▲	▲
		850 hPa	▲	▲	▲	▲	▲	▲	▲	▲	▲	▲	▲	▲	▲	▲	▲	▲	▲	▲	▲	▲
		1000 hPa	▲	▲	▲	▲	▲	▲	▲	▲	▲	▲	▲	▲	▲	▲	▲	▲	▲	▲	▲	▲
	Wind	200 hPa	▲	▲	▲	▲	▲	▲	▲	▲	▲	▲	▲	▲	▲	▲	▲	▲	▲	▲	▲	▲
850 hPa		▲	▲	▲	▲	▲	▲	▲	▲	▲	▲	▲	▲	▲	▲	▲	▲	▲	▲	▲	▲	
Geopotential	100 hPa	▼	▼	▼	▼	▼	▼	▼	▼	▼	▼	▼	▼	▼	▼	▼	▼	▼	▼	▼	▼	
	500 hPa	▲	▲	▲	▲	▲	▲	▲	▲	▲	▲	▲	▲	▲	▲	▲	▲	▲	▲	▲	▲	
	850 hPa	▲	▲	▲	▲	▲	▲	▲	▲	▲	▲	▲	▲	▲	▲	▲	▲	▲	▲	▲	▲	
Extratropical Southern Hemisphere	10 m wind over ocean	▼	▼	▼	▼	▼	▼	▼	▼	▼	▼	▼	▼	▼	▼	▼	▼	▼	▼	▼	▼	
		▲	▲	▲	▲	▲	▲	▲	▲	▲	▲	▲	▲	▲	▲	▲	▲	▲	▲	▲	▲	
		▲	▲	▲	▲	▲	▲	▲	▲	▲	▲	▲	▲	▲	▲	▲	▲	▲	▲	▲	▲	
	Relative humidity	300 hPa	▲	▲	▲	▲	▲	▲	▲	▲	▲	▲	▲	▲	▲	▲	▲	▲	▲	▲	▲	▲
		700 hPa	▲	▲	▲	▲	▲	▲	▲	▲	▲	▲	▲	▲	▲	▲	▲	▲	▲	▲	▲	▲
	Temperature	100 hPa	▲	▲	▲	▲	▲	▲	▲	▲	▲	▲	▲	▲	▲	▲	▲	▲	▲	▲	▲	▲
		500 hPa	▲	▲	▲	▲	▲	▲	▲	▲	▲	▲	▲	▲	▲	▲	▲	▲	▲	▲	▲	▲
		850 hPa	▲	▲	▲	▲	▲	▲	▲	▲	▲	▲	▲	▲	▲	▲	▲	▲	▲	▲	▲	▲
		1000 hPa	▼	▼	▼	▼	▼	▼	▼	▼	▼	▼	▼	▼	▼	▼	▼	▼	▼	▼	▼	▼
	Wind	200 hPa	▼	▼	▼	▼	▼	▼	▼	▼	▼	▼	▼	▼	▼	▼	▼	▼	▼	▼	▼	▼
850 hPa		▲	▲	▲	▲	▲	▲	▲	▲	▲	▲	▲	▲	▲	▲	▲	▲	▲	▲	▲	▲	
Geopotential	100 hPa	▼	▼	▼	▼	▼	▼	▼	▼	▼	▼	▼	▼	▼	▼	▼	▼	▼	▼	▼	▼	
	500 hPa	▲	▲	▲	▲	▲	▲	▲	▲	▲	▲	▲	▲	▲	▲	▲	▲	▲	▲	▲	▲	
	850 hPa	▼	▼	▼	▼	▼	▼	▼	▼	▼	▼	▼	▼	▼	▼	▼	▼	▼	▼	▼	▼	
Tropics	10 m wind over ocean	▲	▲	▲	▲	▲	▲	▲	▲	▲	▲	▲	▲	▲	▲	▲	▲	▲	▲	▲	▲	
		▲	▲	▲	▲	▲	▲	▲	▲	▲	▲	▲	▲	▲	▲	▲	▲	▲	▲	▲	▲	
		▲	▲	▲	▲	▲	▲	▲	▲	▲	▲	▲	▲	▲	▲	▲	▲	▲	▲	▲	▲	
	Relative humidity	300 hPa	▲	▲	▲	▲	▲	▲	▲	▲	▲	▲	▲	▲	▲	▲	▲	▲	▲	▲	▲	▲
		700 hPa	▲	▲	▲	▲	▲	▲	▲	▲	▲	▲	▲	▲	▲	▲	▲	▲	▲	▲	▲	▲
	Temperature	100 hPa	▲	▲	▲	▲	▲	▲	▲	▲	▲	▲	▲	▲	▲	▲	▲	▲	▲	▲	▲	▲
		500 hPa	▲	▲	▲	▲	▲	▲	▲	▲	▲	▲	▲	▲	▲	▲	▲	▲	▲	▲	▲	▲
		850 hPa	▲	▲	▲	▲	▲	▲	▲	▲	▲	▲	▲	▲	▲	▲	▲	▲	▲	▲	▲	▲
		1000 hPa	▲	▲	▲	▲	▲	▲	▲	▲	▲	▲	▲	▲	▲	▲	▲	▲	▲	▲	▲	▲
	Wind	200 hPa	▲	▲	▲	▲	▲	▲	▲	▲	▲	▲	▲	▲	▲	▲	▲	▲	▲	▲	▲	▲
850 hPa		▲	▲	▲	▲	▲	▲	▲	▲	▲	▲	▲	▲	▲	▲	▲	▲	▲	▲	▲	▲	

Symbol legend: for a given forecast step...

- ▲ Cy40r1 better than Cy38r2 – statistically highly significant
- ▲ Cy40r1 better than Cy38r2 – statistically significant
- ▲ Cy40r1 better than Cy38r2 – not statistically significant
- ▲ Little difference between Cy40r1 and Cy38r2
- ▼ Cy40r1 worse than Cy38r2 – not statistically significant
- ▼ Cy40r1 worse than Cy38r2 – statistically significant
- ▼ Cy40r1 worse than Cy38r2 – statistically highly significant

**Summary score card for Cy40r1.** Score card for Cy40r1 versus Cy38r2 verified by the respective analyses at 00 and 12 UTC for 244 days in the period 6 February 2012 to 3 November 2013. Verification is also carried out against observations, but this is not shown. Thanks go to Martin Janousek for providing the figure.

are used over land and sea-ice from AMSU-A, AMSU-B and MHS as well as cloud-affected radiances over the ocean. The satellite radiance quality control includes model background error estimates derived from the EDA, a further step towards a more consistent use of the EDA in 4DVAR. In addition the estimation of observation errors and quality control for atmospheric motion vectors has been fundamentally improved.

The new cycle significantly improves the performance of HRES in the northern hemisphere, especially during autumn and winter, and it has a neutral to slightly negative impact in the southern hemisphere. The temperature and humidity forecasts are significantly improved in the lower troposphere in the tropics, while the 850 hPa winds are slightly degraded in certain tropical regions. The ENS probabilities are generally improved, except for a slight deterioration of tropical and southern hemisphere winds. The inclusion of the EDA-based land-surface temperature and moisture perturbations in ENS improves reliability, especially in the short range.

The diurnal cycle of convection is much improved (see *ECMWF Newsletter No. 136*, pages 15–22) so that the peak precipitation occurs later in the afternoon than in previous cycles. This is apparent in the associated forecast fields including convective indices (CAPE, CIN), precipitation and simulated satellite imagery. The 24-hourly precipitation totals are not significantly affected by the change in timing of the convection.

Changes to the vertical diffusion and sub-grid orography schemes improve the night time low level jets over land (e.g. important for wind energy applications) and significantly improves the large-scale circulation (hence the headline scores) in the northern hemisphere during winter time. The wind turning in the boundary-layer is slightly improved over land and ocean.

The snow analysis has been improved, while perturbations to snow cover in the ENS have a noticeable effect on 2-metre temperature spread. Cy40r1 has a statistically significant positive impact on the monthly forecast skill scores in the stratosphere due to the increased vertical resolution and on the prediction of the Madden-Julian Oscillation due to the ocean-coupling from day 0.

## Retirement of Jean-Jacques Morcrette

**ANTON BELJAARS,  
ANGELA BENEDETTI**

On the 31 December Jean-Jacques Morcrette retired as Principal Scientist on radiation modelling after 27 years of active research in the Physical Aspects and Chemical Aspects Sections of the Research Department at ECMWF.

Jean-Jacques made many contributions to the ECMWF forecasting system – only a few are listed here. Introduction of the ‘Morcrette scheme’ for radiation happened quite soon after he started at ECMWF and this, together with a new convection scheme, resulted in a complete overhaul of the physics package. Interestingly, he was also entrained in the convection work as he was asked to do an independent evaluation of two convection schemes. Comparison with observations to improve cloud optical properties, cloud overlap and surface albedo became a nearly continuous development cycle. He was one of the first to use a forward model allowing comparison with satellite data in radiance space. The work also included many technical developments such as:

- Computation of radiation at reduced spatial and temporal resolution to decrease costs.
- Migration of the physics package from the old spectral model to the new IFS.
- Initial steps towards the development of tangent linear and adjoint code for variational data assimilation.

The radiation work at ECMWF always kept strong links with the international research community, often through international projects which included:

- An inter-comparison of clouds and radiation between GCMs in artificial climate change experiments.
- Cloud/radiation inter-comparison organized by WGNE (Working Group on Numerical Experimentation).
- Model to satellite comparisons using, for example, ISCCP and ERBE.

As one of the lead authors in the IPCC Scientific Assessment in 1990, Jean-Jacques received a personalized certificate with a copy of the Nobel Peace Prize, which was awarded to the IPCC in 2007.

The international developments in



radiation modelling were followed very closely, and around 1990 Jean-Jacques felt that it was time to replace the Morcrette scheme by the more modern RRTM (Rapid Radiative Transfer Model) developed by Atmospheric and Environmental Research (AER, USA). This was a major technical and scientific challenge which was concluded with an operational implementation of the long wave part in June 2000 and the short wave part in 2007. The latter was combined with the introduction of the Monte Carlo Independent Column Approximation (McICA). The computationally efficient sampling of sub-grid columns in McICA provides the necessary flexibility to explore various aspects of sub-grid variability of which cloud overlap is the most obvious one.

More recently it was felt that aerosols contributed considerably to the uncertainty of clear sky radiation computations. Therefore, he was keen to join the GEMS and later the MACC and MACC-II projects to develop an aerosol modelling capability. The aerosol developments carried out by Jean-Jacques in the initial stages of GEMS led to the first aerosol forecast at ECMWF in 2007, and to the aerosol analysis in 2008. He then further refined the aerosol modules,

particularly the formulation of a key aerosol, desert dust. Those modules are still being used in the current near-real-time version of the MACC-II system. His contribution to the success of these projects has been invaluable. In parallel, he has also developed the capability to test the prognostic aerosol impacts on the radiation in IFS. It is hoped that this will contribute to improve the weather forecast in the medium and long ranges.

During the leaving party on 16 December, Erland Källén (Director of Research) thanked Jean-Jacques for his many contributions to the ECMWF modelling system and said: “He already had ideas for a new radiation scheme when joining ECMWF and implemented it successfully into a model cycle that markedly improved the forecast scores. A decade later he introduced another new radiation scheme, this time it came from outside ECMWF and Jean-Jacques was convinced that it was better than his own scheme. I think this is a very nice example of how scientists at ECMWF benefit from external scientific developments to maintain and develop the best forecasting system available in the world.”

As well as accomplished scientist, Jean-Jacques is known for his humanitarian and civil effort. In lieu of a retirement present, he asked that the money collected from ECMWF staff be donated to his favourite charity ‘Practical Action’. This is a charity that fights poverty in developing countries from the bottom up, with small scale projects. ECMWF will miss Jean-Jacques expertise and input to model developments. We wish him a very happy retirement.

### Career of Jean-Jacques before ECMWF

Jean-Jacques has a long career in research starting with a degree from the University of Lille on spectroscopy and radiative transfer. After his PhD he spent two years at Atmospheric Environment Service (later renamed as Meteorological Service of Canada) working on atmospheric corrections for lake temperature retrievals and on radiative transfer modelling for the Canadian General Circulation Model (GCM).

In 1980 he took up a CNRS position at the University of Lille where he developed narrow band models for long wave radiation based on line-by-line models and also wide band approximations for use in GCMs. The code developed at Lille would later become the basis of the so-called ‘Morcrette scheme’ in the ECMWF model. After spending another few years at NCAR in Boulder as visiting scientist working on cloud overlap and cloud heterogeneity, Jean-Jacques joined ECMWF in 1986.

## Handling hyperspectral infrared satellite observations

**TONY MCNALLY**

A workshop was held at ECMWF in November 2013 to bring together expertise in the area of handling hyperspectral infrared satellite observations. By making radiance measurements in many thousands of channels, instruments such as those from AIRS, IASI and CrIS provide comprehensive and highly-detailed information on the atmospheric state and composition. However, exploiting this wealth of information in an efficient manner – that meets the demands of real-time operational NWP and environmental prediction – presents significant scientific and technical challenges.

The workshop focussed on optimizing dissemination practices to allow data

compression with minimal information loss, as well as the development of novel data assimilation techniques that can efficiently convey this information to the analysis. Experts from Europe, the USA and Asia participated in the workshop, which was co-sponsored by the EUMETSAT NWP-SAF.

Two days of formal presentations were followed by highly-productive working group discussions which considered the following.

- **Compression for data dissemination:** possibilities for reducing the cost of disseminating high spectral resolution satellite data.
- **Compression and archiving:** if and how developments in data volume for real-time dissemination should impact the strategy and plans for archiving.

- **Compression for data assimilation:** options for exploiting data compression approaches for assimilation with a view towards communicating information from the observed spectrum to the analysis in an efficient a manner as possible.

Also consideration was given to the timing of key decisions affecting data dissemination strategy when planning future satellite programmes. The working group discussions resulted in a number of recommendations to space agencies and NWP centres, mapping out the way forward on this crucial topic. Presentations and working group discussions are documented at:

[http://www.ecmwf.int/newsevents/meetings/workshops/2013/NWP-SAF\\_satellite\\_observations/presentations/index.html](http://www.ecmwf.int/newsevents/meetings/workshops/2013/NWP-SAF_satellite_observations/presentations/index.html)

## MACC-II General Assembly

**VINCENT-HENRI PEUCH,  
RICHARD ENGELEN,  
REBECCA CALNAN**

The Third General Assembly of MACC-II and associated Open Science Conference took place from 27 to 30 January in Brussels, in the prestigious venue of the Royal Academies for Science and the Arts of Belgium.

Around 160 international participants gave a total of over 80 oral presentations on on-going research and development activities in MACC-II, as well as in a number of related international projects and initiatives concerned with analysing and predicting atmospheric composition. Ranging from specific science questions to consideration of market developments in applications areas such as solar energy, the topics covered at this event were extremely interesting and stimulating. ECMWF's contributions in particular were commented as very impressive, with few or no equivalents worldwide of

actual pre-operational services on atmospheric composition.

The activities in GEMS, MACC and MACC-II have allowed the structuring and organising of an active and healthy community which is significantly larger than the one constituted by the teams directly funded by these

projects. This is a very important element at the time of transitioning to Copernicus, as operational and developmental activities will effectively be rooted in the wider pool of European and international research on atmospheric composition (in-situ and satellite data, modelling, assimilation etc.).



**General Assembly of MACC-II held at the Royal Academies for Science and the Arts of Belgium.** The General Assembly and Open Science Conference consisted of three sessions that focused on (a) specific events and forecasting (e.g. large fires, dust outbreaks, volcanic eruptions and air pollution episodes), (b) retrospective analyses, hind-casts and studies spanning a season or more, and (c) applications such as solar radiation.

# Use and development of Meteorological Operational Systems

**ERIK ANDERSSON,  
STEPHAN SIEMEN,  
ALFRED HOFSTADLER**

The 14<sup>th</sup> biennial Workshop on Meteorological Operational Systems was held at ECMWF from 18 to 20 November 2013. The workshop focused on how to transition developments in research into operational products and services. There was also a session on operational data management and visualisation along with an exhibition where current meteorological data processing and visualisation systems were showcased.

A summary of the key points raised in the discussion sessions is provided in the following.

## From research to operations

As forecasting systems become more realistic there is a tendency for them to also become technically more complex. Consequently, the associated development and change processes become more difficult to manage because of the increased versatility of the operational systems and high user expectations of the services.

The NWP centres present at the

workshop manage between one and four major research-to-operations (R2O) transitions of their forecasting systems per year, though the frequency of upgrades tends to reduce the more complex the forecasting systems become. A 'big bang approach' is nevertheless preferred to many small, incremental changes in order to avoid inconsistencies. Extensive validation is required for each upgrade; validation tests are typically carried out for summer and winter seasons complemented with some tests for spring or autumn. Some NWP centres maintain a catalogue of severe weather cases and these form part of their test plans. Hurricane forecasting centres apply a three-year testing period.

The responsibility for pre-operational testing variously lies with research, operations or a transition unit, or a combination of these. In any case, it is very useful to maintain common test systems (test beds) that can be shared between departments and external user groups to help avoid duplication of effort during testing and validation. Common tools for verification and model diagnostics are required.

Potential problems with the R2O

transition can be mitigated by a well-defined work flow and clear distribution of responsibilities. NWP centres deploy 'science advisory boards' or 'NWP coordination groups' to oversee the change process. Some centres provide early access for forecasters to pre-operational products for validation, whereas others run a continuous test suite alongside their operations for evaluation by forecasters.

If something goes wrong, in spite of extensive testing and verification, it is often unfeasible to roll back a major forecasting system upgrade; too many downstream applications are linked to the change. Strategies to make changes less danger prone include data blending which reduces dependency on the output of only one forecasting system.

## How structured or informal can the transition process be?

It was noted that the handover process from research to operations varies significantly between NWP centres and it depends on organisational structure. There is often a very structured process for model evaluation, but downstream applications are not always tested as rigorously, and are not defined in



**Participants in the 14<sup>th</sup> Workshop on Meteorological Operational Systems.** The workshop was attended by 58 participants from Meteorological Services, the World Meteorological Organization (WMO), the United Nations World Food Programme (WFP), research institutions and commercial weather services coming from 25 countries worldwide.



detail. Emergency changes are possible (if small and fully understood) but larger ones are resisted; it is considered better to correct during post-processing, or document and explain any deficiency to the forecast users.

### Collaboration between research and operations

To maintain a fast upgrade cycle, it is essential that researchers are able to run quasi-operational versions of the forecasting systems. Also, to engage with external researchers and academia, development testbed centres are created (e.g. the Data Assimilation Research Testbed at NCAR and OpenIFS at ECMWF). These require a common code base, best practice documentation and modularity with practical support provided by a Developer Committee (or similar).

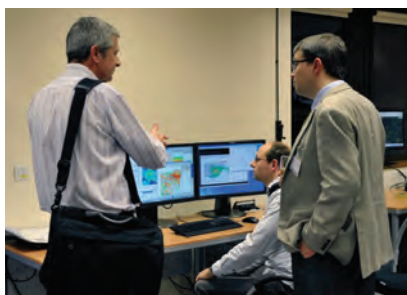
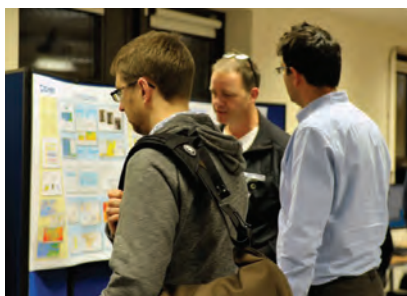
Common verification and diagnostics tools are required for use in research and operations, with well-defined, relevant performance indicators by which the value of new developments can be measured.

### How are HPC resources shared between research and operations?

NWP centres typically devote between 20% and 30% of their high-performance computing (HPC) resources to operations, including pre-operational testing. The peak usage for operational production is however much higher at certain times of day. Many centres use two identical HPC clusters, one for operations and one for research, filling the gaps in the production schedule with research work. In the USA, researchers generally have major resources available on remote (third-party) HPC sites. Their experimental developments can sometimes not be implemented in operations because of insufficient HPC in the operational centre at peak times.

### Visualisation systems

Traditional workstations (Metview, Metcap+, PVA, VisualWeather, Synergie-Next), web based



**Exhibition and poster displays at the workshop.** Informal discussions linked to the exhibition and poster displays played a key role in the success of the workshop.

visualisation (ecCharts, GeoServer) and toolsets (Iris, Metview Macro) were demonstrated. There is a clear trend to make use of more Open Source software in development, such as GIS software packages (proj4) and Python (used as 'glue' rather than for large-scale implementation).

Three-dimensional visualisation has proven to be useful for researchers and important for the diagnostics and understanding of high-impact cases. So far, it is considered less important in the operational forecasting environment.

### Open geospatial consortium (OGC) standards

OGC standards are used for discovery, retrieve and visualise data, and it is satisfying that the meteorological community has been willing to adopt these standards, though there is still a space for bespoke standards. However, it is very important to influence the development of OGC standards to make them more applicable for the meteorological community. If this does not happen, there is the danger that bespoke extensions endanger

interoperability. That is why the MetOcean DWG (Meteorology & Oceanography Domain Working Group) needs support to ensure that OGC standards and profiles allow the meteorological community to develop effective interoperability for web services and content across the wider geospatial domain. During the workshop some possible work priorities for the MetOcean DWG were identified.

### Challenges and opportunities

In the final plenary session it was concluded that in Europe the two main drivers for operational NWP are the establishment of Climate Change Services and new developments in services for the aviation sector. In more general terms the challenges and opportunities discussed at the workshop are:

- Visualising, communicating and standardizing the concept of ensembles, particularly to draw the attention to the risk of events with high impact but low confidence – making ensemble-based products mainstream.
- Communicating with people that do not have meteorological background with emphasis on communicating in terms of impact on people and their activities.
- Engaging researchers in operational forecasting issues.
- Exploiting further the value of re-forecasts and the development of calibration for point-wise (local) forecasts.
- Realizing the potential of (a) international standards to brake our domain-specific habits, (b) the WMO Information System (WIS), (c) open data policy and (d) 'Volunteer Distributed Computing'.

The workshop organisers wish to thank all the speakers, presenters and participants for the contributions to the successful workshop. Presentations are available at:

<http://www.ecmwf.int/newsevents/meetings/workshops/2013/MOS14/>

## ERA-Interim monitors the global warmth of 2013

### ADRIAN SIMMONS

The annual WMO Statement on the status of the climate includes a discussion of the global-mean surface temperature anomaly based primarily on three well-established datasets: those produced by the Met Office's Hadley Centre in collaboration with the Climatic Research Unit of the University of East Anglia (currently the HadCRUT4 version) and by two US institutions, the NASA Goddard Institute for Space Studies (GISS) and the NOAA National Climatic Data Center (NCDC). These datasets are based on analysis of monthly-mean climatological air-temperature reports from land stations and observations of sea-surface temperature. In recent years, the WMO Statement has also taken note of estimates of surface air temperature provided by the ERA-Interim reanalysis that ECMWF initiated in 2006 and updates on a daily basis. Values for a wider set of variables from both ERA-Interim and MACC (Monitoring Atmospheric Composition and Climate) analyses are in addition provided for the annual State of the Climate article published in the Bulletin of the American Meteorological Society.

Readers of two news releases issued on 21 January would have encountered the definitive opening statements "The globally averaged temperature for 2013 tied as the fourth warmest year since record keeping began in 1880, according to NOAA scientists" and "NASA scientists say 2013 tied with 2009 and 2006 for the seventh warmest year since 1880 ...". Digging deeper, readers may have found text that explains that these rankings are sensitive to how data are processed. Indeed the GISS data subsequently made available for downloading puts 2013 in sixth place, due to inclusion of a small amount of late-arriving observational data in an updated analysis.

ERA-Interim adds something different to the mix. Its analysis of temperature at two-metre height is based on synoptic air-temperature observations and its use of background-forecast values from its full four-dimensional

	ERA-Interim	GISS	Hadley Centre	NCDC
1998	0.20 (4=)	0.20 (4=)	0.24 (3)	0.21 (3)
1999	-0.04 (18)	-0.01 (17=)	0.02 (17)	0.04 (16)
2000	-0.02 (17)	-0.01 (17=)	0.01 (18=)	0.01 (18)
2001	0.14 (9=)	0.11 (12)	0.15 (12)	0.13 (12)
2002	0.18 (7=)	0.20 (4=)	0.21 (5=)	0.19 (6)
2003	0.18 (7=)	0.19 (6=)	0.22 (4)	0.20 (4=)
2004	0.10 (11)	0.10 (13)	0.16 (11)	0.16 (10)
2005	0.30 (1)	0.24 (2)	0.26 (1=)	0.23 (2)
2006	0.25 (3)	0.18 (8=)	0.21 (5=)	0.18 (7=)
2007	0.19 (6)	0.21 (3)	0.20 (7=)	0.17 (9)
2008	0.04 (12=)	0.07 (14)	0.10 (14=)	0.09 (15)
2009	0.18 (7=)	0.18 (8=)	0.20 (7=)	0.18 (7=)
2010	0.26 (2)	0.25 (1)	0.26 (1=)	0.24 (1)
2011	0.14 (9=)	0.13 (11)	0.12 (13)	0.11 (13)
2012	0.17 (8)	0.16 (10)	0.17 (10)	0.15 (11)
2013	0.20 (4=)	0.19 (6=)	0.20 (7=)	0.20 (4=)

**Annual global surface temperature anomalies.** Shown are the anomalies (K) relative to 1981–2010 along with the rankings in brackets, with 1 denoting the warmest year. These results indicate that 2005 and 2010 are the warmest two years on record. See the text for more discussion of these results.

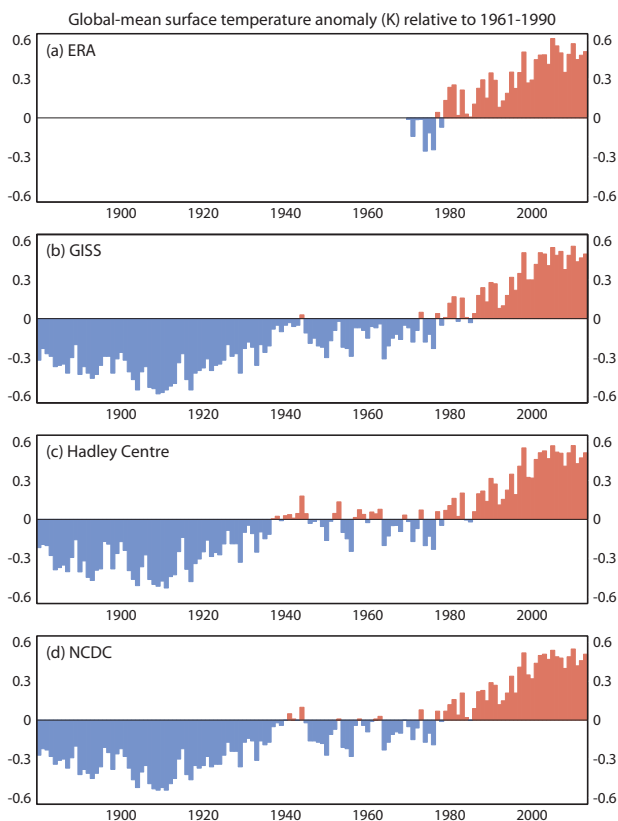
variational analysis provides geographically complete coverage, including high northern latitudes where warming has been strongest over recent decades. The background forecast brings information from the previously assimilated data from the full observing system, including satellite observations of upper-air temperature and land-surface conditions. There is, nevertheless, more uncertainty in ERA-Interim values over areas where synoptic data are sparse, and there are also some issues of temporal homogeneity. More striking though, is the overall level of agreement among the datasets.

The table shows the anomalies from 1998 onwards, the warmest period on record. The range among the ERA-Interim, GISS, Hadley Centre and NCDC datasets is as large as 0.08 K in 1999 and as small as 0.01 K in 2013. The full HadCRUT4 product comprises an ensemble of 100 realisations. The median is used here; the two-standard-deviation uncertainty value is around 0.08 K for this period. The two years when ERA-Interim is substantially warmer than the other analyses are 2005 and 2006, both of which are characterized by relatively warm ERA-Interim values at high northern latitudes. High-latitude anomalies are cold in 1999.

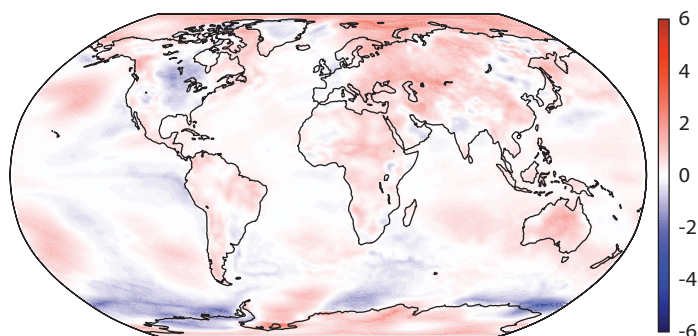
The table also ranks the years for their warmth, for each dataset. Overall, the evidence points to 2005 and 2010 as being the warmest two years on record, with the strong El Niño year of 1998 most likely third, but not clearly distinguishable from a set of six other years (2002, 2003, 2006, 2007, 2009 and 2013), with 2012 being the year that most probably occupies tenth position.

The extent of the disagreement among the datasets is small compared with the variability and net change they depict over multiple decades. This is evident from the first figure, in which the ERA values from 1970 onwards are based on ERA-40 up to 1978 and ERA-Interim thereafter. Values back to 1880 are shown for the other three datasets. Discussions of several features of these graphs can be found in the contribution of Working Group I to the Fifth Assessment Report of the Intergovernmental Panel on Climate Change.

The second figure presents the ERA-Interim temperature anomaly for 2013 in map form. Warmth is evident over many continental areas and at high latitudes, with the average over Australia the warmest on record. Below-average annual values over north-western Europe are a reminder of an unusually cold spring, and



**Annual global surface temperature anomalies.** Shown are the anomalies (K) relative to 1961–1990 for (a) ERA, (b) GISS, (c) Hadley Centre and (d) NCDC. All data are computed first as anomalies relative to the common period of 1981–2010, and then expressed as anomalies relative to 1961–1990 by subtracting the average for 1961–1990 of the GISS, Hadley Centre and NCDC values. The ERA values, based on ERA-40 up to 1978 and ERA-Interim thereafter, are complete global means; for the other datasets the averages do not cover the entire globe as each analysis has to a greater or lesser extent gaps due to sparsity of near-surface data coverage. See the contribution of Working Group I to the Fifth Assessment Report of the Intergovernmental Panel on Climate Change for more discussion of features of these time series.



**Surface air temperature anomaly.** Shown is the anomaly (K) for 2013 relative to 1981–2010, from ERA-Interim. The distribution of the anomaly is discussed in the text.

cold values over the central USA and Canada occurred in both spring and the closing months of the year, and continued into 2014. Cold values over Greenland are indicative of a more widespread cold anomaly at high northern latitudes in the middle troposphere; the warm near-surface anomaly that occurs over lower-lying high-latitude regions is a shallow one. Cold values around Antarctica and between Greenland and Svalbard are likely linked to anomalies in sea-ice cover. Here it should be cautioned that changes in the sea-ice analysis over the course of ERA-Interim have introduced some artefacts. Likewise, changes in source of sea-surface-

temperature analysis have caused ERA-Interim surface-air temperatures over sea to be a little cooler than they would otherwise have been since 2001. Such issues will be addressed in the replacement reanalysis for ERA-Interim, production of which is expected to begin this year. This may, however, introduce a discrepancy between the reanalysis and the other datasets compared here, as the global average from the reanalysis is expected to be warmer in recent years when a consistent sea-surface-temperature analysis is used. More information can be found at the following web links.

- [http://library.wmo.int/opac/index.php?lvl=notice\\_display&id=14750](http://library.wmo.int/opac/index.php?lvl=notice_display&id=14750)
- <http://www.giss.nasa.gov/research/news/20140121/>
- [http://data.giss.nasa.gov/gistemp/updates\\_v3/](http://data.giss.nasa.gov/gistemp/updates_v3/)
- <http://www.metoffice.gov.uk/hadobs/hadcrut4/>
- <http://www.ncdc.noaa.gov/news/ncdc-releases-2013-global-climate-report>
- <http://www.ipcc.ch/report/ar5/wg1>
- [http://www.bom.gov.au/announcements/media\\_releases/ho/20140103.shtml](http://www.bom.gov.au/announcements/media_releases/ho/20140103.shtml)
- <http://dx.doi.org/10.1002/qj.2317>

# Parameter estimation and inverse modelling for atmospheric composition

**RICHARD ENGELEN**

Under the umbrella of the EU-funded projects GEMS, MACC, and MACC-II, ECMWF has extended its data assimilation and forecasting system to include atmospheric composition. Analyses and forecasts of reactive gases, greenhouse gases, and aerosol are now routinely provided on a daily basis. At the same time the EU-funded GEOLAND and GEOLAND2 projects have extended the ECMWF land surface model to include a simple representation of the carbon cycle. As part of the European Copernicus framework it is envisaged that this atmospheric composition data assimilation and forecasting system will become fully operational to provide daily global forecasts complementing ECMWF's meteorological forecasts.

The modelling and data assimilation of atmospheric composition differs in several ways from the modelling and data assimilation for numerical weather prediction, such as the atmospheric chemistry and the available observations. However, another important aspect is the significance of the boundary conditions. Anthropogenic emissions, greenhouse gas surface fluxes, wild fire emissions, and volcanic eruptions form a significant part of the assimilation and forecasting problem, which can therefore not really be treated as an initial condition problem with a (almost) perfect model. Current practice is to prescribe these boundary conditions based on emission

inventories, off-line carbon flux models, off-line fire detection systems, and ad-hoc definition of volcanic emissions. However, for a future operational forecasting system better solutions should be found in order to minimize the model error.

ECMWF organised a workshop on parameter estimation and inverse modelling for atmospheric composition from 22 to 24 October 2013. The aim of the workshop was to explore the options to optimally define the boundary conditions in a near-real-time data assimilation system. The first day and a half was spent with very interesting presentations from mostly external experts providing different angles on the challenge of constraining boundary conditions for atmospheric composition in an NWP environment.

After the presentations, two working groups were formed to discuss in more detail the various aspects, focussing on surface modelling and parameter estimation on the one hand, and constraining emissions from volcanoes, fires, and anthropogenic sources on the other hand. Several recommendations were then presented in the final plenary. Among others this included:

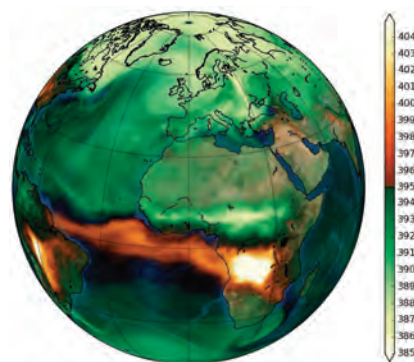
- Improved modelling of emissions to provide better a priori for parameter estimation (e.g. diurnal cycles for anthropogenic emissions and fire emissions).
- Better coordination in the WMO context of greenhouse gas in-situ observations.

- Exploration of the use of Ensemble Data Assimilation for atmospheric composition to better propagate background errors.

All participants, internal and external, left with enough food for further thought after an inspiring 2½ days. Presentations are available at:

[http://www.ecmwf.int/newsevents/meetings/workshops/2013/Parameter\\_estimation/presentations/index.html](http://www.ecmwf.int/newsevents/meetings/workshops/2013/Parameter_estimation/presentations/index.html)

Column-averaged dry-air mole fraction of CO<sub>2</sub> (ppm)  
1 September 2013



**Carbon dioxide concentrations as modelled by the MACC-II system.** Lower concentrations reflecting mainly the impact of photosynthesis are shown in green, while higher concentrations reflecting the impact of respiration and emissions are shown in brown. An animated version of the image is available from:

[http://www.copernicus-atmosphere.eu/pressroom/CO2\\_animation\\_Sep2013.gif](http://www.copernicus-atmosphere.eu/pressroom/CO2_animation_Sep2013.gif)

## Update on the new website

During 2012/2013, ECMWF has been undertaking a significant redesign of its website. We expect to release this new web site during the first quarter of 2014. This update will result in changes to all aspects of our external website including the forecast charts. The first beta release is planned for February 2014. The current website is expected to remain for one further year but its text content will be frozen – forecast charts will continue to be updated.

For more information about the new website go to:

<https://software.ecmwf.int/wiki/display/NWEB/>



## ECMWF's contribution to GEO

### BOB RIDDAWAY

ECMWF had a strong presence at the Tenth Plenary Session of the Group on Earth Observations (GEO-X) and the 2014 GEO Ministerial Summit which took place in Geneva from 15 to 17 January 2014.

ECMWF's stand in the exhibition attracted many visitors every day – some who did not know anything about ECMWF though others had many interesting and relevant questions about ECMWF's work in relation to GEO. Also, as part of the side events, presentations were given on:

- Monitoring the Climate – Jean-Noël Thépaut
- MACC-II and Copernicus Atmosphere Service – Vincent-Henri Peuch
- Benefits of TIGGE weather forecast data for the GEOSS community – Florian Pappenberger

In addition, Jean-Noël Thépaut gave an interview to RTS (Radio Television Suisse) about "La terre sous surveillance" which was broadcast in a programme called "CQFD". It is available in French at:

<http://www.rts.ch/audio/la-1ere/programmes/cqfd/5498499-la-terre-sous-surveillance-16-01-2014.html>.



**GEO-X and the Ministerial Summit.** About 700 delegates attended GEO-X and the Ministerial Summit representing over 50 countries and more than 45 organisations, including ECMWF.

The ECMWF stand concentrated on four major projects that it either leads or to which it is a major contributor: MACC-II, ERA-CLIM2, EFAS and TIGGE.

- MACC-II (Monitoring Atmospheric Composition and Climate - Interim Implementation) is the current pre-operational Copernicus Atmosphere Service which provides data records on atmospheric composition for recent years, data for monitoring present conditions and forecasts of the distribution of key constituents for a few days ahead. It is funded by the European Union under the 7th Framework Programme (2011–2014).
- ERA-CLIM2 aims to develop extended climate reanalyses of the coupled Earth system, including atmosphere, land surface, ocean, sea-ice and the carbon cycle. It is funded by the European Union under the 7th Framework Programme (2014–2016).
- EFAS (European Flood Awareness System) uses forecasts from a number of NWP models to drive a hydrological model to create an ensemble of real-time predicted hydrographs that can be used to provide probabilistic flood forecasts. It is funded by Copernicus (2012–2015).

### Group on Earth Observations (GEO)

The Group on Earth Observations (GEO) is a partnership of governments and international organizations that provides a framework within which these partners can develop new projects and coordinate their strategies and investments aimed at building a Global Earth Observation System of Systems (GEOSS).

GEO's Members include 90 Governments, including the European Commission. In addition, 77 intergovernmental, international, and regional organizations with a mandate in Earth observation or related issues have been recognized as Participating Organizations. ECMWF has been a Participating Organization in GEO since the initiative was started in 2003.

- TIGGE (THORPEX Interactive Grand Global Ensemble) provides a research archive of ensemble forecast data from ten global weather prediction centres from 2006 onwards, along with TIGGE LAM (Limited Area Model) which is an extension of the archive.

The Ministerial Summit was held on the last day of the event. Alan Thorpe, ECMWF Director General, joined the ECMWF team staffing the stand. High profile stakeholders visited the stand and this led to discussions about many important topics including how to build the case for on-going investment in weather predictions and satellite missions. As might be expected, given the flooding in January in the UK, there was interest in the power of medium-range weather forecasts for flood forecasting and monthly to seasonal predictions. The Summit ended up with Ministers endorsing another ten years of GEO.

It was a very positive week which increased awareness of ECMWF and its leading role in numerical weather prediction and associated international meteorological activities.

## New items on the ECMWF website

### *4<sup>th</sup> Meeting of the Global Flood Working Group*

With more population and economic asset at risk, governments, banks, international development and relief agencies, and private firms are investing in flood reduction measures. However, in many countries, the flood risk is not managed optimally because of lack of scientific data and methods or a communication gap between science and risk managers. The 4<sup>th</sup> meeting of the Global Flood Working Group will be hosted by ECMWF on 4 to 6 March 2014.

[http://www.ecmwf.int/newsevents/meetings/workshops/2014/Global\\_Flood\\_WG/](http://www.ecmwf.int/newsevents/meetings/workshops/2014/Global_Flood_WG/)

### *Workshop on High Performance Computing*

Every second year ECMWF hosts a workshop on the use of high performance computing. The 16<sup>th</sup> ECMWF Workshop on High Performance Computing in Meteorology will be held from 27 to 31 October 2014.

[http://www.ecmwf.int/newsevents/meetings/workshops/2014/high\\_performance\\_computing\\_16th/](http://www.ecmwf.int/newsevents/meetings/workshops/2014/high_performance_computing_16th/)

### *WISE Meeting (Waves In Shallow water Environment)*

The WISE meeting is a yearly gathering of ocean wave modellers. It is a continuation of the successful WAM (Wave Model)-group collaboration, which produced the WAM model in the 1980s. This model has been running operationally at ECMWF since 1992.

[http://www.ecmwf.int/newsevents/meetings/workshops/2014/WISE\\_Meeting/](http://www.ecmwf.int/newsevents/meetings/workshops/2014/WISE_Meeting/)

### *ECMWF/EUMETSAT ROM-SAF Workshop on Applications of GPS Radio Occultation Measurements*

This workshop, jointly organized by ECMWF and the EUMETSAT Radio Occultation Meteorology Satellite Application Facility (ROM-SAF), will review the use of the GPS radio occultation (GPS-RO) data at the major NWP centres, and explore how the assimilation of the measurements can be improved using more sophisticated observation operators. The workshop will be held from 16 to 18 June 2014.

[http://www.ecmwf.int/newsevents/meetings/workshops/2014/GPS\\_Radio\\_Occultation/](http://www.ecmwf.int/newsevents/meetings/workshops/2014/GPS_Radio_Occultation/)

### *H-SAF and HEPEX Workshops on Coupled Hydrology*

The EUMETSAT Satellite Application Facility (SAF) that supports operational hydrology and water management (H-SAF) aims to develop and deliver operational satellite-derived products of precipitation, snow and soil moisture as well as continuous validation of these products. Also the mission of HEPEX (Hydrological Ensemble Prediction Experiment) is to demonstrate the added value of hydrological ensemble predictions for emergency management and water resources sectors. Combined H-SAF and HEPEX workshops on coupled hydrology will be held from 3 to 6 November (H-SAF) and 5 to 7 November (HEPEX).

[http://www.ecmwf.int/newsevents/meetings/workshops/2014/H-SAF\\_HEPEX/](http://www.ecmwf.int/newsevents/meetings/workshops/2014/H-SAF_HEPEX/)

## Applying for Special Projects

### ----- **UMBERTO MODIGLIANI**

Each year users within one of ECMWF's Member States may apply for computing resources as a 'Special Project'. These are experiments or investigations of a scientific or technical nature, undertaken by one of more Member States, likely to be of interest to the general scientific community. Information about the current Special Projects is available from:

[http://www.ecmwf.int/about/special\\_projects/index.html](http://www.ecmwf.int/about/special_projects/index.html)

If you wish to begin work on a Special Project in 2014, an application form should be completed and sent to ECMWF via the Director of the appropriate National Meteorological Service. In addition, European organisations with which ECMWF has concluded Co-operation Agreements may apply for resources for a Special Project, with such a request to be considered by the Director-General of ECMWF. The application form is available from:

[http://www.ecmwf.int/computer\\_access\\_registration/forms/Special\\_Projects.html](http://www.ecmwf.int/computer_access_registration/forms/Special_Projects.html)

In this case you will be eligible to receive resources from the 20% of Special Project allocations set aside for applications received during the year. The total allocation in this 'reserve' for 2014 is.

- HPCF: 104 million units
- Data Storage: 2008 terabytes

The deadline to apply for resources for a project to start in 2015 is 30 June 2014. An estimate of the resources available in 2015 will be published on the ECMWF website in May 2014.

# Ten years of ENVISAT data at ECMWF

ROSSANA DRAGANI, SALEH ABDALLA,  
RICHARD ENGELEN, ANTJE INNESS, JEAN-NOËL THÉPAUT

On 8 April 2012 the European Space Agency (ESA) suddenly lost communication with ENVISAT (ENVironmental SATellite) after just over ten years in space. The satellite, launched in February 2002, carried ten instruments to provide continuous observation of the Earth's land, atmosphere, oceans and ice caps from a sun-synchronous orbit at about 800 km altitude (see Table 1 for a full list of the ENVISAT payload).

During its ten years of operations, ENVISAT continually delivered high-quality data to a large user community including ECMWF, where data from seven instruments (out of a payload of ten) was routinely received, monitored and validated. The data from ENVISAT has supported Earth-science research and monitoring of the evolution of environmental and climate changes, as well as development of operational and commercial applications.

This article provides an overview of the contribution of the ENVISAT observations to various components of the ECMWF assimilation and forecasting suite that form part of the Integrated Forecasting System (IFS) – see Box A. The aim is to highlight the way in which ECMWF has exploited data from a research satellite within a Numerical Weather Prediction (NWP) system, and discuss the lessons learnt from a fruitful collaboration with ESA. Furthermore, an outlook on future usage of these valuable data is also presented.

Instrument	Extended name
ASAR	Advanced Synthetic Aperture Radar
GOMOS	Global Ozone Monitoring by Occultation of Stars
MERIS	Medium Resolution Imaging Spectrometer
MIPAS	Michelson Interferometer for Passive Atmospheric Sounding
MWR	MicroWave Radiometer
RA-2	Radar Altimeter 2
SCIAMACHY	Scanning Imaging Absorption Spectrometer for Atmospheric Cartography
AATSR	Advanced Along Track Scanning Radiometer
DORIS	Doppler Orbitography and Radiopositioning Integrated by Satellite
LRR	Laser Retro-Reflector

**Table 1** List of the ENVISAT payload. The top seven ENVISAT instruments were received at and monitored by ECMWF.

A thorough discussion of the activities and lessons learnt from ten years of ENVISAT observations at ECMWF can be found in *Dragani et al.* (2014).

## Data usage and data monitoring

### ENVISAT data usage

Contracted by ESA, ECMWF was involved in the daily monitoring and assimilation of a variety of products from several instruments on board ENVISAT during its ten-year lifetime. Annual summary reports of can be found at <http://www.ecmwf.int/publications/library/do/references/list/18/>.

These activities were performed routinely using the Observation Monitoring Facility, a robust tool developed at ECMWF to provide statistics about how different observations available in the ECMWF system compare with their model equivalent (i.e. the modelled field that simulates the observed parameter). These statistics, updated twice a day, allow ECMWF to provide timely feedback to the data providers when there are events such as data anomalies and loss of performance.

Whenever possible, observations of proven high quality that positively impacted on ECMWF's high-resolution forecast (HRES) were also assimilated in the parallel applications: ERA (reanalysis activities) and MACC (Monitoring Atmospheric Composition and Climate).

Figure 1 summarises the data usage timeline of all the ENVISAT observation types received at ECMWF across the HRES, ERA and MACC applications. In contrast to all the

## The ECMWF system and its applications

A

The ECMWF Integrated Forecasting System (IFS) is a comprehensive system simulating the dynamics, thermodynamics and composition of the Earth's atmosphere and interacting parts of the Earth-system. It includes three forecasting components: a global spectral atmospheric model, an ocean wave model and an ocean model that simulates the ocean circulation and sea ice.

Several ECMWF applications are based on the IFS.

- The core high-resolution forecast (hereafter HRES).
- The environmental atmospheric monitoring and forecasting suite, initiated and recently developed under the FP-7 project Monitoring Atmospheric Composition and Climate, precursor of the future Copernicus Atmosphere service (hereafter MACC).
- The climate reanalysis activities, which are contributing to the development of a European climate monitoring infrastructure (hereafter ERA).

All these applications have heavily relied on and taken full advantage of high-quality information provided by the ENVISAT observations.

other retrieved parameters and owing to its unavailability in near-real time, the SCIAMACHY methane data was mainly used for monitoring purposes in a delayed-mode at ECMWF. It was also used for direct flux inversions in combination with surface flask observations by one of the MACC partners.

In addition to the data usage depicted in Figure 1, it is worth mentioning that:

- ENVISAT derived sea-level data has been assimilated in the ocean reanalysis that provides initial conditions for the operational monthly and seasonal forecasting systems.
- Although never operationally implemented, the assimilation of the MIPAS limb radiances was also tested using both the full spectral resolution radiances in 2004 and the reduced spectral resolution channels in 2009. Both attempts showed that the direct assimilation of limb radiances could be used to provide temperature, humidity and ozone information in the upper troposphere-lower mesosphere region, without significantly degrading the fit to other observations.

The ENVISAT observations have continuously been delivered by ESA in near-real time with a generally good timeliness to guarantee that between 85% and 95% of the data (depending on the instrument) arrived on time to be ingested in the assimilation for the HRES.

Ten years of data monitoring revealed that the ENVISAT data has been stable during the satellite's lifetime and with good long-term consistency. Some changes in the level of agreement between the ENVISAT data and the model equivalent were observed over the years, but in most cases they were the consequences of either upgrades to the IFS model or changes to the retrieval algorithm.

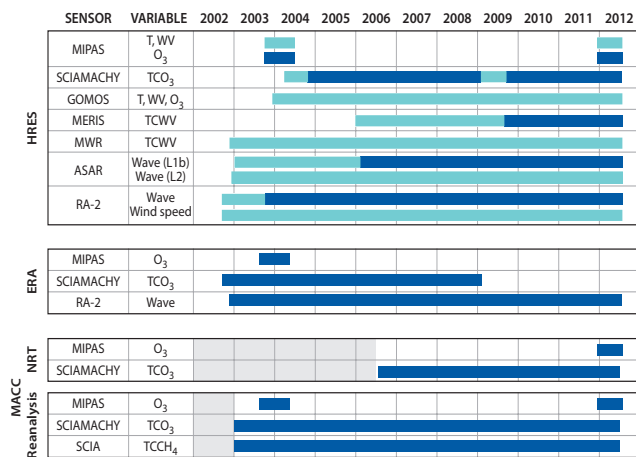


**Figure 1** Data usage across three applications of the ECMWF model, namely the HRES, the ERA-Interim reanalysis, and the MACC near-real-time (NRT) products and reanalysis. The blue bars indicate periods during which their corresponding variables were actively assimilated; the green bars indicate periods during which their corresponding variables were monitored. The MACC system was available in near-real time only from July 2006; whilst the MACC reanalysis was run from January 2003 onwards. Periods during the ENVISAT lifetime for which the MACC applications are not available are shaded in grey.

*Feedback to data producers*

The collaboration between ESA (the data producer) and ECMWF (the operational data user) has produced substantial benefits to both. On one hand, the operational data user contributes to the calibration and validation activities by:

- Monitoring the performance of all the data received in near-real time.
- Detecting anomalies in the data.
- Providing timely feedbacks to the data producer (e.g. in case of anomalies).
- Assessing the impact of changes in the data processing chains.
- Providing support to new instrument assessments.

On the other hand, the availability of long data records allows the operational data users to (a) monitor their own model performance and changes, and (b) take full advantage of observations with sufficiently high quality to positively impact the corresponding forecasts and analyses through data assimilation.

Figure 2 presents an example of time series of the standard deviation of the difference in significant wave height between the radar altimeter data (RA-2) and the model equivalent. This observation–model comparison clearly shows that the introduction of a new version of the RA-2 processing chain (February 2010) resulted in a slight degradation of the wave data quality – this information was fed back to ESA. At the same time, the model improvements affecting the HRES produced the steady and continuous reduction of the standard deviation as shown in the figure.

In some cases, the collaboration between data producer and data user can also lead to improvements in the retrieval algorithms, as in the case of the RA-2 wind speed retrieval algorithm. Such an algorithm was fine-tuned by ECMWF using collocations between RA-2 and model data over two months, and then extensively verified for a numbers of altimeters against ECMWF model and buoy observations. Verifications after the implementation showed a better performance in terms of wind speed retrieval and a 5% reduction in the scatter index (*Abdalla, 2012*).

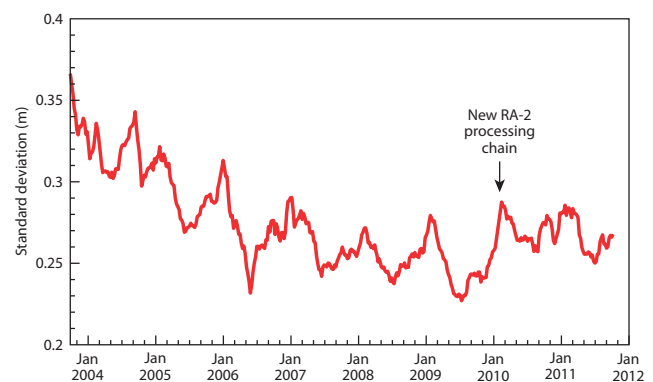


**Figure 2** Time series of the standard deviation of the difference between RA-2 and the model departures of significant wave height.



### Impact of ENVISAT data on NWP

During the satellite lifetime, ECMWF regularly assessed the impact of the assimilated ENVISAT data on the quality of its analyses and forecasts. The assimilation of the MERIS total column water vapour, discussed in detail by Bauer (2009), showed a small impact on the corresponding analyses and forecasts (still visible in the day-3 forecasts) in regions where the total amount was below 30 kg/m<sup>2</sup>.

Two selected examples are discussed here, one for wave data and one for ozone. Both studies were run for the period December 2011 to March 2012, although only the period January to March is discussed here so that the results are not affected by spin-up issues.

#### Impact of wave data

To assess the value of the RA-2 and ASAR wave observations, the impact of adding ENVISAT wave information to a baseline configuration was assessed for one instrument at a time. The following experiments were run.

- *Exp/Base*. A baseline experiment that used neither the RA-2 significant wave height data nor the ASAR level 1b radiances.
- *Exp/RA2*. *Exp/Base* plus the assimilation of the RA-2 wave data.
- *Exp/ASAR*. *Exp/Base* plus the assimilation of ASAR radiances.

For both instruments, the results suggest a statistically significant positive impact on the ECMWF analyses and forecasts.

Figure 3 shows the reduction in tropical random error against in-situ data as function of the forecast day. This random error reduction is computed as the relative difference between the standard deviation of the residual between the model and in-situ wave values for *Exp/Base* and that of either *Exp/RA2* or *Exp/ASAR*, both of which benefitted from the assimilation of the ENVISAT data. Positive values mean that *Exp/Base* exhibits larger model random error than either *Exp/RA2* or *Exp/ASAR*. Results are presented for the significant wave height (SWH) and the peak wave period (PWP).

Figure 3 shows that both observing system leads to a reduction of the model random error in the tropics of the significant wave height. This reduction is largest at the analysis time (8% in the case of RA-2 and 4% for ASAR) and shows a persistence of up to day 5 of the forecast for both sets of data. A similar but somewhat less persistent impact was found in the extra-tropics, where the assimilation of the ENVISAT wave data could lead to a reduction of the model random error visible up to day 2.

Additionally, the assimilation of wave information has a positive impact on the characterisation of other wave parameters. Figure 3 shows that the peak wave period error is reduced with a change at analysis time that can be as high as 6%.

#### Impact of ozone data

To assess the impact of the ENVISAT ozone products,

two denial experiments were run at reduced horizontal resolution of T511 with 91 levels referred to as follows.

- *Exp/Ctrl*. Control experiment that used all observations assimilated for the HRES, including the ENVISAT ozone data.
- *Exp/NoO3*. Like *Exp/Ctrl* after withdrawing the SCIAMACHY and MIPAS ozone observations.

The results from the assessment of withdrawing the ENVISAT ozone information from the HRES showed a statistically significant negative impact on the ECMWF ozone field, and only a limited impact on the main meteorological variables (e.g. temperature and wind).

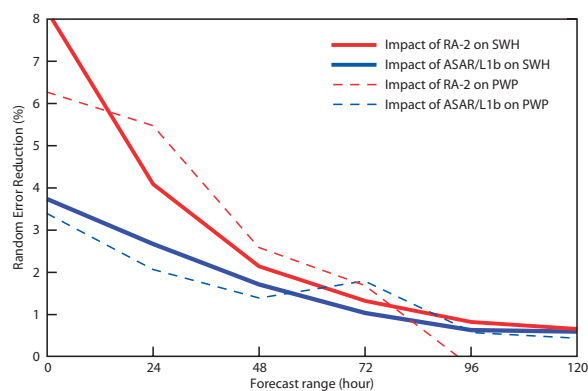


**Figure 3** Random error reduction (%) in the tropics against buoys as function of the forecast day and computed for either *Exp/ASAR* or *Exp/RA2* with respect to *Exp/Base* during the period 1 January to 31 March 2012. The impact is shown for significant wave height (SWH) and the peak wave period (PWP).

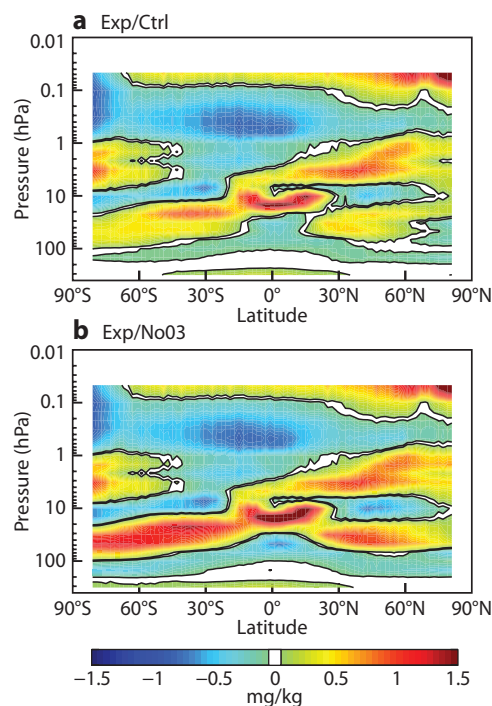


**Figure 4** Mean difference between the MLS ozone profiles (v2.2) and the co-located ozone analyses computed for (a) *Exp/Ctrl* and (b) *Exp/NoO3* averaged over January to March 2012.

This is because the ozone-radiation coupling and the coupling through the 4DVAR data assimilation scheme are not currently exploited in the IFS, although ozone is included in the radiative transfer model used to assimilate the radiances.

Figure 4 shows the comparisons of the ozone analyses from Exp/Ctrl (top panel) and Exp/NoO3 (bottom panel) with the reprocessed Aura Microwave Limb Sounder (MLS) ozone retrievals given in terms of their zonally-averaged temporal mean difference. These results indicate that the loss of ENVISAT ozone data substantially degraded the mean ozone state, particularly in the stratosphere between 10 and 100 hPa. This degradation is also confirmed by comparisons of the ozone analyses with the ozone sonde profiles from the World Ozone and Ultraviolet Radiation Data Centre.

**Ozone impact across different applications**

The loss of the ENVISAT products has led to degraded analyses and forecasts across the various ECMWF applications, but – as one would expect – the actual impact strongly depended on the particular observing system used. For instance, a pair of experiments equivalent to Exp/Ctrl and Exp/NoO3 was also run using the MACC system. As the MACC ozone analyses benefitted from the assimilation of MLS ozone profiles, the results of the study only showed a marginal impact from the loss of ENVISAT ozone products.

It is, however, interesting to assess the impact of several data sources, including those from ENVISAT, on the skill that the ozone analyses have in fitting independent observations (e.g. in-situ measurements, across different IFS applications). An example is presented in Figure 5 for the Neumayer station in Antarctica where the Common Area Fraction (CAF) score – an indicator of how well the analysis profile fits the observation profile – is computed for the HRES and MACC ozone analyses for the period 2010–2012. A CAF value of one means a perfect fit.

Three periods can be identified in Figure 5.

- *January 2010 to November 2011.* The MACC system performed better than the HRES. That is because the MACC assimilated the height-resolved MLS ozone profiles on top of ozone products retrieved from ultra-violet sensors that were also used for the HRES.
- *November 2011 to April 2012.* The two ozone analyses show similar skill. The combination of the assimilation of ozone-sensitive radiances in the infrared (introduced in HRES in November 2011) and the MIPAS ozone profiles (introduced in both systems on 8 December) produced a substantial improvement in the high-resolution ozone analyses.
- *April 2012 onwards.* After the loss of MIPAS, both systems show a slightly degraded agreement with the ozone sondes. This reduced performance is more visible in the high-resolution analyses than in those from MACC. This is particularly evident from June onwards with the start of the southern hemisphere winter period where limited constraint is provided by ozone observations retrieved from ultra-violet sensors due to the lack of sunlight.

Two conclusions can be drawn from these results. The first one concerns the obvious reduction in performance of the HRES with respect to MACC following the loss of ENVISAT data: in terms of the CAF score, this is approximately 5%. The second concerns the impact of the ozone-sensitive radiances in the infrared: it is argued that, although this data improved the high-resolution ozone analyses and their corresponding CAF score (of about 10% compared with the same period of 2011), having their vertical sensitivity limited to the upper troposphere–lower stratosphere (*Dragani & McNally, 2013*) means this radiance data cannot provide a constraint as strong as that of MLS.

**The second life of ENVISAT**

Although the ENVISAT mission officially ended in 2012, its observations are expected to continue and contribute to our understanding of the Earth system and its evolution for many years to come thanks to the on-going reprocessing activity. Such an activity will deliver more consistent data than has been available so far in near-real time.

The need for reprocessing satellite data arises from the main requirements to:

- Improve the quality of the satellite products by implementing the up-to-date algorithms and format over the whole life of the product.
- Produce a long, consistent data record suitable for climate studies.

The long-term consistency and homogeneity is a constant preoccupation in the production of any data record. Operational near-real-time products cannot fulfil this requirement due to the frequent algorithm updates implemented to either improve their products or solve problems. For example, Figure 6 shows the time series of difference in significant wave height between two RA-2 products (the operational near-real-time product and the newly reprocessed dataset) and the reanalysis equivalent using ERA-Interim. The processor that was used for the reprocessing was also used operationally since 1 February 2010 when the difference between the two timeseries became marginal. On one hand, it is clear that the

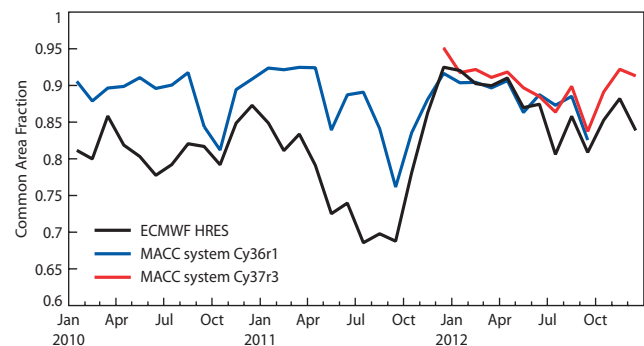


**Figure 5** Time series of the common area fraction (CAF) score for ozone analyses computed for the Neumayer station (8.25°W, 70.65°S) in the Antarctic for three streams: high-resolution ozone analysis and two versions of the MACC ozone analysis (Cy36r1 and Cy37r3). A CAF value of one means a perfect fit.

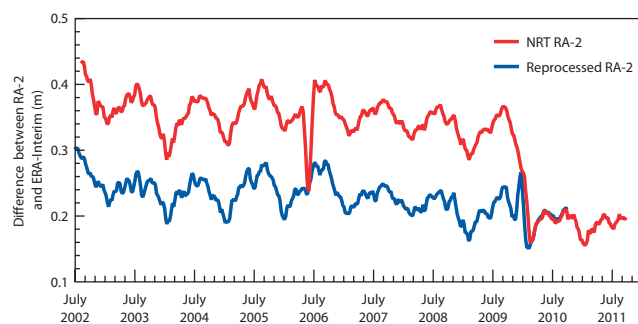


**Figure 6** Time series of the difference between RA-2 and ERA-Interim for significant wave height computed for two sets of RA-2 data: the operational near-real-time (NRT) RA-2 data and version 2.1 reprocessed RA-2 data.

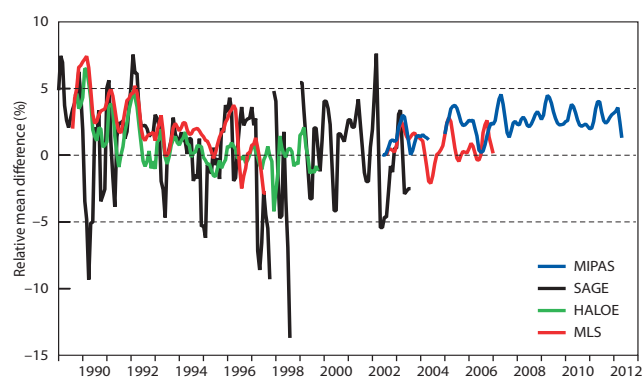


**Figure 7** Relative mean difference at 10 hPa in the tropics between the ERA-Interim ozone analyses and reprocessed ozone data from the MIPAS, SAGE, HALOE and MLS instruments (computed as  $100 \times (\text{Observations} - \text{Analysis}) / \text{Observations}$ ). The period runs from January 1989 to December 2012. The two dotted lines indicate where the relative differences are within  $\pm 5\%$ . The plot is an adaptation of Figure 5 (panel d) presented by Dragani (2011).

implementation of the new algorithm in the near-real-time stream produced an improved data set, but on the other hand it also led to an artificial jump in its data record.

Motivated by this, ESA has embarked upon a substantial reprocessing activity of all its observations using the latest available algorithms to produce long records of consistent data products. This activity started before the end of the ENVISAT mission, and has been successfully concluded for most instruments at the time of writing. Different applications and studies can benefit from these reprocessed datasets.

On their own, thanks to its ten-year lifetime, the ENVISAT data records provide a unique opportunity to perform short-term and decadal variability analysis studies. Furthermore, they will also provide an invaluable contribution to forthcoming reanalysis productions (e.g. the one that will replace ERA-Interim planned to start in 2014). In preparation for this future reanalysis, an initial pre-assessment of the value of these reprocessed data records has already been performed at ECMWF using the ERA-Interim reanalyses (Figure 7). The results of this assessment show that the MIPAS ozone profiles are in very good agreement with the ERA-Interim co-located reanalyses.

Moreover, the ERA-Interim residuals from MIPAS also exhibit a very good long-term agreement with those from several other instruments. This result, together with those from the denial assimilation presented above, pave the way for the assimilation of the MIPAS reprocessed ozone profiles in future reanalyses.

Although the reprocessed satellite data record from a given instrument is not long enough to perform climate analysis, there is an on-going effort in both Europe and the USA to merge observations of the same variable derived from different instruments in one consistent and homogeneous dataset. Although this is not possible for all variables, in some cases data records spanning most of the satellite era can be achieved.

These activities are important as such homogeneous and consistent data records can be used to study climate variability and perform trend analysis. Furthermore, the merging procedure can provide useful information about the offsets between different instruments (inter-instrumental biases), which can also be valuable in undertakings such as a reanalysis when the original, unmerged records are assimilated. Moreover, these activities also feed into a number of climate research projects: they help improve our current understanding of how, how much and possibly why the climate system has evolved to its current state. This understanding, in particular identifying the cause(s) of these changes, gives a scientific underpinning for predicting future climate. It is recognised that satellite data play a major role in all these activities.

In this context, ESA has launched the Climate Change Initiative that aims at providing satellite-based climate data records of essential climate variables that fulfil the requirements – set by the Global Climate Observing System (GCOS) – for satellite data to be useful in climate studies. These satellite-based climate data records will strongly rely on ENVISAT observations. ECMWF's involvement in the assessment of these essential climate variables ensures the continuation of the collaboration with ESA.

Alongside ESA, reprocessing work is also carried out by EUMETSAT through its various Satellite Application Facilities. In addition, in the USA, NOAA has initiated a Climate Data Record Program aimed at long-term data preservation.

#### FURTHER READINGS

- Abdalla, S.**, 2012: Ku-band radar altimeter surface wind speed algorithm. *Mar. Geod.*, **35**, 276–298.
- Bauer, P.**, 2009: 4D-Var Assimilation of MERIS Total Column Water Vapour retrievals over land. *Q. J. R. Meteorol. Soc.*, **135**, 1852–1862.
- Dragani, R.**, 2011: On the quality of the ERA-Interim ozone reanalyses: Comparisons with satellite ozone data. *Q. J. R. Meteorol. Soc.*, **137**, 1312–1326.
- Dragani, R., S. Abdalla, R.J. Engelen, A. Inness & J.-N. Thépaut**, 2014: Ten years of ENVISAT observations at ECMWF: a review of activities and lessons learnt. *Q. J. R. Meteorol. Soc.*, under review.
- Dragani, R & A.P. McNally**, 2013: Operational assimilation of ozone-sensitive infrared radiances at ECMWF. *Q. J. R. Meteorol. Soc.*, DOI 10.1002/qj.2106.

# Have ECMWF monthly forecasts been improving?

FRÉDÉRIC VITART, FRANCO MOLteni,  
ROBERTO BUIZZA

Monthly forecasts (32-day forecasts) have been produced routinely at ECMWF since March 2002, and operationally since October 2004. In the current configuration, the monthly forecasts are generated by extending the 15-day ensemble integrations to 32 days twice a week (at 00 UTC on Mondays and Thursdays). Forecasts are based on the medium-range/monthly ensemble forecast (ENS) which is part of ECMWF's Integrated Forecasting System. ENS includes 51 members run with a horizontal resolution of T639 (about 32 km) up to forecast day 10, and T319 (about 65 km) thereafter. Initial perturbations are generated using a combination of singular vectors and perturbations generated using the ECMWF ensemble of data assimilations, and model uncertainties are simulated using two stochastic schemes.

The climatology (re-forecasts) used to calibrate the real-time forecasts is computed using the re-forecast suite that includes only 5 members of 32-day integrations with the same configuration as the real-time forecasts, starting on the same day and month as the real-time forecast over the past 20 years. The re-forecasts are created a couple of weeks before the corresponding real-time forecast. This strategy for re-forecasts is different to the one used for seasonal forecasting where the model version is frozen for a few years and the re-forecasts are created only once.

An extract of the results published in a recent article (Vitart, 2013) is presented hereafter. They document that, on average, the skill of monthly forecasts for weeks 2 to 4 has significantly improved over the past decade.

## Monthly forecast skill: how do we measure it?

The skill of the monthly forecasts is routinely evaluated by scoring the 51-member real-time forecasts, mainly against analyses, using a range of measures. For instance, Figure 1 shows skill scores of 2-metre temperature anomalies based on all the real-time forecasts since October 2004, when the monthly forecasts became operational. The skill score is the area under the Relative Operating Characteristic (ROC), which is a measure of the capability of the monthly forecasts to discriminate between occurrence and non-occurrence of events (in this case the event is '2-metre temperature anomaly above the upper tercile of the climatological distribution'). With this measure 1 indicates a perfect forecast and 0 a forecast with the same skill as climatology.

Figure 1 shows a drop of skill with increased time range as expected. For the 12–18 day forecast, the ROC area exceeds 0.7 over large portions of the northern extra-tropics. One week later (i.e. the 19–25 day forecast), the northern extra-tropics still display some skill in predicting 2-metre temperature anomalies, but the highest skills scores are in the tropics. At days 26–32, the skill in the northern extra-tropics is low, although larger than climatology, while in the tropics the skill is still positive. An issue with this type of verification is that it mixes forecasts which have been produced using different versions of the IFS since 2004.

A methodology for evaluating the evolution of the monthly forecast skill scores over the past 10 years could be to compute the skill scores of the real-time forecasts for each season or each year. Figure 2 shows an example of the evolution of the ROC area of 2-metre temperature for days 12–18 since winter 2004. It can be seen that the forecasts at this time range consistently outperform persistence of the previous week's forecast (i.e. using the forecast for days 5–11). However, a major issue with this methodology is that

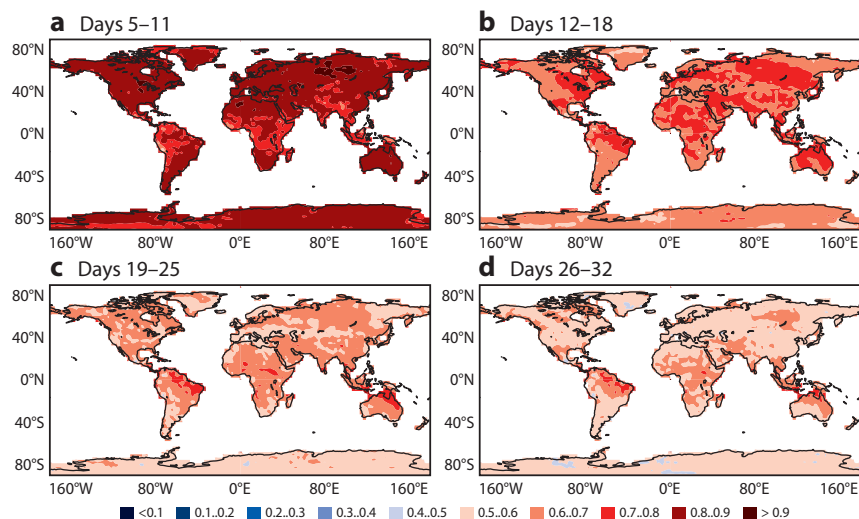


**Figure 1** Area under the Relative Operating Characteristic (ROC) curve for the probabilistic prediction of 2-metre temperature anomalies in the upper tercile for weekly periods: (a) days 5–11, (b) days 12–18, (c) days 19–25 and (d) days 26–32. This plot has been produced using all the real-time monthly forecasts since October 2004.

the monthly forecast skill scores are strongly dependant on the large-scale circulation that was predominant during a season. For instance, Figure 2 shows that the skill of the monthly forecasts has decreased since winter 2009–2010. However, the winter 2009–2010 was exceptionally predictable (e.g. *Jung et al., 2011*) with a persistent strong negative North Atlantic Oscillation (NAO) pattern. It is likely that the higher skill score in 2010 is due to this exceptional condition rather than to a degradation in the model performance after 2010. Low frequency variability associated with El Niño Southern Oscillation (ENSO) events can also impact the skill scores for the extended-range forecasts in the tropics and extra-tropics. This makes it difficult to identify trends from a time series of skill scores of real-time forecasts.

Another option for assessing the evolution of the monthly forecast skill scores based on the monthly re-forecasts is discussed in details in the next section.

**Methodology for assessing the evolution of the skill scores in the re-forecasts**

As shown in Figure 3, the number of re-forecast years has been changing since 2002, but all the re-forecasts since 2002 have the period 1995–2001 in common. The starting days of the re-forecasts may vary from one year to another, but this should not have a significant impact on the skill scores averaged over a complete year or a season. The scores can be compared for re-forecasts covering the same years and seasons: i.e. all the re-forecasts from 1995 to 2001 that were produced each year between April of a given year until March of the following year. For instance, the scores of 2006 will refer to the scores of all the re-forecasts from 1995 to 2001 that were produced between April 2006 and March 2007 (4 April, 11 April, 18 April.....27 March 1995–2001) using the IFS versions that were operational between April 2006 and March 2007.

Please note that averages have been computed over a period starting from April to March of the following year

to ensure a consistency in the model versions used for a complete winter and a complete summer.

As mentioned above, an advantage of this methodology is that it ensures that all the re-forecasts cover the same seasons and years. There are however two weaknesses of this approach that is worth mentioning – these are associated with differences in ensemble size and changes to the model. For more detail see Box A.

Despite weaknesses in the methodology, the approach taken provides a valuable assessment of the time evolution of monthly forecasts' scores for various aspects of the ECMWF monthly forecasts, as will be shown.

**Evolution of average skill over the northern extra-tropics**

The classical ranked probability skill score (RPSS) is a measure of the degree to which a forecast outperforms a reference forecast, in this case climatology. However, a disadvantage of the RPSS is its strong negative bias for

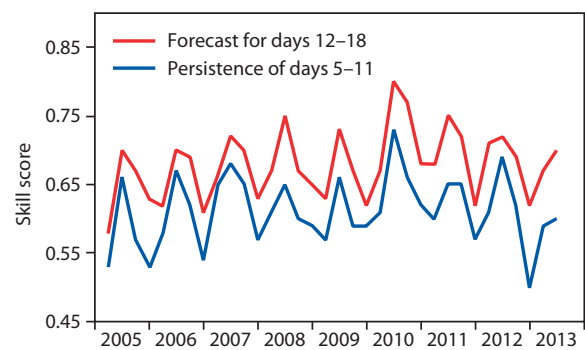


**Figure 2** Evolution of the skill scores of the real-time forecast and the corresponding persistence forecast based on probabilities of the previous week. The skill score is the area under the Relative Operating Characteristic (ROC) curve for the probabilistic prediction of 2-metre temperature anomalies in the upper tercile over the northern extra-tropics (north of 30°N) calculated for each season since winter 2004.

	March 2002	October 2004	February 2006	March 2008	January 2010	November 2011	June 2012
<b>Frequency</b>	Every 2 weeks	Once a week				Twice a week*	
<b>Horizontal resolution</b>	100 km days 0-32			50 km days 0-10 80 km days 10-32	30 km days 0-20 60 km days 10-32		
<b>Vertical resolution</b>	40 levels Top at 10 hPa		62 levels Top at 5 hPa				
<b>Ocean/Atmosphere coupling</b>	Every hour from day 0			Every 3 hours from day 10			
<b>Re-forecast period</b>	Past 12 years			Past 18 years		Past 20 years	
<b>Re-forecast size</b>	5 members						
<b>Initial conditions</b>	ERA-40			ERA-Interim			

\* Only for real-time forecasts. The frequency of re-forecasts is still once a week.

**Figure 3** Evolution of the main changes in the ECMWF monthly re-forecasts since 2002.

**Weaknesses of the methodology used to assess changes in skill scores with time**

A

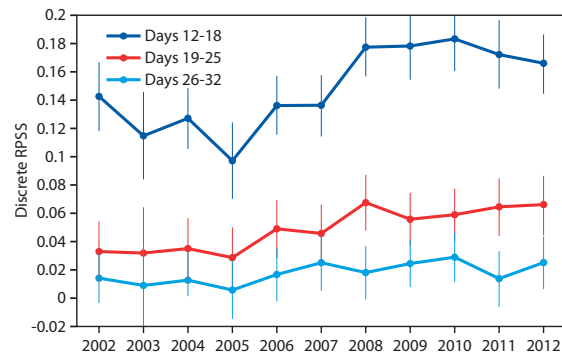
Firstly, the ensemble size of the re-forecasts is limited to only 5 members instead of 51 members for the real-time forecasts. This can be an issue when considering probabilistic forecasts of rare events for which skill scores are very sensitive to ensemble size. *Weigel et al. (2008)* faced the same issue when they scored the ECMWF re-forecasts produced in 2006 and used a correction of the probabilistic skill score which takes into account the ensemble size. It is worth noting that this is less an issue for the present study than that carried out by *Weigel et al.* because the goal here is to assess the evolution of the monthly forecast skill scores during the period 2002–2012 rather than evaluate the skill of the monthly forecasting system.

Secondly, the model may have changed more than once during the period that has been used to compute the skill scores. This makes the attribution of the variation of skill scores to a specific change in the model physics more difficult. An alternative would be to run a large set of re-forecasts covering the same period with the various versions of the IFS model. But this is too expensive to be done systematically and impossible to be done for old versions of IFS which are no longer supported in the current ECMWF operating systems. Apart from the change of the reanalysis from ERA-40 to ERA-Interim in March 2008, all the re-forecasts have been initialised from the same dataset. Therefore this verification will not take into account possible improvements due to changes in the ECMWF data assimilation from 2002 to 2012.

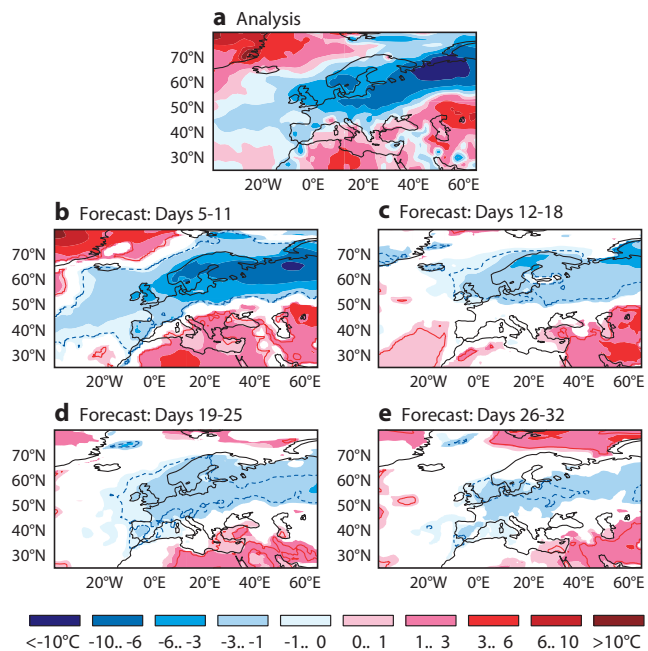
small ensemble size. Therefore, a de-biased version of the RPSS, the so-called discrete ranked probability skill score (*Weigel et al., 2008*), has been used to assess the skill evolution of the re-forecasts of 2-metre temperature anomalies produced since 2002. This measure has the advantage of being insensitive to the unreliability due to small ensemble sizes.

Figure 4 displays the evolution of the discrete RPSS of 2-metre weekly-average temperature anomalies since 2002, for three forecast weekly periods: days 12–18, days 19–25 and days 26–32. Though there is a drop in the probabilistic skill score between days 12–18 and days 19–25, the monthly forecasts still display better skill than climatology (positive RPSS). These results also suggests that there have been improvements in the RPSS scores of 2-metre temperature anomaly re-forecasts over the northern extra-tropics for all three time ranges (days 12–18, days 19–25 and days 26–32) since 2002. The values of the discrete RPSS for days 26–32, although still very low, are now close to the values for the previous week (days 19–25) re-forecasts that were produced in 2002. The skill scores of days 19–25 have also improved in time almost linearly and get close to the skill scores of days 12–18 in the early years of the ECMWF monthly forecasts.

According to Figure 4, the forecasts for weeks 3 and 4 are now more skilful than 10 years ago and therefore



**Figure 4** Evolution of the discrete ranked probability skill score (RPSS) of 2-metre temperature weekly mean anomalies over the northern extra-tropics (north of 30°N) since 2002 for days 12–18, days 19–25 and days 26–32. Only land points have been scored. The RPSS has been computed from terciles and for all the ECMWF re-forecasts for the extended boreal winter (October to March).



**Figure 5** Weekly mean 2-metre temperature anomaly ensemble mean forecasts verifying on the 18–24 March 2013 for the time ranges days 5–11, days 12–18, days 19–25 and days 26–32. The top panel shows the verification computed from ERA-Interim.

the current monthly forecasts are more likely to produce useful early warnings of cold or heat waves. For instance, Figure 5 shows the prediction at various time ranges of 2-metre temperature anomalies during the cold wave over Europe in March 2013. It is impressive that the 32-day ensemble forecasts predicted cold anomalies over Europe three weeks in advance. Figure 6 shows an example of prediction of a summer heat wave in Southern Europe.

**Evolution of the predictive skill of the Madden-Julian Oscillation (MJO)**

The Madden-Julian oscillation (MJO) is a main source of predictability in the tropics on time scales exceeding one

week but less than a season (Madden & Julian, 1971). It is characterised by an eastward propagation of convective rainfall from the Indian Ocean to the western Pacific.

For convenience the MJO has been split into eight phases starting with enhanced rainfall over the western Indian Ocean which moves slowly eastwards across the Indian Ocean (phases 2 and 3). The rainfall then crosses the ‘maritime continent’ of Indonesia and surrounding countries (phases 4 and 5) and arrives in the western Pacific before dying out in the central Pacific (phases 6 and 7). The MJO then continues its eastward propagation in the upper atmosphere over the western hemisphere and Africa (phases 8 and 1). Typically an MJO event lasts between 30 and 60 days.

The Wheeler and Hendon index (WHI, see Wheeler & Hendon, 2004) has been applied to all the model re-forecasts and to ERA-Interim over the period 1995–2001 to evaluate the skill of the monthly forecasting system in predicting MJO events and to produce composites for the eight phases of the MJO.

Principal Component Analysis is a method of identifying the characteristic spatial patterns of data set by a much smaller number of ‘new’ variables. It identifies the underlying structure of the data and extracts the principal components that account for most of the variation in the data. For the MJO the two principle components (PC1 and PC2) are such that:

- Enhanced convection occurs over the maritime continent when PC1 is positive and over the western hemisphere and Africa when PC1 is negative.
- Enhanced convection occurs over the Pacific Ocean when PC2 is positive and over the Indian Ocean when PC2 is negative.

To evaluate the skill of the monthly forecasting system to predict the MJO, a linear bivariate correlation is performed between the time series of PC1 and PC2 from the forecast

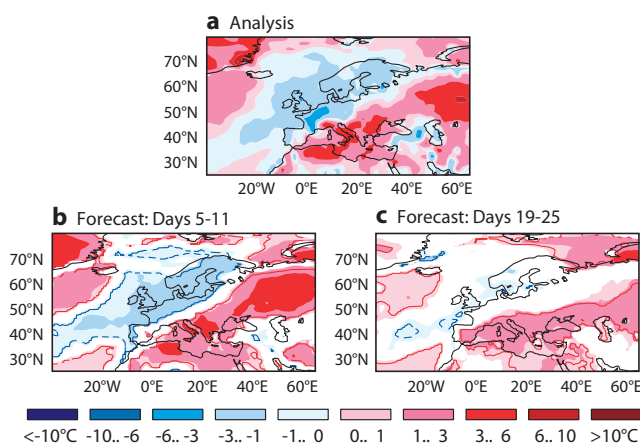


**Figure 6** Weekly mean 2-metre temperature anomaly ensemble mean forecasts verifying on the 9–15 July 2012 (top panel) for the time ranges days 5–11, days 12–18, days 19–25 and days 26–32. The top panel shows the verification computed from ERA-Interim.

ensemble-mean time series for different lead times and the corresponding time series computed from ERA-Interim.

Figure 7 shows the evolution of the MJO bivariate correlation skill score from 2002 until 2012 between the ensemble mean re-forecasts and ERA-Interim. In this figure, the three lines show the forecast day in which the bivariate correlation reached 0.5, 0.6 and 0.8. If we consider the MJO bivariate correlation of 0.6 as a limit of MJO prediction skill, the ECMWF monthly forecasting system displayed skill to predict the MJO up to about 15 days in 2002. In 2012, the limit of 0.6 was reached around day 25, suggesting an averaged gain of about 1 day of lead-time per year. The bivariate correlation of 0.5 is now reached beyond day 30 instead of day 22 in 2002. For the bivariate correlation of 0.8, the gain has been of about 5 days over the 10-year period. The difference of MJO skill scores between 2002 and 2012 is statistically significant for the three thresholds (bivariate correlations of 0.5, 0.6 and 0.8) within the 5% level of confidence.

The evolution of the amplitude error of the MJO, calculated from each individual ensemble member and then averaged, does not display an improvement as regular as for the forecast skill scores. According to Figure 8, forecasts produced a too weak MJO in the early years of the monthly forecasting system, with the amplitude about 30% too low beyond forecast day 20. There has been a clear improvement between 2006 and 2008. In 2008, when Cy32r3 was used operationally, the MJO was even slightly too strong. Since 2008, the amplitude of the MJO displays a trend towards weaker MJOs, with amplitudes in the recent years only about 10% weaker than in the ERA-Interim analyses.

Using reanalysis data, Cassou (2008) showed that there is a link between the MJO and North Atlantic Oscillation (NAO). The probability of a positive phase of the NAO (i.e. the

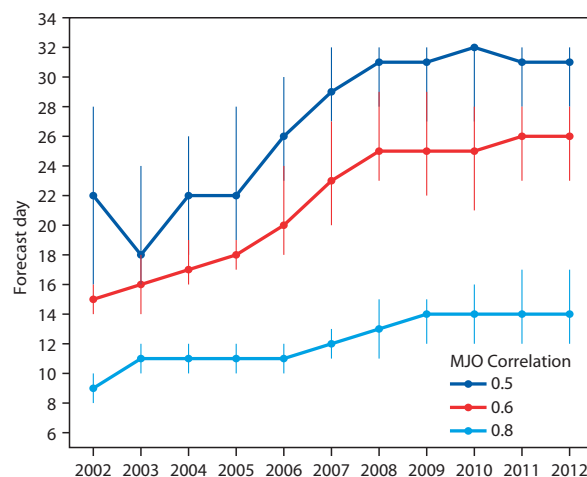


**Figure 7** Evolution of the MJO skill scores (bivariate correlations applied to the WHI) since 2002 as indicated by the days when the MJO bivariate correlation reaches 0.5, 0.6 and 0.8. The MJO skill scores have been computed on the ensemble mean of the ECMWF re-forecasts produced during a complete year. The vertical bars represent the 95% confidence interval computed using a 10,000 bootstrap re-sampling procedure.

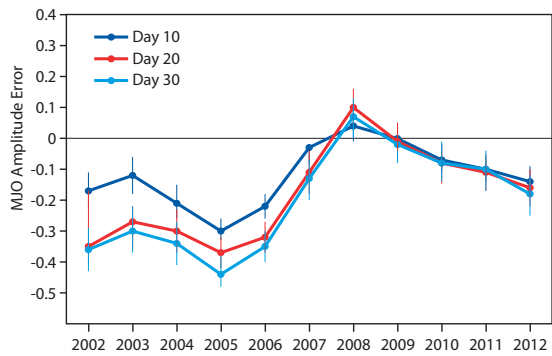


**Figure 8** Amplitude error of the re-forecasts relative to the mean MJO amplitude obtained from ERA-Interim analyses. Negative (positive) numbers in the top panel indicate that the MJO simulated by IFS is weaker (stronger) than in the ECMWF reanalysis. The vertical bars represent the 95% confidence interval computed using a 10,000 bootstrap re-sampling procedure.

difference of atmospheric pressure at sea level between the Icelandic low and the Azores high) is significantly increased about 10 days after the MJO is in Phase 3 (Phase 3 + 10 days), and significantly decreased about 10 days after the MJO is in Phase 6 (Phase 6 + 10 days). The probability of a negative phase of the NAO is decreased (increased) about 10 days after the MJO is in Phase 3 (Phase 6).

Let us now focus on evaluating whether the MJO teleconnections on the northern extra-tropics have improved by comparing the re-forecasts produced each year from 2002 until 2012 with ERA-Interim. This is based on the 500 hPa geopotential height composites 10 days after an MJO in Phase 3 with an amplitude larger than a standard deviation. Only the re-forecasts covering the extended boreal winter season are considered (from October to March).

According to Figure 9, the MJO teleconnections (10 days after an MJO in Phase 3) are more realistic over the northern extra-tropics in 2011 (middle panel) than in 2002 (left panel) compared to ERA-Interim (right panel). The re-forecasts produced in 2011 simulate a stronger

positive NAO anomaly than in 2002. However, the impact of the MJO on the NAO is still underestimated in the 2011 re-forecasts compared to ERA-Interim. On the other hand, the ECMWF forecasting system overestimates the positive 500 hPa geopotential anomaly over the northern Pacific. The same conclusions are valid for the composites of 500 hPa geopotential height 10 days after an MJO in Phase 6 (not shown). The improved MJO teleconnections are likely to impact the monthly forecast skill scores in the northern extra-tropics, and in particular the skill of the model to predict the NAO.

**Evolution of the predictive skill of the North Atlantic Oscillation (NAO)**

The prediction of the NAO is of particular importance for the prediction of European weather. An NAO index has been constructed by projecting the daily 500 hPa height anomalies over the northern hemisphere onto a pre-defined NAO pattern based on an EOF (Empirical Orthogonal Function) analysis – a technique used to study possible spatial patterns of variability and how they change with time. The NAO pattern was defined as the first leading mode of EOF applied to the reanalysis of monthly mean 500 hPa height during the 1950–2000 period produced by NCEP (National Centers for Environmental Prediction). NAO skill scores have been produced for each year from 2002 until 2012 by applying the NAO index to the re-forecasts and to ERA-Interim, and by computing the linear correlation between the ensemble-mean re-forecasts and ERA-Interim.

Let us focus on extended winter cases (from October to March). Figure 10 shows that there has been improvement in the prediction of the daily values of the NAO with a gain of about 4 days of lead time for a correlation of 0.5, 3 days for a correlation of 0.6 and 2 days for a correlation of 0.8. As for the MJO, the improvement in the prediction of the NAO cannot be attributed to a single change of the ECMWF forecasting system. The difference of NAO skill scores between 2002 and 2011 are statistically significant within the 5% level of confidence.

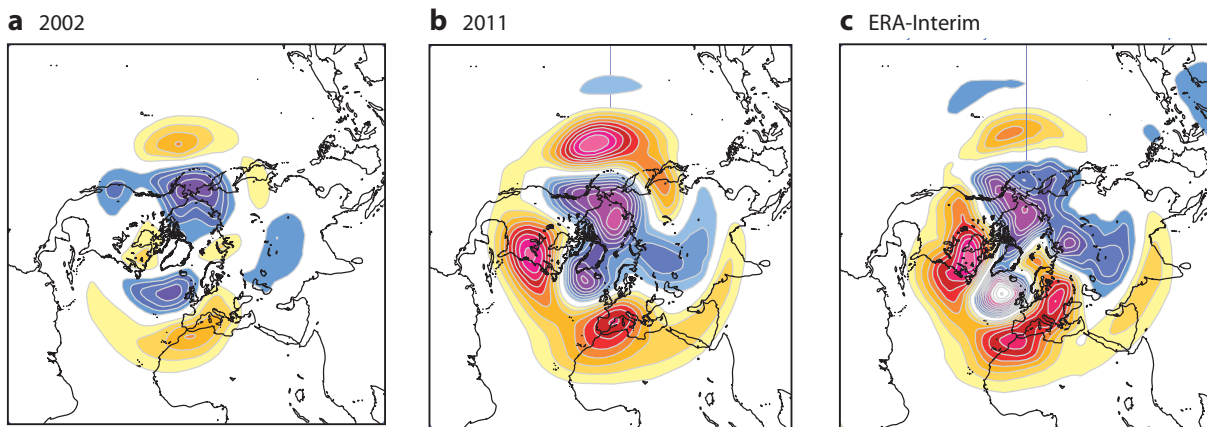


**Figure 9** MJO Phase 3 10-day lagged composites of 500 hPa geopotential height anomaly over the northern extra-tropics for all the October to April re-forecasts that were produced in (a) 2002, (b) 2011 and (c) ERA-Interim. Red and orange colours indicate positive anomalies. Blue colours indicate negative anomalies. The lowest contour is at 10 metres and the contour interval is 5 metres.



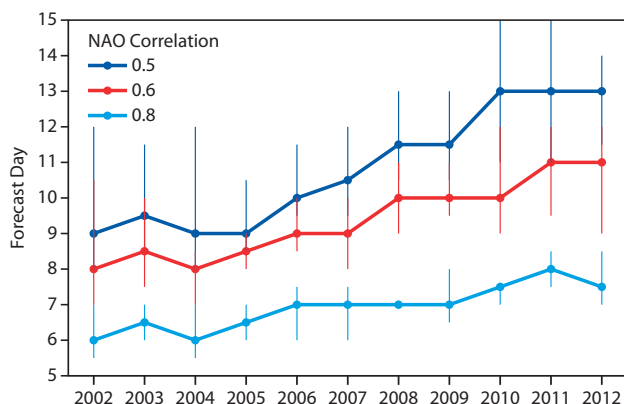


**Figure 10** Evolution of daily NAO skill scores since 2002 as indicated by the days when the NAO index correlation reaches 0.5, 0.6 and 0.8. The daily NAO skill scores (correlations applied to the NAO index) have been computed on the ensemble mean of the ECMWF re-forecasts produced from October to March 1995–2001 and ERA-Interim. The vertical bars represent the 95% confidence interval computed using a 10,000 bootstrap re-sampling procedure.

### Concluding, have ECMWF monthly forecast been improving?

This study has shown that the skill of the ECMWF monthly forecasts has improved since 2002, the time when ECMWF started producing monthly forecasts. The improvements in the skill scores are particularly high for the prediction of the Madden-Julian Oscillation (MJO), an important source of predictability at the sub-seasonal time scale. Over the northern extra-tropics, the prediction skill of the North Atlantic Oscillation (NAO) and of 2-metre temperature anomalies have also increased, particularly for days 12–18. Vitart (2013) shows that a large portion of the improvements in the NAO skill scores can be attributed to the improvements in the prediction of the MJO. For 2-metre temperature, the skill of the 19–25 day forecast in 2012 is getting closer to the skill that the 12–18 day forecast had in 2002. Similar improvements are visible at upper levels, for example in the prediction of the NAO pattern.

The improvements in the monthly re-forecast skill scores reported in this study are likely to be an underestimation of the improvements in the real-time forecasts since this study does not take into account improvements in the generation of atmospheric initial conditions, except for the change from ERA-40 to ERA-Interim in 2008. These improvements are due to a combination of model improvements, better initial conditions (associated with better data assimilation schemes, model improvements and the use of new observing systems), and improvements in the design of more reliable ensemble systems (e.g. thanks to improvements in the simulation of model uncertainties).

Recent changes of the ECMWF medium-range/monthly ensemble forecast (ENS) will help to further increase sub-seasonal forecast skill. In November 2013, three major configuration changes have been implemented affecting the ENS: the atmospheric model is coupled to a new version of the ocean model and from day 0 instead of from day 10, land-surface initial conditions are perturbed, and the vertical resolution has been increased with the introduction

of 91 instead of 62 vertical levels and the rise of the top of the atmosphere from 5 to 0.01 hPa (model cycle Cy40r1). Future changes will include the implementation of a sea-ice model instead of persisting sea-ice and of a higher-resolution,  $\frac{1}{4}^\circ$  ocean model instead of the current  $1^\circ$  model.

It is also worth mentioning that, as part of ECMWF's contribution to the Weather Research Programme (WWRP) and World Climate Research Program 'Sub-seasonal to Seasonal prediction' (S2S) project ([http://www.wmo.int/pages/prog/arep/wwrp/new/S2S\\_project\\_main\\_page.html](http://www.wmo.int/pages/prog/arep/wwrp/new/S2S_project_main_page.html)), ECMWF will extend its existing TIGGE (ThorpeX Interactive Grand Global Ensemble experiment) archive to include sub-seasonal forecasts from other operational centres. This initiative will provide a unique uniform archive of S2S forecasts that will help scientists and developers to understand the sources of S2S predictability, and make it possible to compare the performance of monthly forecasts of different systems.

### FURTHER READING

- Cassou, C.**, 2008: Intraseasonal interaction between the Madden-Julian Oscillation and the North Atlantic Oscillation. *Nature*, doi:10.1038/nature07286.
- Jung, T., F. Vitart, L. Ferranti & J.-J. Morcrette**, 2011: Origin and predictability of the extreme negative NAO winter of 2009/10. *Geophys. Res. Lett.*, **38**, L07701, doi:10.1029/2011GL046786.
- Madden, R.A. & P.R. Julian**, 1971: Detection of a 40-50 day oscillation in the zonal wind in the tropical Pacific. *J. Atmos. Sci.*, **5**, 702–708.
- Vitart, F.**, 2013: Evolution of ECMWF sub-seasonal forecast skill scores. *Q. J. R. Meteorol. Soc.*, in press.
- Weigel, A., D. Baggenstos, M.A. Liniger, F. Vitart & C. Appenzeller**, 2008: Probabilistic verification of monthly temperature forecasts. *Mon. Weather Rev.*, **136**, 5162–5182.
- Wheeler, M.C. & H.H. Hendon**, 2004: An all-season real-time multivariate MJO index: Development of an index for monitoring and prediction. *Mon. Weather Rev.*, **132**, 1917–1932.

# Improving the representation of stable boundary layers

IRINA SANDU, ANTON BELJAARS,  
GIANPAOLO BALSAMO

**H**igh-quality near-surface wind forecasts are particularly valuable for wind energy applications. As more and more forecast users are becoming interested in providing services for such applications, considerable efforts were made in the past three years to improve the representation of stable boundary layers in the ECMWF forecasts. The forecast errors in such conditions, encountered typically over land during night or in winter time, are among the most systematic and longstanding errors of global weather forecasts. The representation of the wind is perhaps the most problematic in terms of both wind speed and wind direction in the first hundreds of metres above the surface.

A revision of the parametrization of turbulent diffusion (or vertical mixing) in stable conditions was recently implemented in cycle 40r1 (November 2013) of the Integrated Forecasting System (IFS). This revision has been combined with changes to the representation of surface drag (or friction) in regions with orography and to the strength of the heat exchange between the land surface and the atmosphere. This set of changes improves the forecasts of near-surface winds in stable boundary layers, but also leads to better forecasts of the large-scale circulation patterns during autumn and winter in the northern hemisphere.

## Background

In the framework of GEWEX Atmospheric Boundary Layer Studies (GABLS, *Holtstlag et al., 2013*) it has been demonstrated that most operational global NWP models are less skilful in representing the key features of stably stratified boundary layers than limited area or research models. In global NWP forecasts:

- Stable boundary layers are often too deep.
- Low-level jets are too weak and located too high above the surface.
- Near-surface ageostrophic wind angles are too small, so that the wind turning between the surface and the boundary layer top is underestimated.

The cause of these errors is well-known: most of them stem from the fact that the operational NWP models in question use turbulence schemes which maintain more turbulent diffusion in stable conditions than justified by observations or very high resolution simulations. To date, the turbulent diffusion in stable conditions is still excessive to various degrees in world-leading operational weather forecasting systems such as those run by ECMWF, Met Office, National Centers for Environmental Prediction (NCEP) and Japan

Meteorological Agency (JMA). It is often argued that the artificial enhancement of the mixing in stable conditions is needed to account for contributions to vertical mixing associated with surface heterogeneity, gravity-waves and mesoscale variability which are not explicitly represented in models. But it is difficult to estimate by how much the mixing in stable conditions should be enhanced.

In theory, reducing the degree of mixing should lead to better forecasts of the key features of stable boundary layers. However, in practice it is difficult to make such a change in a global NWP model. At ECMWF, all previous attempts to use a less diffusive turbulence scheme in stable conditions have been unsuccessful. Back in the 1990s, scientists at ECMWF showed that maintaining more mixing in stable conditions represents an effective way of (a) reducing the cold near-surface temperature biases that are frequently encountered in stable boundary layers and (b) improving the representation of synoptic cyclones (*Beljaars & Viterbo, 1998; Viterbo et al., 1999*). At that time, artificially enhancing the diffusion appeared to be the best compromise for improving the quality of medium-range weather forecasts. Thereafter, attempts were made to get back to mixing levels which are closer to observational evidence and would allow a better representation of stable boundary layers. Unfortunately, such attempts were not successful because they degraded the large-scale performance of the forecasts, especially in the northern hemisphere in winter (*Brown et al., 2005*).

## The way forward

A detailed investigation was conducted in 2011/2012 at ECMWF (*Sandu et al., 2013*) in order to understand whether artificially enhancing the diffusion is still necessary, despite the numerous model improvements and increase in resolution that have occurred in recent years. The study explored the effects of reducing the mixing in stable conditions on the quality of the forecasts produced with the latest version of the IFS.

It was demonstrated that reducing the mixing in stable conditions improves, as expected, the quality of the wind forecasts in stable boundary layers. But, at the same time, it deteriorates to some extent the prediction of near-surface temperatures. Perhaps even more importantly, it also impacts on the atmospheric flow by leading to deeper low pressure systems and stronger high pressure systems. These effects were apparent both at the scale of individual synoptic cyclones and anticyclones and in the mean state. This implies that reducing the diffusion in stable layers near the surface has a direct effect on the amplitude of the stationary planetary-scale waves. For some regions and seasons these effects are detrimental for the quality of the forecasts. The most important drawbacks are similar to

those found with previous attempts to reduce the mixing in stable conditions: a deterioration of the geopotential height scores during winter in the northern hemisphere and an increase of the near-surface night-time cold biases, especially over Europe and North America.

The boundary layer winds, which arguably depend primarily on the representation of turbulence, thus benefit from reduced mixing in stable conditions, while other features (e.g. the large-scale flow and the 2-metre temperatures) sometimes deteriorate. This suggests that excessive mixing is still needed in stable situations, as it has been for more than 20 years, to compensate for errors in other processes that play a role in the evolution of the large-scale flow and 2-metre temperatures. Therefore, a less diffusive turbulence scheme for stable conditions can still not be implemented as a stand-alone change in the IFS.

### Turbulent diffusion in a nutshell

A

A first order local turbulence closure is used in the IFS to parametrize the diffusion in stable layers. Such layers are found close to the surface in stable boundary layers and in most parts of the free-troposphere.

For each stable layer, the flux  $F_\phi$  of a quantity  $\phi$  (temperature, moisture or wind) is parametrized with a K-diffusion approach:

$$F_\phi = K \frac{\partial \phi}{\partial z}$$

The diffusion coefficients  $K$  are proportional to the wind shear across the layer, a mixing length scale  $l$  and an empirical function depending on stability through the Richardson Number  $R_i$ :

$$K = \left| \frac{\partial u}{\partial z} \right| l^2 f(R_i)$$

The mixing length  $l$  is proportional to the height above the surface when the stable layer is in vicinity of the surface, and is bounded by an asymptotic value in stable layers situated far away from the surface. Two types of empiric stability functions of  $f(R_i)$  are used in atmospheric models:

- Long tail functions, which maintain a certain degree of mixing in very stable layers with  $R_i > 1$ .
- Short tail functions, for which there is virtually no mixing in such layers.

The CTL and NEW diffusion closures are summarized below.

#### Up to Cy38r2

- Asymptotic mixing length: 150 m.
- Long tail function close to the surface and short tail functions far away from the surface.
- The shear consists of resolved shear and subgrid shear, parametrized as a height dependent term with a maximum around 850 hPa.

#### From Cy40r1

- Asymptotic mixing length: 10% of the boundary layer height in stable boundary layers; 30 m in free-shear layers.
- Long tail functions in all stable layers.
- Only resolved shear is considered.

*Sandu et al.* (2013) also explored possible strategies for mitigating the detrimental impacts of reducing the turbulent diffusion in stable conditions to more realistic levels. It was found that (a) adjusting the strength of the drag over orography can help improve the representation of the large-scale flow and (b) adjusting the strength of the land-atmosphere heat exchange can be used to compensate for the near-surface cooling induced by reducing the diffusion in stable conditions. These processes are among the most uncertain processes that need to be parameterized at current resolutions, with observational evidence being scarce.

### The changes to the forecasting system

An optimal set of changes to the IFS was found which combines a revision of the turbulence closure (see Box A) with an increase in the drag over orography and a strengthening of the land-atmosphere heat exchange for forested areas. The revised turbulence closure leads to less diffusion in stable boundary layers and in the inversions layers capping boundary layers situated around 850 hPa, while not changing too much the diffusion above this level.

These combined changes were tested for a six month period (January to March and June to August 2012) in a T511 configuration (grid spacing of 39 km) with 137 levels in analysis mode. This means 10-day forecasts were initialized daily at 00 UTC from their own analysis (i.e. analysis performed with the same version of the forecasting system). Hereafter, we will focus on either the June to August or the January to March results of the control (CTL) and of the NEW T511 experiments, depending on which ones are more relevant for the features we want to highlight. Shorter experiments performed at T1279 (grid spacing of 15.6 km) confirmed that the impact of these changes is consistent across resolutions.

### Impacts on near-surface winds

In the northern hemisphere the wind generally turns clockwise with height throughout the boundary layer; the opposite being true for the southern hemisphere. In the IFS, the modelled surface wind directions are generally rotated clockwise with respect to surface

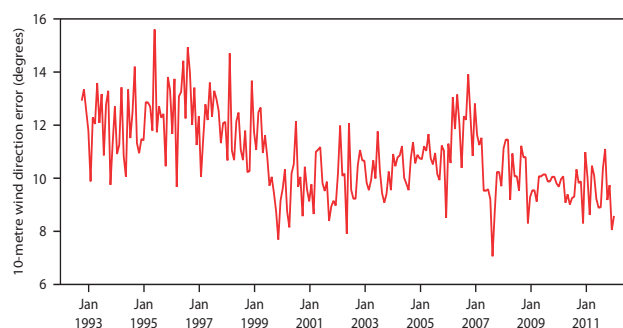


**Figure 1** Historic evolution of 10-m wind direction errors of the IFS. These are monthly values of mean errors at a lead time of 60 hours of the daily forecasts initialized at 12 UTC (verifying time 00 UTC). The verification includes 800 SYNOP stations over Europe (30°–72°N, 22°W–42°E).

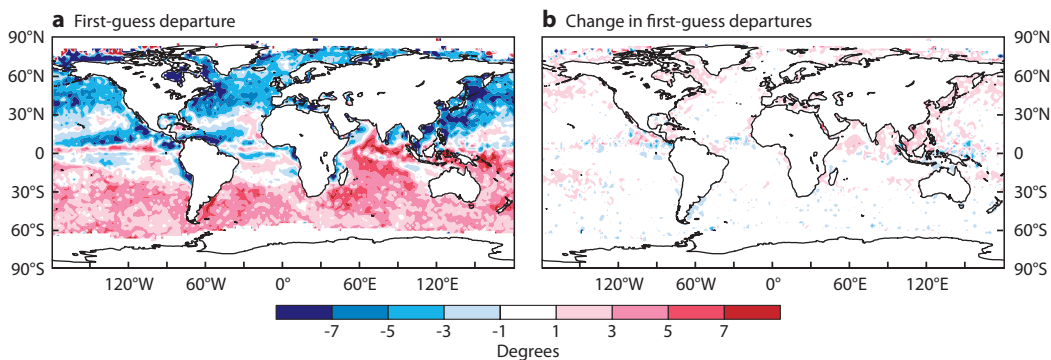


**Figure 2** (a) Mean first-guess departure (observations minus model) of wind direction at the surface (degrees) with respect to ASCAT scatterometer observations in the CTL analysis run and (b) the mean change in these first-guess departures in the NEW experiment with respect to the CTL. These quantities represent the average over the 00 and 12 UTC analyses. Results shown here are for June to August when the stable regions over the oceans are more extended than in January to March.

observations in the northern hemisphere, while in the southern hemisphere they are rotated anticlockwise (Brown *et al.*, 2005, Figure 1 and Figure 2a). The model therefore underestimates the wind turning within the boundary layer. These biases are increasingly pronounced in stable conditions (Brown *et al.*, 2005), where they are amplified by the too strong mixing maintained in such conditions. The bias of the near-surface wind direction predicted for night-time over land clearly illustrates the systematic nature of these biases in stable boundary layers. Indeed, this bias varied only a little over the past 20 years with values ranging between 15° and 10° (Figure 1).

The revision of the turbulence closure significantly reduces these biases in wind direction. Thus, the wind direction bias at the surface, which approaches 10° over Europe for night-time conditions in the CTL experiments, is reduced on average by 3° in winter and by 1° in summer in the NEW experiments. A similar positive impact can be seen for oceanic regions where stable boundary layers prevail (i.e. where warm air is advected over a cold sea surface). This is inferred from the first-guess departures with respect to scatterometer observations of the wind direction at the surface. In the NEW experiments these first-guess

departures are reduced in both hemispheres with respect to the CTL runs (Figure 2b) over the regions where the boundary layer is stably stratified.

The revision of the turbulence closure also diminishes the longstanding biases in near-surface wind speeds. To evaluate the impact of these model changes on the near-surface winds, model results from the CTL and NEW experiments were compared with observations obtained at three sites with differing characteristics: Cabauw (open pasture), Hamburg (urban area) and Falkenberg (rural landscape, open pasture around the site, forest patches in the surroundings). The data was kindly provided by KNMI (Netherlands), University of Hamburg and DWD (Germany).

The observed wind speeds have at night a minimum at 10 m and a maximum at approximately 200 m. This maximum, also known as the nocturnal low-level jet, is a distinct feature of stable boundary layers. In the CTL experiment the model underestimates the wind speed at night in the upper part of the boundary layer. Therefore the amplitude of the diurnal cycle of the wind speed at these levels is too small (Figure 3). The reason is that the strong mixing applied in stable conditions has a tendency to smear out the nocturnal low-level jet by excessively transporting

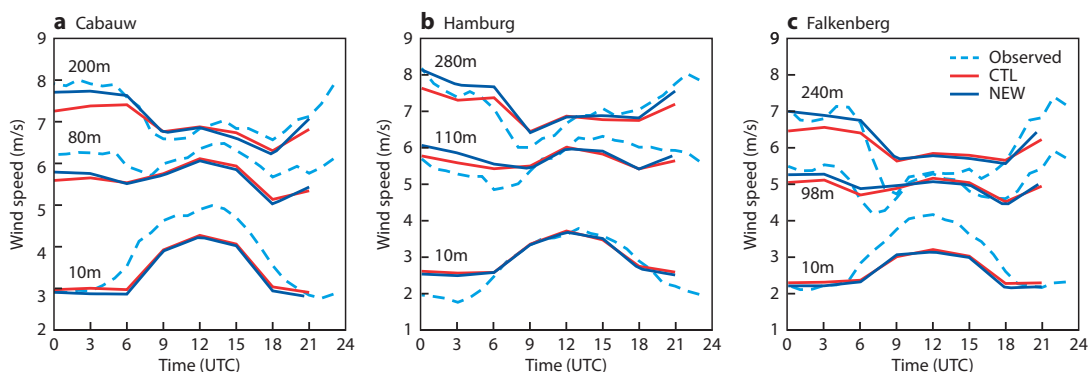


**Figure 3** Averaged diurnal cycle of wind at (a) Cabauw, (b) Hamburg and (c) Falkenberg from forecasts produced in the CTL and NEW experiments (lead times 24 to 42 hours) compared to observations. Note that for Falkenberg the jump around 100 metres is due to the data below 100 metres coming from tower measurements and above 80 metres from sodar. Results are shown for June to August when the diurnal cycles are the most pronounced.

momentum towards the surface. As expected, the low-level jets are strengthened when the turbulent diffusion in stable boundary layers is reduced in the NEW experiment. The improvement in the upper part of stable boundary layers can be seen in terms of both the mean wind speed and root-mean-square error (Figure 4).

At 10 m, the model appears to reproduce well the mean wind speed at night but to underestimate it during daytime at the towers situated in the countryside (Cabauw and Falkenberg); for Hamburg, which is in a strongly urbanized area, it is the opposite. This points to uncertainties in the representation of the roughness length for momentum, which may not be representative of the respective sites.

**Impacts on near-surface temperatures**

Near-surface temperature cold biases are often found in stable boundary layers that typically occur over land at night or in winter (Figure 5a). They may result from errors in the representation of various processes, such as energy exchange between the land and the atmosphere, radiative loss at the surface, turbulent diffusion, horizontal advection or clouds. Nevertheless, these biases are very sensitive to the degree of turbulent diffusion in stable conditions. Indeed, less diffusion means the cooling due to the radiative loss at the surface is distributed in a shallower layer, so there is a drop in near-surface temperature and the existing cold biases increase. This was one of the main factors that have prevented the reduction of the turbulent diffusion in stable conditions in the past.

The revised turbulence closure leads as well to a cooling at the surface. However, the magnitude of this cooling is modulated by the dependence of the diffusion coefficients on the stability of the boundary layer (through the new formulation of the asymptotic mixing length described in Box A). Consequently, the induced cooling is more pronounced in strongly (hence shallower) boundary layers than in weakly stable (hence deeper) ones. Moreover, the increase of the heat exchange between the land surface and the atmosphere for areas where high vegetation is present leads to a warming during night-time. So, it partially outweighs the cooling induced by the revision of the turbulence closure. It follows that the combined changes included cycle 40r1 of the IFS lead to only relatively small changes in near-surface temperatures (Figure 5b).

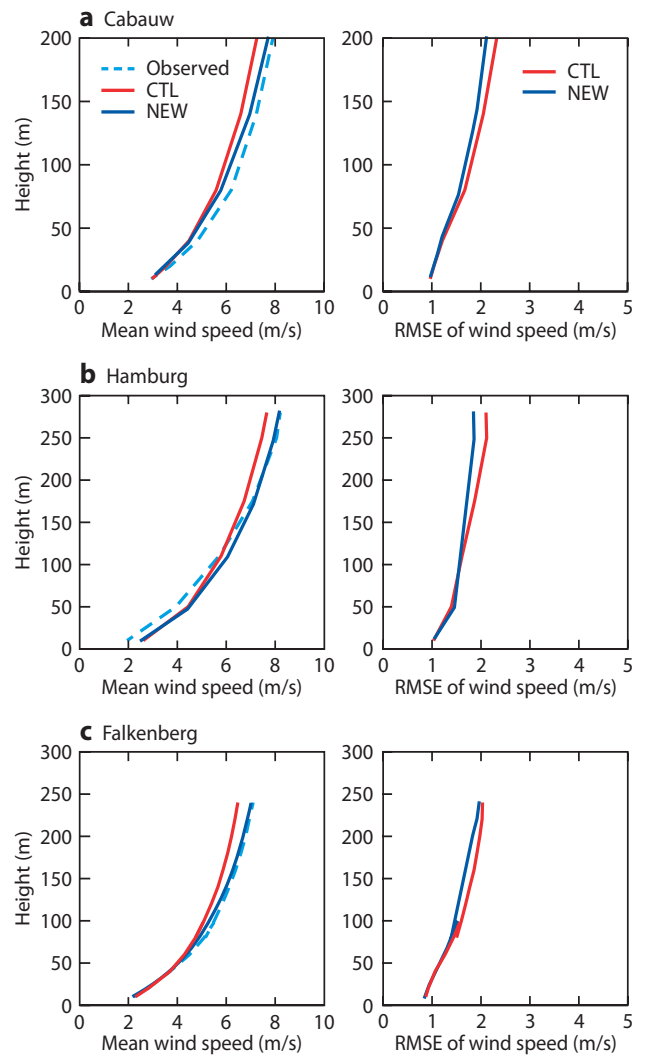


**Figure 4** Mean wind speed (left) and root-mean-square error (RMSE) of wind speed (right) from forecasts produced in the CTL and NEW experiments with respect to the observations from the towers at (a) Cabauw, (b) Hamburg and (c) Falkenberg. The modelled profiles correspond to lead time 24 hours of the daily 00 UTC forecasts (verifying at 00 UTC). Results are shown for June to August when the low-level jets are the most pronounced. Note that for Falkenberg the jump around 100 m is because the data below 100 m comes from tower measurements and above 80 m from sodar.

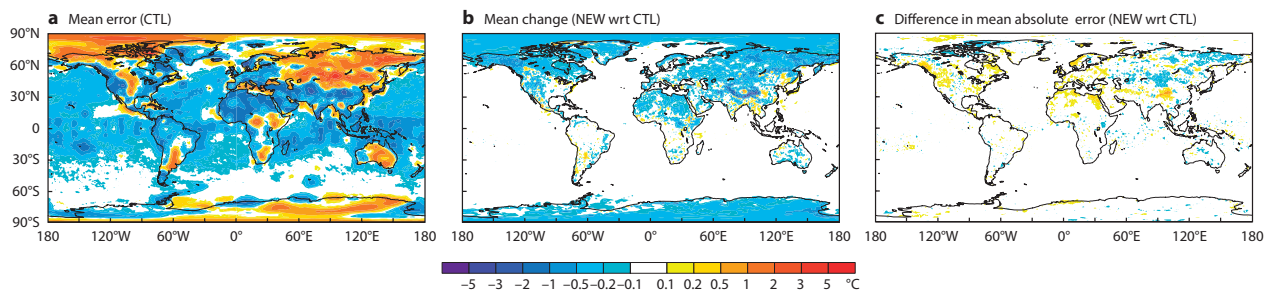


**Figure 5** (a) Mean 2-metre temperature error (°C) for the CTL daily forecasts performed for January–March 2012 with respect to the analyses from which the forecasts were initialized. (b) Mean change in 2-metre temperature in the NEW experiment with respect to the CTL. (c) Difference in mean absolute error in the 2-metre temperature in the NEW experiment with respect to the CTL. The plots correspond to the time of the minimum of the diurnal cycle in 2-metre temperature derived from the lead times 24 to 42 hours of the daily 00 UTC forecasts.

Figure 5a illustrates the patterns of the 2-metre temperature forecast biases occurring over continental areas during night-time in the winter season. These biases are complicated and not understood – they are positive in some areas and negative in others. Consequently the near-surface cooling associated with our changes (Figure 5b) leads to an improvement in some areas and to a slight deterioration in others. The improvement (deterioration) in forecast performance is indicated by a decrease (increase) of the mean absolute error in 2-metre temperature in the NEW versus the CTL experiments (Figure 5c).

**Impacts on large-scale circulation**

Sandu *et al.* (2013) demonstrated that changes made to surface drag, by modifying either the diffusion in stable boundary layers or the drag over orography, affect the large-scale circulation through their impact on the synoptic systems and on stationary planetary waves. To illustrate these impacts, Figure 6 shows how the changes to the turbulent closure in stable conditions and to the drag over orography discussed here modify the mean of the 1000 hPa geopotential height during a winter month when these impacts are the most pronounced. To emphasize the changes affecting the weather systems, in the figure the regions of mean low sea-surface pressure (lows) are indicated by dashes and the regions of high sea-surface pressure (highs) are indicated by full lines.

The mean bias of the 1000 hPa geopotential height suggests that in the short range of the CTL forecasts the highs are on average too weak (i.e. the geopotential is too low). Meanwhile, the lows are either relatively well represented or not deep enough (i.e. the geopotential is too high), especially in the storm track region in the southern hemisphere (Figure 6a). The reduction of the diffusion in stable boundary layers (experiment DIFF) leads to an increase of the geopotential height at 1000 hPa in the highs and decrease in the lows from the beginning of the forecasts (Figure 6b). This corroborates the idea that a reduction in surface drag strengthens the pressure systems, most likely by diminishing the integrated cross-isobaric flow (Beare, 2007; Svensson & Holtslag, 2009). When this change is combined with the increase in the drag over orography (Figure 6c), the highs strengthen even more and the lows deepen less with respect to the CTL compared to when the turbulence changes were tested individually (Figure 6b).

The benefit of combining the two changes is clearly emphasized by the changes in the root-mean square error of the geopotential height for the northern hemisphere shown for various levels in Figure 7. The reduction of the root-mean-square error, which is indicative of an improvement in the large-scale forecast performance, is more substantial and becomes significant when the two changes are combined. The combined changes thus lead to a substantial improvement both in terms of mean and root-mean square errors of the geopotential height in the northern hemisphere (especially over Eurasia and North America), but also in the storm track region in the southern hemisphere at all levels (not shown).

**Outlook**

Although the solution described here is not entirely satisfactory, it is an important step towards reducing some of the most longstanding errors in ECMWF’s parametrization of physical processes – the errors related to the representation of near-surface winds in stable boundary layers. Meanwhile, this work allowed the definition of

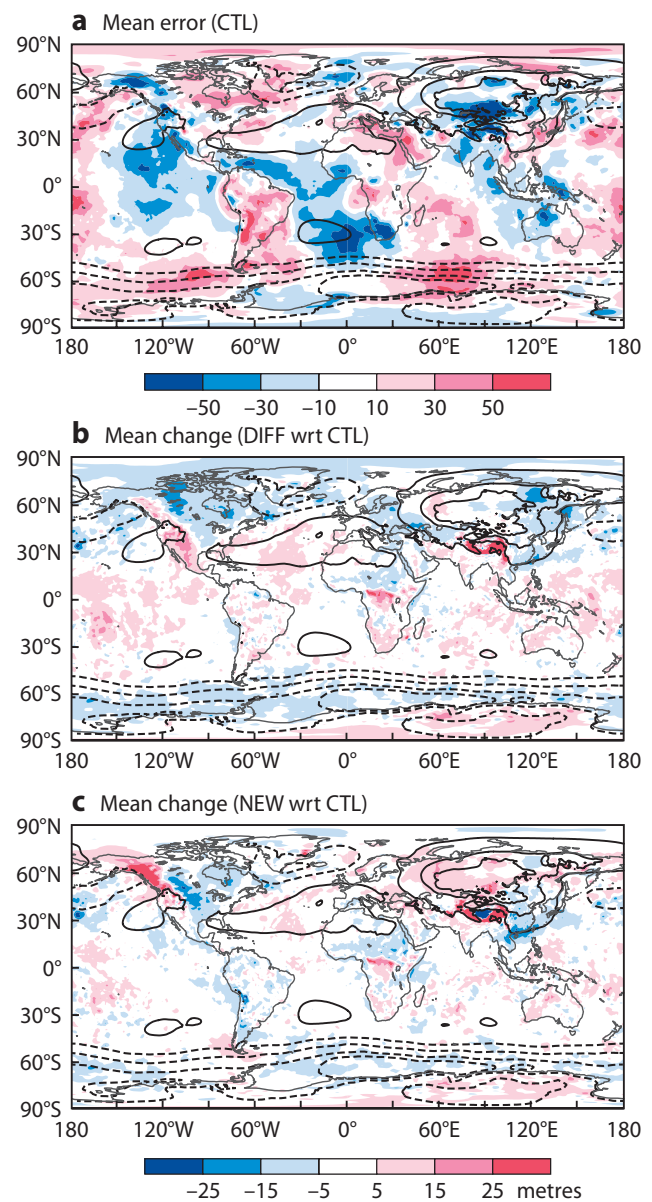


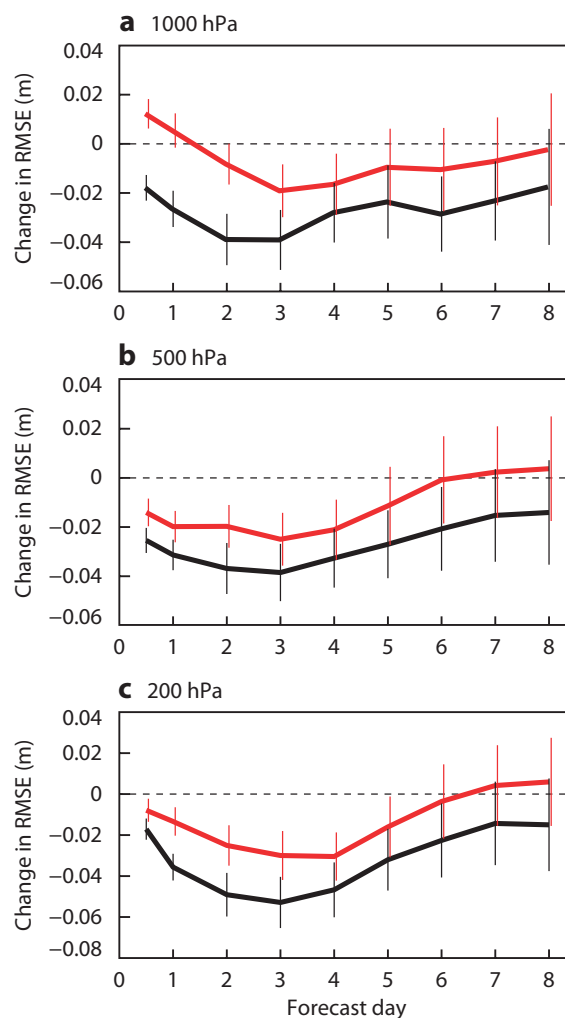
**Figure 6** (a) Mean error of the 1000 hPa geopotential height of the CTL experiment for January 2012, with respect to the analyses from which the forecasts were initialized, at forecast lead time of 24 hours (verifying at 00 UTC). (b) Change in mean of the 1000 hPa geopotential height in an experiment where only the changes to the turbulence closure in stable conditions are tested (experiment DIFF) with respect to the CTL run. (c) Same as (b) but for the NEW experiment where the changes to the turbulence closure are combined with the ones to the surface drag (all in metres). The low pressure systems (dashes) and high pressure systems (full lines) are defined from the monthly mean analyzed fields of 1000 hPa geopotential height.

further research paths that need to be pursued. Namely, it revealed the importance of:

- Improving the representation of drag over orography, which proves to be crucial for the large-scale forecast performance.
- Representing the coupling between the land surface and the atmosphere, which plays a large role in the quality of near-surface temperature forecasts.

The importance of these topics has recently been acknowledged by the research community and two ongoing intercomparison exercises are focusing on these aspects in the frameworks of WGNE (Working Group on Numerical Experimentation), GASS (Global Atmospheric System Studies) and GLASS (Global Land/Atmosphere System Study). These intercomparison studies, in which ECMWF is currently participating, are going to highlight how differently the orographic drag and the land-atmosphere coupling are treated in various NWP models. Hopefully they will stimulate further research on the factors governing land-atmosphere fluxes, the coupling strength, and the representation of drag over orography.

**Figure 7** Change in root-mean-square error (RMSE) of the geopotential height for the northern hemisphere extratropics (20°–90°N) at (a) 1000 hPa, (b) 500 hPa and (c) 200 hPa in an experiment where only the changes to the turbulence closure in stable conditions are tested (red) and in the NEW experiment where the changes to the turbulence closure are combined with the ones to the surface drag (black), both with respect to the CTL experiment for January to March 2012. If vertical lines do not intersect the 0 line, it means the NEW experiment is significantly better, or worse (95% interval), than the CTL.



#### FURTHER READING

**Beare, R.**, 2007: Boundary layer mechanism in extra tropical cyclones. *Q. J. R. Meteorol. Soc.*, **133**, 503-515.

**Beljaars, A. & P. Viterbo**, 1998: The role of the boundary layer in a numerical weather prediction model. *Clear and Cloudy Boundary Layers*, A.A.M. Holtslag and P.G. Duynkerke, Eds., Royal Netherlands Academy of Arts and Sciences, North Holland Publishers, Amsterdam, 287-304.

**Brown, A., A. Beljaars, H. Hersbach, A. Hollingsworth, M. Miller & D. Vasiljevic**, 2005: Wind turning across the marine atmospheric boundary layer. *Q. J. R. Meteorol. Soc.*, **131**, 1233-1250.

**Holtslag, A., G. Svensson, P. Baas, S. Basu, B. Beare, A. Beljaars, F. Bosveld, J. Cuxart, J. Lindvall, G. Steeneveld, M. Tjernström & B.V.D. Wiel**, 2013: Stable atmospheric boundary layers and diurnal cycles challenges for weather and climate models. *Bull. Am. Meteorol. Soc.*, doi 10.1175/BAMS-D-11-00187.1.

**Sandu, I., A. Beljaars, P. Bechtold, T. Mauritsen & G. Balsamo**, 2013: Why is it so difficult to represent stably stratified conditions in Numerical Weather Prediction (NWP) models? *J. Adv. Model. Earth Syst.*, **5**, 117-133.

**Svensson, G. & A. Holtslag**, 2009: Analysis of model results for the turning of the wind and the related momentum fluxes and depth of the stable boundary layer. *Boundary-Layer Meteorol.*, **132**, 261-277.

**Viterbo, P., A. Beljaars, J.-F. Mahfouf & J. Teixeira**, 1999: The representation of soil moisture freezing and its impact on the stable boundary layer. *Q. J. R. Meteorol. Soc.*, **125**, 2401-2426.

# iCOLT – Seasonal forecasts of crop irrigation needs at ARPA-SIMC

GIULIA VILLANI, LUCIO BOTARELLI, VITTORIO MARLETTO, ANDREA SPISNI, VALENTINA PAVAN, WILLIAM PRATIZZOLI, FAUSTO TOMEI  
ARPA-SIMC, Bologna, Italy

Every year, ARPA-SIMC, the Hydro-Meteo-Climate Service of the Environmental Agency of Emilia-Romagna provides a probabilistic assessment of potential irrigation demand of crops for the plain area of Emilia-Romagna (Northern Italy) and for each of the eight reclamation and irrigation consortia (hereafter referred to as 'consortia'), as shown in Figure 1. This is carried out using the iCOLT system (irrigazione e Classificazione delle cOLTure in atto tramite Telerilevamento – irrigation and classification of current crops by remote sensing) which integrates satellite data, seasonal weather forecasts and water balance predictions.

An early assessment of the irrigation water need is of great importance, especially in a region like Emilia-Romagna that is located in the Northern Mediterranean area and exposed to water scarcity in summer. In recent years, the region has faced several droughts combined with very large summer temperature anomalies. This led to major problems in water management, which needs to balance the demands from civil, agricultural and industrial activities. In particular, the whole of Northern Italy was affected by an intense precipitation deficit, extending from September 2011 to September 2012, and by intense heat-waves. These conditions led to dramatic consequences for agriculture, especially in those Italian regions where water scarcity made it impossible to irrigate crops.

- The production was reduced by 20% for tomatoes, between 30% and 50% for corn (whose quality was also lower due to very high temperatures), by 40% for soya-beans, by 25% for rice and between 10% and 20% for sunflower seeds.
- Reductions in production were recorded for peaches

(between 10% and 25%), pears (about 40%) and apples (about 20%).

The iCOLT system takes advantage of the ECMWF facilities made available as part of the Special Project SPIT-SPIA, aimed at producing seasonal predictions for Italian agriculture. It was mostly developed in the framework of the Italian national project Agrosenari, which is concerned with evaluating the impact of climate change on agriculture and devising specific adaptation strategies. The system has been operational at ARPA-SIMC since 2010, with the results made available via the agency's official website. It is an example of a climate service for agriculture, with specific application in the field of water management at regional and irrigation consortium scales. In the following, we give a description of the system, of its workflow in operational conditions, and of the results obtained for the summers of 2011, 2012 and 2013.

The iCOLT system has recently been officially recognized by the regional authorities of Emilia-Romagna as a strategic adaptation tool, amongst others, to address growing uncertainties in water availability for agriculture due to climate change.

## The operational system

Figure 2 shows the iCOLT operational workflow producing seasonal predictions of summer irrigation water need for Emilia-Romagna. The operational process spans two years.

- The process starts in mid-October of year one with the acquisition of the first satellite image of the region.
- By April of the following year, all satellite images have been acquired and the information on crop distribution can be classified (Spisni *et al.*, 2010).
- By the third week of May, the calibrated probabilistic seasonal predictions for Emilia-Romagna are made available and the seasonal predictions of water irrigation need can be generated.

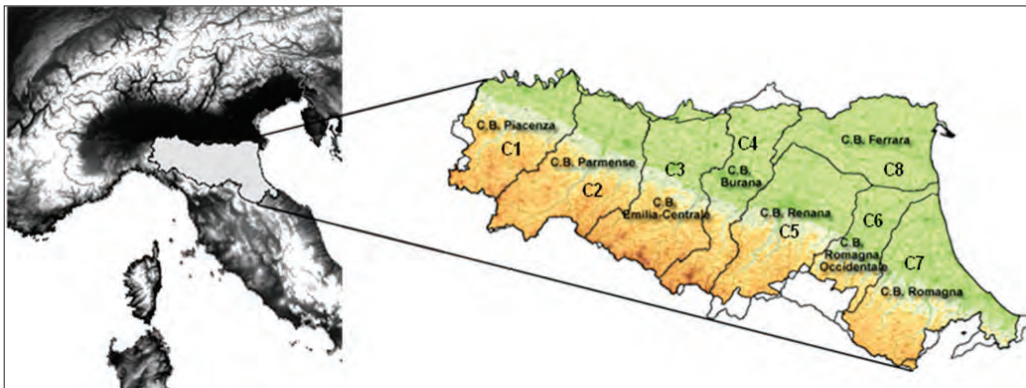
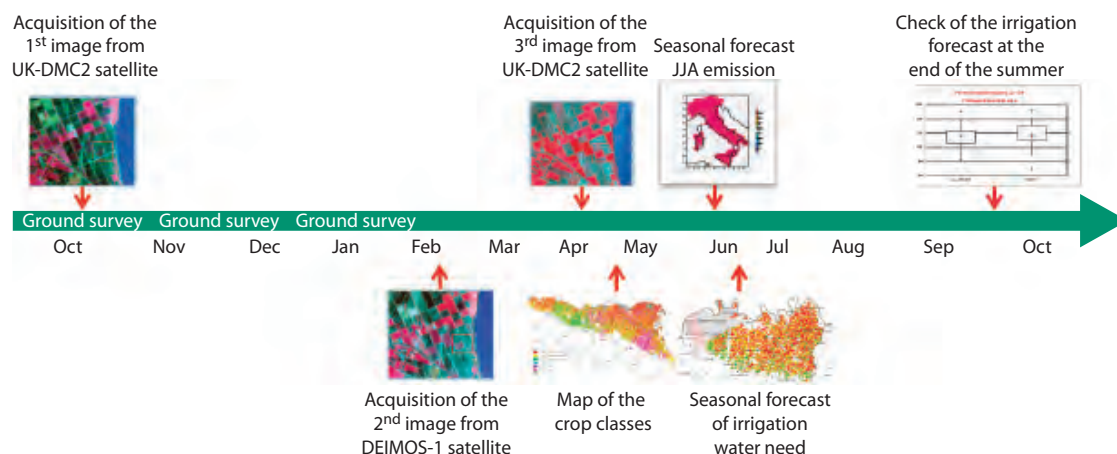


Figure 1 Emilia-Romagna region and the eight consortia.





**Figure 2** The iCOLT system workflow.

- At the end of summer, meteorological observations are used to estimate the actual irrigation needs using the CRITERIA water balance model (Controllo Riserve Idriche Territoriali per la Riduzione dell’Impatto Ambientale – Local water resource monitoring to reduce the environmental impact) developed by ARPA-SIMC (see, for example, *Marletto et al., 2007*).

Wherever possible, forecast results are also verified using observed irrigation data. Each element of this workflow will now be described in detail.

### Crop classification and mapping with remote sensing

The first step of the iColt system consists of the classification of current agricultural crops on the whole regional plain (about 1,180,000 hectare). The classification is based on field surveys and on the analysis of visible and near infrared satellite images taken in October, February and April. The three temporal windows for the satellite images are chosen to enhance the differences between the phenological stages of crop macro-classes. In any particular year, the satellite data sources used depend upon availability and image quality. As an example, for 2013, the three images were taken on 16 October 2012 (satellite UK-DMC2), 8 February 2013 (satellite DEIMOS-1) and 18 April 2013 (satellite UK-DMC2).

Crops are grouped into five macro-classes: summer herbaceous, winter herbaceous, multiannual fodder crops, fruit orchards and vines, and rice paddies. The results are available by the end of April each year.

### Seasonal forecasts

ARPA-SIMC has been producing local probabilistic seasonal forecasts since 2007 by calibrating the operational multi-model ensemble global seasonal predictions to the local climate. The multi-model ensemble is produced at ECMWF by the EUROSIP system (see Box A and *Pavan & Doblas-Reyes, 2013*). The final predictions are made available on a 35 km regular latitude-longitude grid covering the whole of Italy. These predictions represent the contribution of ARPA-SIMC to the Task Team on Monthly and Seasonal Predictions created by the Italian National Civil Protection Agency. This Task Team gives technical support to decision making

at national level concerning water management, health care and wild fires prevention.

Summer seasonal forecasts for the June to August are issued in mid-May. Calibrated ensemble predictions of seasonal anomalies are produced for several variables needed as input of the weather generator scheme. These variables are:

Seasonally cumulated precipitation, wet day frequency and wet-wet frequency (i.e. the frequency of occurrence of a wet day after another wet day).

### EUROSIP

A

The EUROSIP multi-model seasonal forecasting system consists of a number of independent coupled seasonal forecasting systems integrated into a common framework. From September 2012, the system included forecasts from ECMWF, the Met Office, Météo-France and NCEP (National Centers for Environmental Prediction). The reason for using a multi-model forecasting system is that research has shown that in most cases the multi-model combination is better than the best single model.

Data from all component models is archived at ECMWF, and can be accessed subject to the terms of the policy EUROSIP data.

ECMWF produces a number of multi-model products that are created from the integrated output of the component models. They are officially referred to as ‘EUROSIP products’. Most of these products are provided in graphical form only, although also some numerical data are made available. These multi-model products can be accessed just like any other ECMWF product.

Data from the individual models is also archived at ECMWF, but the data can only be accessed subject to specific terms in the EUROSIP data policy.

For more information go to:  
<http://www.ecmwf.int/products/forecasts/seasonal/documentation/eurosip/ch3.html>

Minimum and maximum seasonal averaged temperature and the average difference in maximum temperature between dry and wet days.

A weather generator produces time series of daily precipitation and minimum and maximum temperature data that are statistically compatible with the seasonal anomalies given as input (Tomei *et al.*, 2010). These synthetic daily time series are finally fed into the CRITERIA water balance model (see Box B for more information). Moreover, ARPA-SIMC has developed an empirical equation to assess the current value of the depth of the shallow water table using temperature and precipitation observations (Tomei *et al.*, 2010). Seasonal forecasts of these two variables also allow the production of probabilistic seasonal predictions of water table level, a crucial source of water for the crops located in the Emilia-Romagna plain.

**Results**

Figure 3 presents, for each consortium, the time series of the box plots for the probabilistic seasonal predictions of irrigation need anomaly for the last three summers. Climatological values of the irrigation need and validation data are estimated using the CRITERIA water balance model forced by meteorological observations over the period 1991 to present. The irrigation need anomalies are computed by subtracting the climatological values from those predicted values. It should be noted that these results are obtained in forecast mode, so that the reference period includes only data preceding the forecast season.

**The CRITERIA model**

B

The water balance model CRITERIA describes the dynamics of water in agricultural soils. In the iCOLT system it makes use of:

- Observed (until May) and predicted (for the rest of summer) daily data: namely minimum and maximum temperatures, precipitation, and water table depth.
- Yearly regional crop type maps derived from remote sensing classification.
- Static soil type data taken from the official Emilia-Romagna soil atlas.

CRITERIA is based on the approach of Driessen & Konijn (1992), though it has been improved by assuming a multi-layered soil and explicitly computing approximate values of daily evaporation, transpiration, water flows between layers, deep drainage, runoff and subsurface runoff. Crop development and the dynamics of related processes (e.g. those associated with the leaf area index and the rooting depth) are simulated in CRITERIA by means of empirical equations based on degree-day sums.

To assess the crop water demand, the irrigation process is controlled by a number of parameters, including the irrigation season duration, irrigation shift minimum period, maximum volume for a single irrigation, crop coefficients reached by the crop in the maximum development, crop sensitivity values to the water stress and, if applicable, percentage of controlled stress.

For each consortium, at least two out of three forecasts are able to capture the sign of the observed anomaly and in some cases the forecast also gives a correct indication of the intensity. Furthermore, in some cases, the system captures differences in irrigation needs between consortia within the region. The particularly good skill of these predictions exceeded the expectations, since the products are obtained using probabilistic seasonal forecasts which do not have a high skill over Southern Europe (Pavan & Doblaz-Reyes, 2013). It is possible that the ability of the system to capture the observed interannual variability is linked to the strong dependence of the water table level on the meteorological conditions that occurred over the preceding few months. As a consequence, a good estimate of the initial conditions of this quantity may have a positive impact on the final product, thereby improving the overall skill of the system.

In 2012, Emilia-Romagna suffered from an intense drought that substantially lowered the water table level, while in 2013 the opposite took place. These conditions favoured irrigation needs being higher than their climatic values in 2012, but lower in 2013. Furthermore, in these two years, although the meteorological seasonal predictions

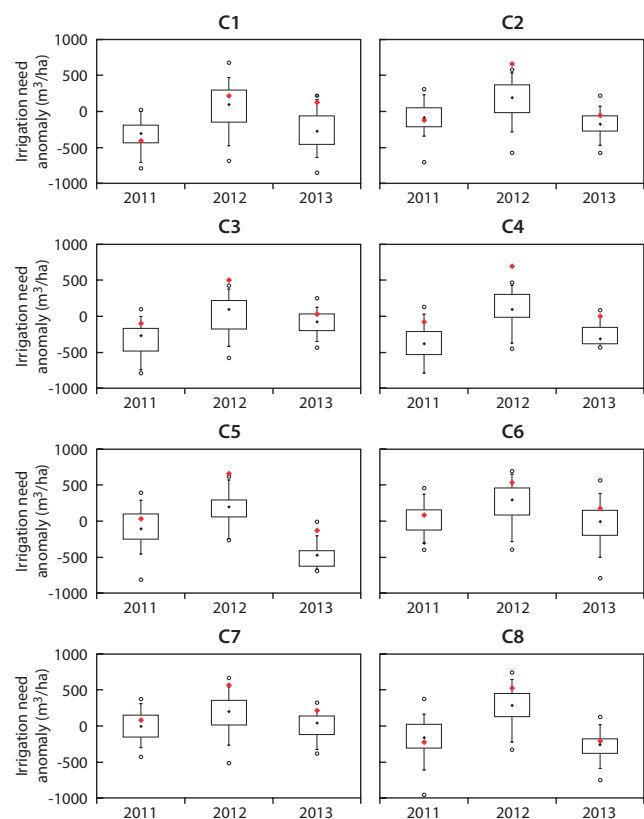


**Figure 3** The panels refer to each Emilia-Romagna consortium and show the box plot for the probabilistic seasonal predictions of irrigation need anomaly (in m<sup>3</sup>/ha) obtained using the iCOLT system for the years 2011, 2012 and 2013. Climatological values and validation values (red dots) are estimated using the CRITERIA water balance model forced with meteorological observations. Boxes cover from the 25<sup>th</sup> to the 75<sup>th</sup> percentiles, whiskers extend to the 5<sup>th</sup> and 95<sup>th</sup> percentiles while extreme values are indicated by black dots. Red, solid dots indicate the observed values.

could not capture the exact intensity of the climate anomaly, they reproduced its general characteristics and made at least a partial contribution to the overall good performance of the system.

The ability of the system to capture differences between water irrigation needs between consortia might be linked to (a) a correct evaluation of the initial conditions of the local water table level and (b) the good quality of the evaluation of the geographical distribution of different crop macro-classes since each of them is characterized by different water needs.

Table 1 is based on data for summer 2013 and presents one of the typical operational products of iCOLT that provides an assessment of crop water needs at regional and local level to water management authorities. The table shows the median, the 25<sup>th</sup> percentile and the 75<sup>th</sup> percentile of the probabilistic seasonal predictions of irrigation (466 million cubic metres) for each consortium and for the region as a whole, together with the estimated irrigation need. These last values are obtained by the end of the season by running the CRITERIA water balance model forced with meteorological observations. Actual observed data are currently being collected, but, as for now, are not yet available for all consortia. The table shows that there is a difference of about 20% between the median of the probabilistic forecast and the estimated values of water irrigation needs.

### Current performance and future developments

The iCOLT system is used operationally at ARPA-SIMC to provide information about seasonal probabilistic irrigation needs over the plains of Emilia-Romagna. The system combines information on land use (obtained from high-resolution satellite data), meteorological observations (provided by the local regional meteorological office), and probabilistic seasonal predictions (obtained by calibrating the operational EUROSIP multi-model seasonal forecasts over the regional climate).

The results for the last three seasons indicate that this

Consortium	25 <sup>th</sup> Percentile	Median	75 <sup>th</sup> Percentile	Estimate
C1	50.0	63.1	78.2	92.0
C2	27.3	35.5	44.2	44.7
C3	26.2	36.8	46.6	48.7
C4	5.2	11.4	26.6	42.3
C5	6.7	21.1	28.4	56.1
C6	83.9	97.0	110.7	108.1
C7	59.7	71.6	80.9	80.3
C8	102.3	129.6	147.4	156.6
<b>TOTAL</b>	<b>361.2</b>	<b>466.0</b>	<b>563.0</b>	<b>628.8</b>

**Table 1** Summer (June to August) 2013 predicted and estimated irrigation water needs (millions of cubic metres) for each consortium. The table reports the median and the 25<sup>th</sup> and 75<sup>th</sup> percentiles of the predicted values and the estimate of the irrigation need obtained from the CRITERIA model forced with meteorological observations.

product has a relatively good skill. In particular, at least two out of three probabilistic predictions for each consortium are able to capture the sign of the observed anomaly, if not its amplitude. Furthermore, to some degree, the dependence of the predictions on the geographical position of each consortium is similar to that observed.

### With regard to the ability of the system:

On the one hand it can capture the interannual variability which seems to be partly due to the dependence of the predictions on the soil water table level at the beginning of the prediction season. The calibrated probabilistic seasonal prediction skill in the last three years was possibly higher than the average, contributing to the overall good performance of the system.

On the other hand it can capture differences in irrigation need between consortia. This might be due partly to the differences in initial condition of soil water table level and partly to a good evaluation of the geographical distribution of crop classes, characterized by different water needs.

These promising results prompt the continuation of the current provisional operational practice for the next few years and a more thorough study of seasonal irrigation water need predictions over a longer period to evaluate their actual skill. Particular attention will be paid to the evaluation of the dependence of the quality of the final product on the various components of the system. The study will also cover a comparison between observed irrigation data and estimated data obtained by forcing the CRITERIA water balance model with meteorological observations.

### FURTHER INFORMATION (in Italian)

CRITERIA model: [www.tinyurl.com/criteriamodel](http://www.tinyurl.com/criteriamodel)

Seasonal forecasts: [http://www.arpa.emr.it/sim/?previsioni/lungo\\_termine](http://www.arpa.emr.it/sim/?previsioni/lungo_termine)

iColt reports and results: <http://www.arpa.emr.it/sim/?telerilevamento/colt>

Agrosenari project: <http://www.agrosenari.it>

### FURTHER READING

**Driessen, P.M. & N.T. Konijn**, 1992: *Land-use Systems Analysis*. Wageningen Agricultural University, 230 pp.

**Marletto, V., F. Ventura, G. Fontana & F. Tomei**, 2007: Wheat growth simulation and yield prediction with seasonal forecasts and a numerical model. *Agric. Forest Meteorol.*, **147**, 71–79.

**Pavan, V. & F. Doblas-Reyes**, 2013: Calibrated multi-model ensemble summer temperature predictions over Italy. *Climate Dynamics*, doi 10.1007/s00382-013-1869-7.

**Spisni, A., W. Pratzzoli, F. Tomei, M.C. Mariani, G. Villani, V. Pavan, R. Tomozeiu & V. Marletto**, 2010: Forecasting seasonal water needs under current and future climate. *ESA Special Publication SP-686*, Ed.: H. Lacoste-Francis, Proceedings of the ESA Living Planet Symposium, 28 June–2 July 2010, Bergen, Norway.

**Tomei, F., G. Antolini, R. Tomozeiu, V. Pavan, G. Villani & V. Marletto**, 2010: Analysis of precipitation in Emilia-Romagna (Italy) and impacts of climate change scenarios. In *Proc. International Workshop on Statistics in Hydrology*, 23–25 May 2010, Taormina, Italy.

# GPU based interactive 3D visualization of ECMWF ensemble forecasts

MARC RAUTENHAUS, CHRISTIAN M. GRAMS,  
ANDREAS SCHÄFLER, RÜDIGER WESTERMANN

Nowadays Graphics Processing Units (GPUs) and three-dimensional (3D) visualization are state of the art in the entertainment industry. However, the power that GPUs provide has not been used widely in meteorological data visualization. In the context of weather forecasting during aircraft-based field campaigns, the Technical University of Munich's Chair for Computer Graphics and Visualization is, in collaboration with the DLR (German Aerospace Centre) Institute of Atmospheric Physics, developing a GPU powered 3D weather forecasting tool for ECMWF ensemble forecasts. In our project, we are interested in how we can exploit the computational power of GPUs to create interactive 3D visualizations of ensemble predictions that enable the forecaster to (a) quickly identify atmospheric features of interest to a campaign and (b) assess the features' uncertainty. This includes technical issues as well as the question of how the forecast meteorological fields and the uncertainty information derived from the ensemble can best be presented in three dimensions.

Our research is motivated by forecasting cases from the T-NAWDEX-Falcon field campaign (hereafter TNF, see Box A), which in October 2012 aimed at taking in-situ measurements in warm conveyor belts (WCBs). In this article we describe our visualization approach to predict WCB situations. The weather situation of 19 October 2012 serves as an illustration of the visualization methods and their implementation using the GPU. As it is difficult to convey the full power of interactive 3D visualization in printed, static images, you can find supplementary video content on our project website. Please point your web browser to <http://www.wcg.in.tum.de/research/research/projects/met3d.html>.

## Using GPUs to visualize meteorological data fields

GPUs have become increasingly powerful in recent years. First designed as highly specialized co-processors to speed up graphics operations, they have evolved into massively parallel multi-purpose processors that nowadays can be used for arbitrary computations including numerical simulation (e.g. *Owens et al.*, 2008). In our work we use them

### AFFILIATIONS

**Marc Rautenhaus, Rüdiger Westermann**, Computer Graphics and Visualization Group, Technische Universität München, Germany

**Christian M. Grams**, Institute for Atmospheric and Climate Science, ETH Zürich, Switzerland

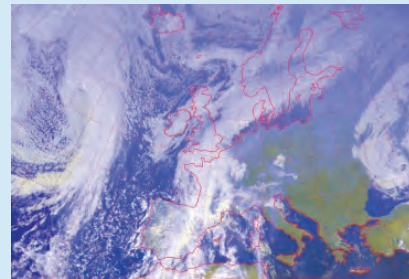
**Andreas Schäfler**, Institut für Physik der Atmosphäre, Deutsches Zentrum für Luft- und Raumfahrt, Oberpfaffenhofen, Germany

### T-NAWDEX-Falcon

A

The T-NAWDEX-Falcon field campaign, jointly organised by DLR and ETH Zurich, took place in October 2012 at DLR's Oberpfaffenhofen base. Several research flights were conducted with the German research aircraft Falcon to take in-situ measurements in warm conveyor belts (WCBs; a WCB is an air stream in an extratropical cyclone that rapidly ascends in the warm sector ahead of the cold front along the sloped isentropes of the midlatitude baroclinic zone). The major forecasting challenge was to predict how favourable the weather situation was for the occurrence of a WCB within aircraft range. *Schäfler et al.* (2014) describe the campaign and the challenges for flight planning in detail.

The visualizations shown in this article consider the T-NAWDEX-Falcon case of 19 October 2012. The figure shows the visible Meteosat image at 12 UTC on 19 October (Meteosat operated by EUMETSAT with image processing by DLR-IPA).



A distinct narrow trough was located to the west of the British Isles. Cold air was advected far south, as can be seen from the convective clouds east of the Iberian Peninsula. The former hurricane 'Rafael', having undergone extratropical transition, can be seen upstream of the trough, south of Iceland. This strong cyclone largely influenced the predictability over Europe and, in particular, the shape and location of the WCB manifest in the cloud band extending from Spain to the British Isles.

to execute visualization algorithms, as well as to speed up data processing operations. Current GPUs allow the execution of increasingly complex visualization algorithms at interactive frame rates, that is, a single image can be rendered in a fraction of a second. This enables smooth animations of a scene.

Box B gives further information on GPUs. For visualizing meteorological forecast data, current models provide sufficient power to enable interactivity for scenes such as the example shown in Figure 1. The images are generated by uploading the forecast data to the graphics card. Spatial interpolation, isosurface extraction, contour line generation

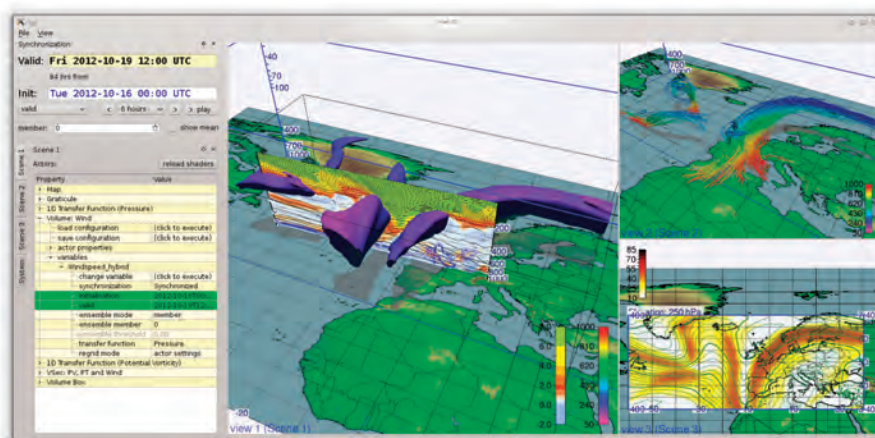


**Figure 1** Screenshot of the forecasting tool 'Met.3D' with three views visualizing different variables of the control run of the ensemble forecast started at 00 UTC on 16 October 2012 at 84 hours lead time. View 1 (middle):  $40 \text{ ms}^{-1}$  isosurface of wind speed together with a vertical cross-section of potential vorticity. View 2 (upper right): Trajectories ascending more than 500 hPa in 48 hours. View 3 (lower right): Horizontal cross-section of geopotential height and wind speed at 250 hPa.

and colour mapping is all carried out by the GPU. The user can move around in the scene and change visualization parameters, including the position of cross-sections, isosurface values and colour mappings without having to wait for a new image.

### How to visualize the ensemble?

During aircraft based field campaigns, flights often have to be planned several days in advance. Hence, being able to assess the uncertainty of the forecast on whose basis a flight route is designed is very valuable. In contrast to the surface products provided operationally by ECMWF's ensemble forecast (e.g. surface wind gust probabilities), planning of flights with high-flying aircraft focuses on upper-level features, which inherently are of a three-dimensional nature. Hence it seems natural to aid the identification of such features (which can be clouds, the jet stream or, in the case of TNF, warm conveyor belts) in the forecast data with three-dimensional visualization elements. Nevertheless, until now research flight planning at DLR has been based on the 'classic' two-dimensional (2D) plots widely used in meteorology (Rautenhaus *et al.*, 2012). We thus considered it essential to provide familiar 2D cross-sections in the new 3D environment, thereby 'building a bridge' from 2D to 3D visualization. By enabling the forecaster to interactively move a cross-section in the scene and to add, for instance, a 3D

isosurface, the 3D structure of the forecast atmosphere can be explored very quickly. Figure 2 illustrates the approach with a vertical cross-section of cloud cover (colour) and potential temperature (contour lines) to which trajectories indicating a WCB (see below) are added.

With regard to the ensemble, we are, as a first step, interested in animating the ensemble members and exploring statistical metrics including mean, standard deviation and probabilities derived from the ensemble. Similar to the operational stamp maps showing all the members of an ensemble, animating over the ensemble members helps identify regions of large variation and determine the scenarios indicated by the ensemble forecast. Figure 3 shows a few members of a vertical cross-section of potential vorticity together with a  $40 \text{ ms}^{-1}$  isosurface of wind speed (indicating the jet stream). The jet stream on the western, upstream side of the trough is influenced by the interaction of hurricane Rafael with the midlatitude flow during its extratropical transition. It is clearly visible that the wind speed isosurface in this region varies much more between the members than on the eastern, downstream side of the trough.

Probabilities can refer to simple thresholds (e.g. the probability of wind speed exceeding  $40 \text{ ms}^{-1}$  or the probability of temperature being between 260 K and 270 K), or to features.

### Graphics Processing Units

A graphics processing unit (GPU) is a highly parallel processor, with current models possessing up to 1,500 processing cores. Originally designed as special-purpose graphics engines with fixed functionality, GPUs have evolved into fully-programmable processors featuring extremely fast memory. In recent years, the term GPGPU (general-purpose computing on the GPU) has been coined to describe the mapping of arbitrary computations to the GPU.

GPUs are programmed following the single program multiple data (SPMD) paradigm, allowing the processing of many elements (e.g. grid points for fluid simulation or rays casted through a data volume for 3D visualization) in parallel using the same program. This ability to simultaneously use a large

number of processing units, paired with the fast memory interface, leads to very high performance in applications where parallelism is abundant. The very high performance combined with high bandwidth interfaces to the CPU, through which the GPU might even be able to directly access CPU memory in the near future, enables the implementation of streaming methods. Streaming allows the efficient exploitation of the GPU's power to process and visualize datasets too large to fit into its local memory, an approach particularly interesting for ensemble datasets.

For further information on GPUs, we refer the reader to, for example, the survey by Owens *et al.* (2008).

B

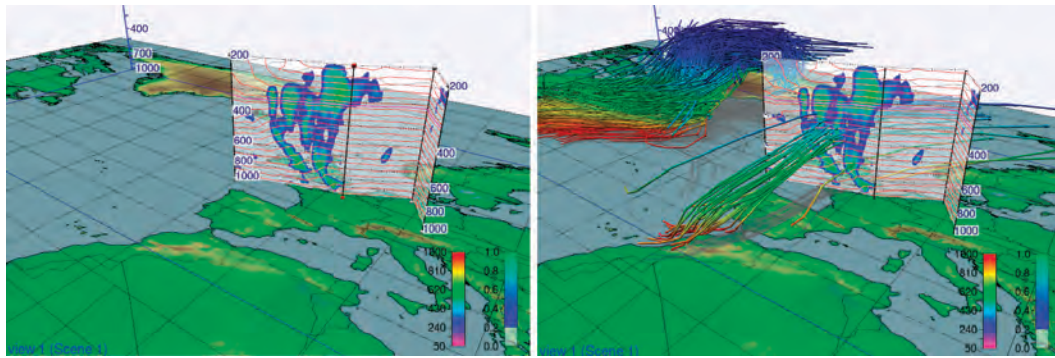


**Figure 2** A vertical cross-section of cloud cover along a possible flight route (forecast from 00 UTC on 16 October valid at 12 UTC on 19 October 2012). The waypoints defining the section can be moved by dragging the spherical handles. On the right, 3D trajectory lines are added to the scene to visualize where trajectories and flight route intersect. Trajectory lines are coloured with pressure (hPa) and the vertical section is coloured with cloud cover fraction per grid box (0-1).

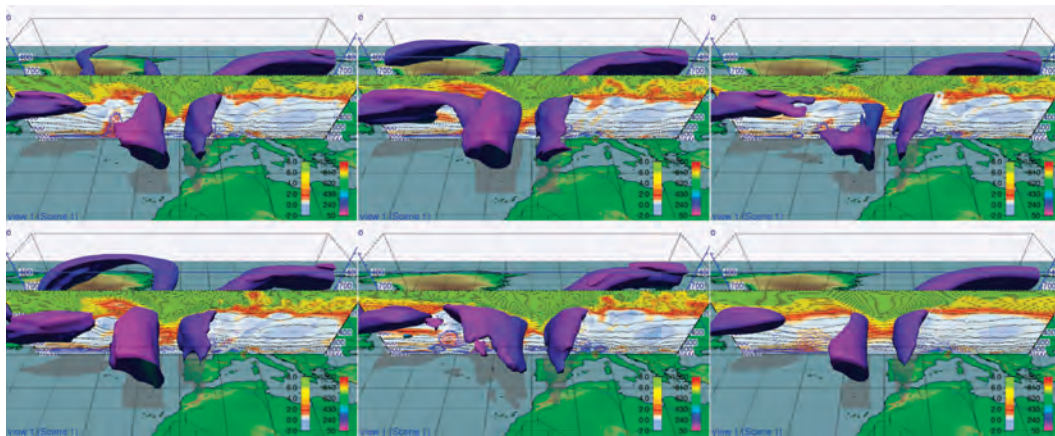


**Figure 3** Screenshots from navigating through the ensemble dimension (forecast from 00 UTC on 16 October valid at 12 UTC on 19 October 2012). The vertical cross-section shows potential vorticity in PVU (reddish colours denote the dynamic tropopause at 2 PVU) and the 3D isosurface shows a wind speed of  $40 \text{ ms}^{-1}$  (colour coded by pressure in hPa). From left to right, top to bottom: Control run, members 8, 16, 31 and 32 and the ensemble mean.

Figure 4 shows the probability of cloud cover exceeding a grid box fraction of 0.2. Knowledge about clouds along a flight track is important information for many research flights. For TNF, we were particularly interested in the probability of a WCB occurring. To identify WCBs, we followed the approach of *Wernli & Davis (1997)* and computed Lagrangian trajectories for each member of the ensemble with the ETH Zurich LAGRANTO model. Trajectories starting close to the surface and ascending more than 500 hPa in 48 hours were classified as WCB trajectories. By gridding each member’s trajectory position at a given time and counting the number of members for which a grid box contains a trajectory, a probability of WCB occurrence can be derived. Figure 5 illustrates the approach. Thresholds for computing probabilities or parameters for feature detection, such as the filter criterion of vertical distance per time to identify WCBs, may not be specifiable in advance. Hence, we provide interactivensess with regard to parameter adjustments in the visualization system. Figure 5 shows an example of adjusting the trajectory filter criterion from 500 hPa to 550 hPa in 48 hours, thereby focussing more strongly on the core region of the WCB where the ascent is strongest.

**Met.3D – a 3D forecasting tool**

We have integrated the visualization methods into a software tool that is intended to be used for forecasting during future field campaigns. Figure 1 shows a screenshot of the current version of the tool, which we have called ‘Met.3D’. The software provides multiple views that can display the same or different datasets from arbitrary viewpoints in 3D space. A number of global parameters concerning time and ensemble dimensions and camera position can be synchronized and hence be changed simultaneously for all views. As common in meteorology, the logarithm of pressure serves as the vertical coordinate.

To achieve the best possible vertical accuracy in the visualizations and trajectory computations, we use ensemble forecast data on the original hybrid sigma-pressure model levels. Although these datasets are not operationally archived in the ECMWF Meteorological Archive and Retrieval System (MARS), the last three forecast runs are available and can be retrieved during field campaigns. For our project, we have recorded multiple ensemble forecasts for the TNF period. As we are typically

not interested in the entire global forecast but only in a limited domain, we use the data on the regular horizontal grid that is output by the MARS system.

To enable smooth animation over time and ensemble dimensions, Met.3D uses caching and pre-fetching techniques to avoid time-consuming disk reads when the user changes time or ensemble settings. Depending on the resolution of the dataset to be visualized, the system hence requires multiple GB of system and video memory. However, for a dataset covering the domain shown in Figure 1 with a horizontal resolution of one degree, Met.3D can already be used on a standard Laptop equipped with 4 GB of system memory and 1 GB of video memory.

**Ongoing developments**

Our current focus is to continue research on how to best visualize the uncertainty information derived from the ensemble. Uncertainty visualization is an active field of research in the visualization community, and meteorological data visualization may greatly benefit from it. Relevant recent research includes work on the positional uncertainty of isosurfaces (Pfaffelmoser et al., 2011), uncertain particle trajectories (Bürger et al., 2012) and using non-parametric probabilistic models to compute feature probabilities (Pöthkow & Hege, 2013). We are, for example, pursuing further experiments to visualize probabilities of atmospheric features such as fronts and jet streams.

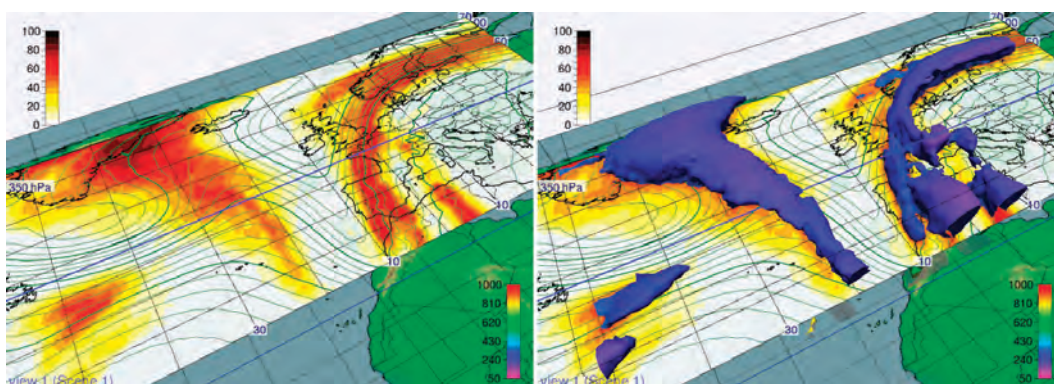


**Figure 4** Left: Horizontal section at 350 hPa showing the probability (%) of cloud cover fraction exceeding 0.2. Contour lines show the mean geopotential height field. Right: An isosurface of 50% added to the horizontal section (forecast from 00 UTC on 16 October valid at 12 UTC on 19 October 2012).

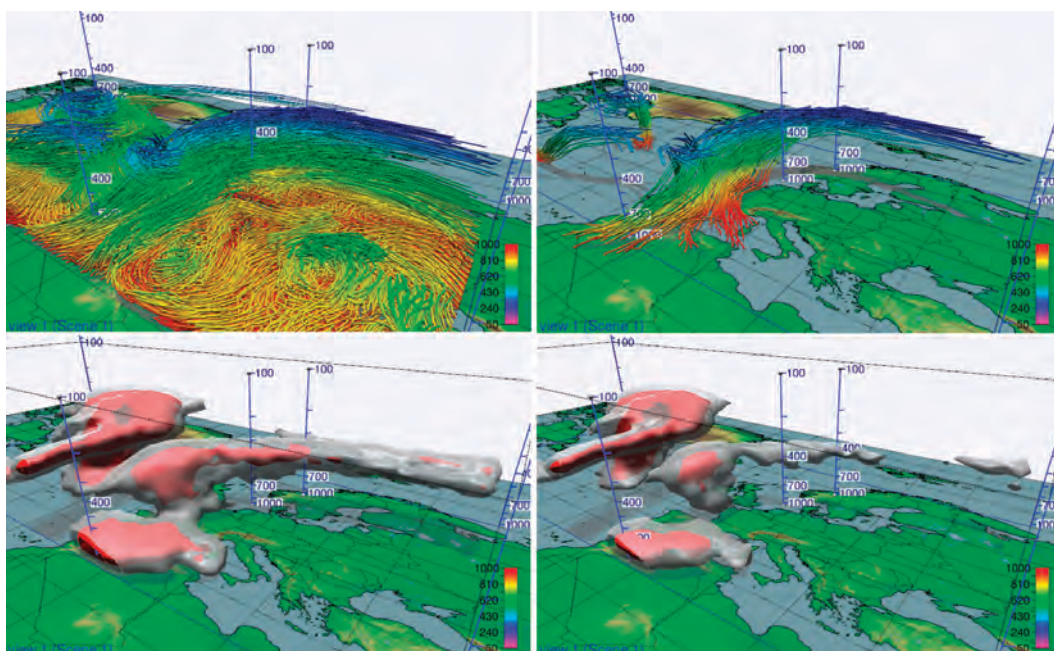


**Figure 5** Probability of warm conveyor belt occurrence  $p(\text{WCB})$  computed from trajectories. Top row: Single member of 48-hour trajectories started near the surface (left) and filtered according to an ascent of 500 hPa in 48 hours (right). Bottom: Volume rendering of  $p(\text{WCB})$  with two different probability surfaces, derived from gridded trajectories ascending 500 hPa in 48 hours (left) and 550 hPa in 48 hours (right).

Furthermore, spatial perception is an important issue with 3D visualization. In particular, in meteorology it often is essential to know the exact location of a feature. In Met.3D, we currently use shadows (all figures) and user-placed poles (Figure 5) to aid the perception of the spatial location of a feature. Nevertheless, we are continuing to investigate the issue to further improve spatial perception. The same applies to detailed labelling of the elements shown in an image. Real-time label placement in three dimensions is a difficult problem, though labels can greatly improve the quantitative information conveyed by an image.

When using model data on hybrid sigma-pressure levels, every ensemble member is defined on a different model grid (the surface pressure field defining the elevation of the individual grid points varies with the ensemble). Hence, computing ensemble statistics on a grid-point basis strictly speaking requires a regridding of the members to

a common grid. However, the difference in the produced images often is small. We will soon publish a discussion on the impact of regridding on the visualization of derived statistical quantities.

Beside the usage of Met.3D for planning research flights, the software's modular architecture allows the straightforward integration of new visualization methods. Hence, the system also serves as an infrastructure for atmospheric visualization research, enabling the development and evaluation of methods for visualizing ensemble simulation data. It is thus usable for applications other than flight planning. In this context, we are considering the release of Met.3D as open source software in 2014. If you are interested in collaboration, or if you are encountering any unsolved issues with regard to uncertainty visualization in your work, please do not hesitate to contact us.

**FURTHER READING**

**Bürger, K., R. Fraedrich, D. Merhof & R. Westermann**, 2012: Instant visitation maps for interactive visualization of uncertain particle trajectories. In *Proc. Visualization and Data Analysis*, SPIE 8294, 82940P–82940P-12.

**Owens, J.D., M. Houston, D. Luebke, S. Green, J.E. Stone & J.C. Phillips**, 2008: GPU Computing. *Proceedings of the IEEE*, **96**, 879–899.

**Pfaffelmoser, T., M. Reitingner & R. Westermann**, 2011: Visualizing the positional and geometrical variability of isosurfaces in uncertain scalar fields. *Computer Graphics Forum*, **30**, 951–960.

**Pöthkow, K. & H.-C. Hege**, 2013: Nonparametric models for uncertainty visualization. *Computer Graphics Forum*, **32**, 131–140.

**Rautenhaus, M., G. Bauer & A. Dörnbrack**, 2012: A web service based tool to plan atmospheric research flights. *Geoscientific Model Development*, **5**, 55–71.

**Schäfler, A., M. Boettcher, C.M. Grams, M. Rautenhaus, H. Sodemann & H. Wernli**, 2014: Planning of aircraft measurements within a warm conveyor belt. *Accepted by Weather*.

**Wernli, H. & H.C. Davies**, 1997: A Lagrangian-based analysis of extratropical cyclones. I: The method and some applications. *Q. J. R. Meteorol. Soc.*, **123**, 467–489.

**ECMWF Calendar 2014**

Mar 10–14	NWP Training: Data assimilation	Jun 8–12	WISE Meeting
Mar 17–21	NWP Training: ECMWF/EUMETSAT NWP-SAF satellite data assimilation	Jun 16–18	ROM SAF Workshop on 'Applications of GPS radio occultation measurements'
Mar 24–28	NWP Training: Advanced numerical methods for Earth-system modelling	Jul 9–10	Council (81st Session)
Mar 31–Apr 10	NWP Training: Parametrization of subgrid physical processes	Sep 8–12	Annual Seminar on 'Use of satellite data'
Mar 30–Apr 1	Advisory Committee for Data Policy (14th Session)	Oct 6–8	Scientific Advisory Committee (43rd Session)
Apr 23–25	Computing Training: Introduction to ecFlow	Oct 9–10	Technical Advisory Committee (46th Session)
Apr 28–May 2	Computing Training: Magics	Oct 13–16	EUMETNET STAS and PFAC
Apr 28	Policy Advisory Committee (37th Session)	Oct 16–17	Finance Committee (94th Session)
Apr 29–30	Finance Committee (94th Session)	Oct 20	Policy Advisory Committee (38th Session)
Apr 29–2 May	Computing Training: Metviews	Oct 27	Advisory Committee of Co-operating States (20th Session)
May 7–16	NWP Training: Predictability and ocean-atmosphere ensemble forecasting	Oct 27–31	Workshop on 'High performance computing in meteorology'
May 12–13	Security Representatives' Meeting	Nov 3–7	Combined H-SAF and HEPeX workshops on 'Coupled hydrology'
May 13–15	Computer Representatives' Meeting	Dec 3–4	Council (82nd Session)
Jun 4–6	Using ECMWF's Forecasts (UEF2014)		



## ECMWF Council and its committees

The following provides some information about the responsibilities of the ECMWF Council and its committees. More detail can be found at:

<http://www.ecmwf.int/about/committees>

### Council

The Council adopts measures to implement the ECMWF Convention; the responsibilities include admission of new members, authorising the Director to negotiate and conclude co-operation agreements, and adopting the annual budget, the scale of financial contributions of the Member States, the Financial Regulations and the Staff Regulations, the long-term strategy and the programme of activities of the Centre.



**President** Prof Dr Gerhard Adrian (Germany)

**Vice President** Dr Miguel Miranda (Portugal)

### Policy Advisory Committee (PAC)

The PAC provides the Council with opinions and recommendations on any matters concerning ECMWF policy submitted to it by the Council, especially those arising out of the Four-Year Programme of Activities and the Long-term Strategy.



**Chair** Mr Juhani Damski (Finland)

**Vice Chair** Mr Arni Snorrason (Iceland)

### Finance Committee (FC)

The FC provides the Council with opinions and recommendations on all administrative and financial matters submitted to the Council and shall exercise the financial powers delegated to it by the Council.



**Chair** Mr Detlev Frömming (Germany)

**Vice Chair** Mr Marco Viljanen (Finland)

### Scientific Advisory Committee (SAC)

The SAC provides the Council with opinions and recommendations on the draft programme of activities of the Centre drawn up by the Director and on any other matters submitted to it by the Council. The 12 members of the SAC are appointed in their personal capacity and are selected from among the scientists of the Member States.



**Chair** Dr Jan Barkmeijer (KNMI)

**Vice Chair** Prof Sarah Jones (Deutscher Wetterdienst)

### Technical Advisory Committee (TAC)

The TAC provides the Council with advice on the technical and operational aspects of the Centre including the communications network, computer system, operational activities directly affecting Member States, and technical aspects of the four-year programme of activities.



**Chair** Dr Daniel Gellens (Belgium)

**Vice Chair** Mr Jean-Marie Carrière (France)

### Advisory Committee for Data Policy (ACDP)

The ACDP provides the Council with opinions and recommendations on matters concerning ECMWF Data Policy and its implementation.



**Chair** Mr Frank Lantsheer (Netherlands)

**Vice Chair** Mr Soren Olufsen (Denmark)

### Advisory Committee of Co-operating States (ACCS)

The ACCS provides the Council with opinions and recommendations on the programme of activities of the Centre, and on any matter submitted to it by the Council.



**Chair** Mr Martin Benko (Slovakia)

**Vice Chair** Ms Inita Stikute (Latvia)

## TAC Representatives, Computing Representatives and Meteorological Contact Points

Member States	TAC Representatives	Computer Representatives	Meteorological Contact Points
Austria	Dr G. Kaindl	Mr M. Langer	Dr A. Schaffhauser
Belgium	Dr D. Gellens	Mrs L. Frappez	Dr J. Nemeghaire
Denmark	Mr C. Simonsen	Mr T. Lorenzen	Mr H. Gisselø
Finland	Mr J. Hyrkkänen	Mr M. Aalto	Mr P. Nurmi
France	Mr J.-M. Carrière	Mr N. Merlet	Ms N. Girardot
Germany	Dr D. Schroeder	Dr E. Krenzien	Mr T. Schumann
Greece	Mr A. Emmanouil	Mr. N. Andritsas	Mr A. Lalos Ms C. Petrou Mr P. Skrimizeas Ms T. Tzeferi
Iceland	Mr T. Hervarsson	Mr V. Gislason	Mrs K. Hermannsdóttir
Ireland	Ms S. O'Reilly	Mr T. Daly	Mr G. Fleming
Italy	Lt. Col. L. Torrasi	Mr A. Vocino	Dr T. La Rocca
Luxembourg	Mrs M. Reckwerth	Mrs. M. Reckwerth	Mrs. M. Reckwerth
Netherlands	Mr R. van Lier	Mr H. de Vries	Mr J. Diepeveen
Norway	Mrs C. Husum Vold	Mr K. Steinar Dale	Dr B Røsting
Portugal	Mrs T. Abrantes	Mr B. Anjos	Mr N. M. Moreira
Slovenia	Mr J. Jerman	Mr P. Hitij	Mr B. Gregorčič
Spain	Mr P. del Rio	Mr R. Corredor	Mrs A. Casals
Sweden	Mr F. Linde	Mr R. Urrutia	Mr F. Linde
Switzerland	Dr P. Steiner	Mr P. Roth	Mr E. Müller
Turkey	Mr M. Fatih Büyükkasabbaşı	Mr M. Emre Yakut	Mr A. Guser
United Kingdom	Mr I. Forsyth	Mr R. Sharp	Mr I. Forsyth
<b>Co-operating States</b>			
Bulgaria	Ms I. Etropolska	Ms I. Etropolska	Mrs A. Stoycheva
Croatia	Ms B. Matjacic	Mr V. Malović	Mr Č. Branković
Czech Republic	Ms A. Trojakova	Mr K. Ostatnický	Mr F. Sopko
Estonia	Mr A. Männick Mr A. Luhamaa	Mr H. Kaukver	Mrs M. Merilain Mrs T. Paljak
The former Yugoslav Republic of Macedonia	Mr V. Dimitriev	Mr B. Sekirarski	Ms N. Aleksovska
Hungary	Mr I. Ihász	Mr I. Ihász	Mr I. Ihász
Israel	Mr I. Rom	Mr V. Meerson	Mr N. Stav
Latvia	Mr A. Bukšs	Mr A. Bukšs	Ms A. Niznika
Lithuania	Mrs V. Auguliene	Mr M. Kazlauskas	Mrs V. Raliene
Montenegro	Mr A. Marčev	Mr A. Marčev	Mr B. Micev
Morocco	Mr H. Haddouch	Mr M. Jidane	Mr K. Lahlal
Romania	Mrs A. Ristici	Mr R. Cotariu	Ms M. Georgescu
Serbia	Ms L. Dekic	Mr V. Dimitrijević	Mr B. Bijelic
Slovakia	Mr J. Vivoda	Dr O. Španiel	Dr M. Benko Dr J. Csaplár
<b>Observers</b>			
EUMETSAT	Mr A. Ratier	Dr S. Elliott	
WMO	Mr M. Jarraud		

## ECMWF publications

(see <http://www.ecmwf.int/publications/>)

### Technical Memoranda

- 716 **Breivik, O., P.A.E.M. Janssen & J.-R. Bidlot:** Approximate Stokes drift profiles in deep water. *December 2013*
- 715 **Muñoz Sabater, J., P. de Rosnay, C. Jimenez, L. Isaksen & C. Albergel:** SMOS brightness temperatures angular noise: characterization, filtering and validation. *November 2013*
- 714 **Cardinali, C. & S. Healy:** Impact of GPS radio occultation measurements in the ECMWF system using adjoint based diagnostics. *November 2013*
- 713 **Diamantakis, M. & J. Flemming:** Global mass flux algorithms for conservative tracer transport in the ECMWF model. *October 2013*
- 712 **Janssen, P.A.E.M., O. Breivik, K. Mogensen, F. Vitart, M. Balmaseda, J.-R. Bidlot, S. Keeley, M. Leutbecher, L. Magnusson, & F. Molteni:** Air-sea interaction and surface waves. *November 2013*
- 711 **English, S., T. McNally, N. Bormann, K. Salonen, M. Matricardi, A. Horanyi, M. Rennie, M. Janisková, S. Di Michele, A. Geer, E. Di Tomaso, C. Cardinali, P. de Rosnay, J. Muñoz Sabater, M. Bonavita, C. Albergel, R. Engelen & J.-N. Thépaut:** Impact of satellite data. *November 2013*
- 710 **Richardson, D.S., J. Bidlot, L. Ferranti, T. Haiden, T. Hewson, M. Janousek, F. Prates & F. Vitart:** Evaluation of ECMWF forecasts, including 2012–2013 upgrades. *November 2013*

### ERA Report Series

- 16 **Hersbach, H., C. Peubey, A. Simmons, P. Poli, D. Dee & P. Berrisford:** ERA-20CM: a twentieth century atmospheric model ensemble. *November 2013*
- 15 **Simmons, A.J., P. Poli, D.P. Dee, P. Berrisford, H. Hersbach & C. Peubey:** Estimating low-frequency variability and trends in atmospheric temperature using ERA-Interim. *September 2013*
- 14 **Poli, P., H. Hersbach, D. Tan, D. Dee, J.-N. Thépaut, A. Simmons, C. Peubey, P. Laloyaux, T. Komori, P. Berrisford, R. Dragani, Y. Trémolet, E. Holm, M. Bonavita, L. Isaksen & M. Fisher:** The data assimilation system and initial performance evaluation of the ECMWF pilot reanalysis of the 20<sup>th</sup>-century assimilating surface observations only (ERA-20C). *September 2013*

### EUMETSAT/ECMWF Fellowship Programme Research Report

- 32 **Salonen, K. & N. Bormann:** Atmospheric motion vector observations in the ECMWF system: third year report. *November 2013*
- 31 **Lupu, C. & A.P. McNally:** Wind tracing with ozone-sensitive radiances from SEVIRI. *December 2013*
- 30 **Baordo, F., A.J. Geer & S. English:** All-sky assimilation of SSMI/S humidity sounding channels over land: second year report. *September 2013*

### ESA Contract Reports

- Abdalla, S.:** Evaluation of radar altimeter path delay using ECMWF pressure-level and model-level fields. *October 2013*

## Contact information

ECMWF, Shinfield Park, Reading, Berkshire RG2 9AX, UK

Telephone National 0118 949 9000

Telephone International +44 118 949 9000

Fax +44 118 986 9450

ECMWF's public website <http://www.ecmwf.int/>

E-mail: The e-mail address of an individual at the Centre is firstinitial.lastname@ecmwf.int. For double-barrelled names use a hyphen (e.g. j-n.name-name@ecmwf.int).

Problems, queries and advice	Contact
General problems, fault reporting, web access and service queries	calldesk@ecmwf.int
Advice on the usage of computing and archiving services	advisory@ecmwf.int
Queries regarding access to data	data.services@ecmwf.int
Queries regarding the installation of ECMWF software packages	software.support@ecmwf.int
Queries or feedback regarding the forecast products	meteorological_support@ecmwf.int

## Index of newsletter articles

This is a selection of articles published in the *ECMWF Newsletter* series during recent years.  
Articles are arranged in date order within each subject category.  
Articles can be accessed on the ECMWF public website – <http://www.ecmwf.int/publications/newsletter/index.html>

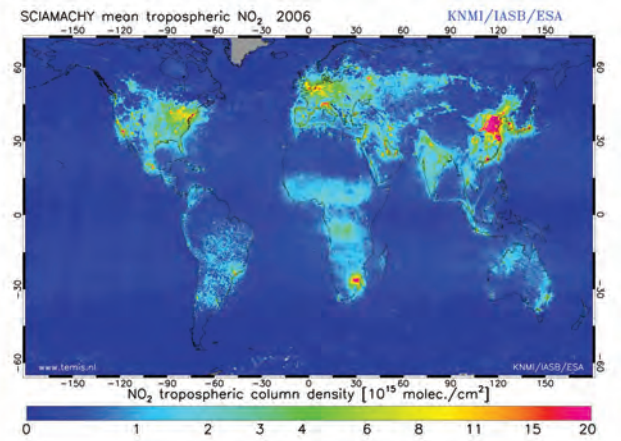
	No.	Date	Page		No.	Date	Page
<b>NEWS</b>							
Metview's 20 <sup>th</sup> anniversary	138	Winter 2013/14	2	ERA-20C production has started	134	Winter 2012/13	6
New model cycle 40r1	138	Winter 2013/14	3	ecCharts service	134	Winter 2012/13	7
Retirement of Jean-Jacques Morcrette	138	Winter 2013/14	4	Improving cloud and precipitation parametrization	134	Winter 2012/13	9
Handling hyperspectral infrared satellite observations	138	Winter 2013/14	5	Application of the new EFI products to a case of early snowfall in Central Europe	133	Autumn 2012	4
MACC-II General Assembly	138	Winter 2013/14	5	Metview 4.3 released under Open Source Licence	133	Autumn 2012	6
Use and development of Meteorological Operational Systems	138	Winter 2013/14	6	ECMWF forecasts help aid workers	133	Autumn 2012	7
Parameter estimation and inverse modelling for atmospheric composition	138	Winter 2013/14	8	Training courses: reaching out to the international community	133	Autumn 2012	8
Update on the new website	138	Winter 2013/14	8	High performance computing in meteorology	133	Autumn 2012	8
ERA-Interim monitors the global warmth of 2013	138	Winter 2013/14	9	ECMWF forecasts of 'Superstorm Sandy'	133	Autumn 2012	9
ECMWF's contribution to GEO	138	Winter 2013/14	11	Training courses: a success story	131	Spring 2012	5
New items on the ECMWF website	138	Winter 2013/14	12	Honorary degree awarded to Alan Thorpe	130	Winter 2011/12	2
Applying for Special Projects	138	Winter 2013/14	12	Co-operation with EFAS	130	Winter 2011/12	3
Florence Rabier – Director of Forecasts	137	Autumn 2013	3	An appreciation of Dominique Marbouty	128	Summer 2011	2
Accession agreement between Serbia and ECMWF	137	Autumn 2013	4	<b>VIEWPOINT</b>			
A reanalysis tale on the Earth's climate	137	Autumn 2013	4	Using ECMWF's Forecasts: a forum to discuss the use of ECMWF data and products	136	Summer 2013	12
New look for the NWP training course	137	Autumn 2013	5	Describing ECMWF's forecasts and forecasting system	133	Autumn 2012	11
Using Earth System science at ECMWF	137	Autumn 2013	6	Discussion about the ECMWF Newsletter and communicating science	133	Autumn 2012	13
An assessment of solar irradiance components produced by the IFS	137	Autumn 2013	6	<b>COMPUTING</b>			
MACC-II Summer School 2013	137	Autumn 2013	8	GPU based interactive 3D visualization of ECMWF ensemble forecasts	138	Winter 2013/14	34
The role of mathematics in understanding weather	137	Autumn 2013	9	RMDCN – Next Generation	134	Winter 2012/13	38
Walter Zwielfhofer	136	Summer 2013	3	A new trajectory interface in Metview 4	131	Spring 2012	31
University of Helsinki meeting on OpenIFS	136	Summer 2013	4	A new framework to handle ODB in Metview 4	130	Winter 2011/12	31
ECMWF's new departmental structure	136	Summer 2013	4	Managing work flows with ecFlow	129	Autumn 2011	30
NWP training 2013	136	Summer 2013	5	Support for OGC standards in Metview 4	127	Spring 2011	28
Improving polar predictions	136	Summer 2013	6	Metview 4 – ECMWF's latest generation meteorological workstation	126	Winter 2010/11	23
Annual Report 2012	136	Summer 2013	6	Green computing	126	Winter 2010/11	28
Contract for a new High-Performance Computing Facility at ECMWF	136	Summer 2013	7	Metview Macro –			
New model cycle 38r2	136	Summer 2013	8	A powerful meteorological batch language	125	Autumn 2010	30
RMDCN – Next Generation	136	Summer 2013	9	The Data Handling System	124	Summer 2010	31
Floods in Central Europe in June 2013	136	Summer 2013	9	Update on the RMDCN	123	Spring 2010	29
Webinars: what are they?	135	Spring 2013	2	<b>METEOROLOGY</b>			
Routine verification of radiation and cloudiness	135	Spring 2013	3	<b>OBSERVATIONS &amp; ASSIMILATION</b>			
Flow dependent background error modelling in 4DVAR	135	Spring 2013	4	Ten years of ENVISAT data at ECMWF	138	Winter 2013/14	13
Use of GIS/OGC standards in meteorology	135	Spring 2013	5	Impact of the Metop satellites in the ECMWF system	137	Autumn 2013	9
ECMWF's plans for 2013	134	Winter 2012/13	3	Ocean Reanalyses Intercomparison Project (ORA-IP)	137	Autumn 2013	11
Republic of Slovenia becomes ECMWF's twentieth Member State	134	Winter 2012/13	4	The expected NWP impact of Aeolus wind observations	137	Autumn 2013	23
Polar-orbiting satellites crucial in successful Sandy forecasts	134	Winter 2012/13	5				

	No.	Date	Page		No.	Date	Page
Winds of change in the use of Atmospheric Motion Vectors in the ECMWF system	136	Summer 2013	23	Representing model uncertainty: stochastic parametrizations at ECMWF	129	Autumn 2011	19
New microwave and infrared data from the S-NPP satellite	136	Summer 2013	28	Simulation of the Madden-Julian Oscillation and its impact over Europe in the ECMWF monthly forecasting system	126	Winter 2010/11	12
Scaling of GNSS radio occultation impact with observation number using an ensemble of data assimilations	135	Spring 2013	20	On the relative benefits of TIGGE multi-model forecasts and reforecast-calibrated EPS forecasts	124	Summer 2010	17
ECMWF soil moisture validation activities	133	Autumn 2012	23	Combined use of EDA- and SV-based perturbations in the EPS	123	Spring 2010	22
Forecast sensitivity to observation error variance	133	Autumn 2012	30				
Use of EDA-based background error variances in 4D-Var	130	Winter 2011/12	24	<b>METEOROLOGICAL APPLICATIONS &amp; STUDIES</b>			
Observation errors and their correlations for satellite radiances	128	Summer 2011	17	iCOLT – Seasonal forecasts of crop irrigation needs at ARPA-SIMC	138	Winter 2013/14	30
Development of cloud condensate background errors	128	Summer 2011	23	Forecast performance 2013	137	Autumn 2013	13
Use of SMOS data at ECMWF	127	Spring 2011	23	An evaluation of recent performance of ECMWF's forecasts	137	Autumn 2013	15
Extended Kalman Filter soil-moisture analysis in the IFS	127	Spring 2011	12	Cold spell prediction beyond a week: extreme snowfall events in February 2012 in Italy	136	Summer 2013	31
Weak constraint 4D-Var	125	Autumn 2010	12	The new MACC-II CO2 forecast	135	Spring 2013	8
Collaboration on Observing System Simulation Experiments (Joint OSSE)	123	Spring 2010	14	Forecast performance 2012	134	Winter 2012/13	11
The new Ensemble of Data Assimilations	123	Spring 2010	17	Teaching with OpenIFS at Stockholm University: leading the learning experience	134	Winter 2012/13	12
Assessment of FY-3A satellite data	122	Winter 2009/10	18	Uncertainty in tropical winds	134	Winter 2012/13	33
				Monitoring and forecasting the 2010-11 drought in the Horn of Africa	131	Spring 2012	9
<b>FORECAST MODEL</b>				Characteristics of occasional poor medium-range forecasts for Europe	131	Spring 2012	11
Improving the representation of stable boundary layers	138	Winter 2013/14	24	A case study of occasional poor medium-range forecasts for Europe	131	Spring 2012	16
Interactive lakes in the Integrated Forecasting System	137	Autumn 2013	30	The European Flood Awareness System (EFAS) at ECMWF: towards operational implementation	131	Spring 2012	25
Effective spectral resolution of ECMWF atmospheric forecast models	137	Autumn 2013	19	New tropical cyclone products on the web	130	Winter 2011/12	17
Breakthrough in forecasting equilibrium and non-equilibrium convection	136	Summer 2013	15	Increasing trust in medium-range weather forecasts	129	Autumn 2011	8
Convection and waves on small planets and the real Earth	135	Spring 2013	14	Use of ECMWF's ensemble vertical profiles at the Hungarian Meteorological Service	129	Autumn 2011	25
Global, non-hydrostatic, convection-permitting, medium-range forecasts: progress and challenges	133	Autumn 2012	17	Developments in precipitation verification	128	Summer 2011	12
Development of cloud condensate background errors	129	Autumn 2011	13	New clustering products	127	Spring 2011	6
Evolution of land-surface processes in the IFS	127	Spring 2011	17	Use of the ECMWF EPS for ALADIN-LAEF	126	Winter 2010/11	18
Non-hydrostatic modelling at ECMWF	125	Autumn 2010	17	Prediction of extratropical cyclones by the TIGGE ensemble prediction systems	125	Autumn 2010	22
Increased resolution in the ECMWF deterministic and ensemble prediction systems	124	Summer 2010	10	Extreme weather events in summer 2010: how did the ECMWF forecasting system perform?	125	Autumn 2010	10
Improvements in the stratosphere and mesosphere of the IFS	120	Summer 2009	22	Monitoring Atmospheric Composition and Climate	123	Spring 2010	10
Parametrization of convective gusts	119	Spring 2009	15	Tracking fronts and extra-tropical cyclones	121	Autumn 2009	9
<b>PROBABILISTIC FORECASTING &amp; MARINE ASPECTS</b>							
Have ECMWF monthly forecasts been improving?	138	Winter 2013/14	18				
Closer together: coupling the wave and ocean models	135	Spring 2013	6				
20 years of ensemble prediction at ECMWF	134	Winter 2012/13	16				

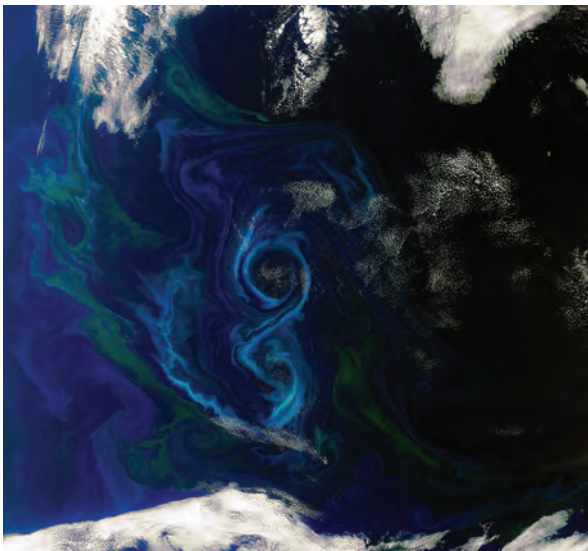
# ENVISAT



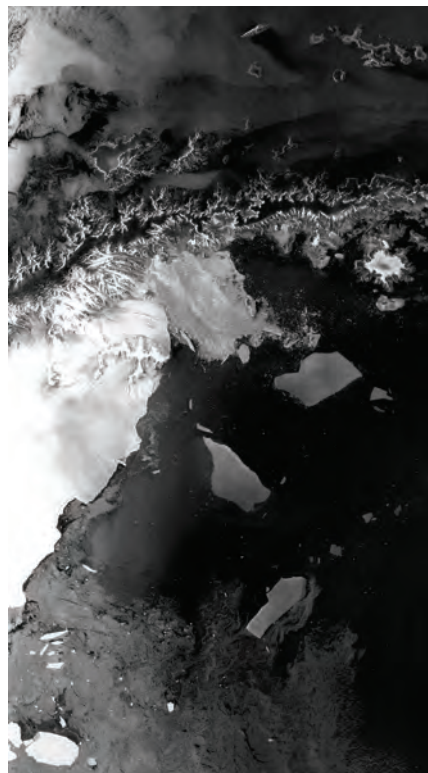
ENVISAT in testing (courtesy of ESA–A.Van Der Geest)



NO<sub>2</sub> pollution map (courtesy of KNMI/IASB/ESA)



Southern summer bloom (courtesy of ESA)



Antarctic peninsular – Advanced Synthetic Aperture Radar (courtesy of ESA)

An article about 10 years of ENVISAT data at ECMWF is on pages 13 to 17.